Picornavirus IRES: Accessibility and Inhibition of Viral Gene Expression

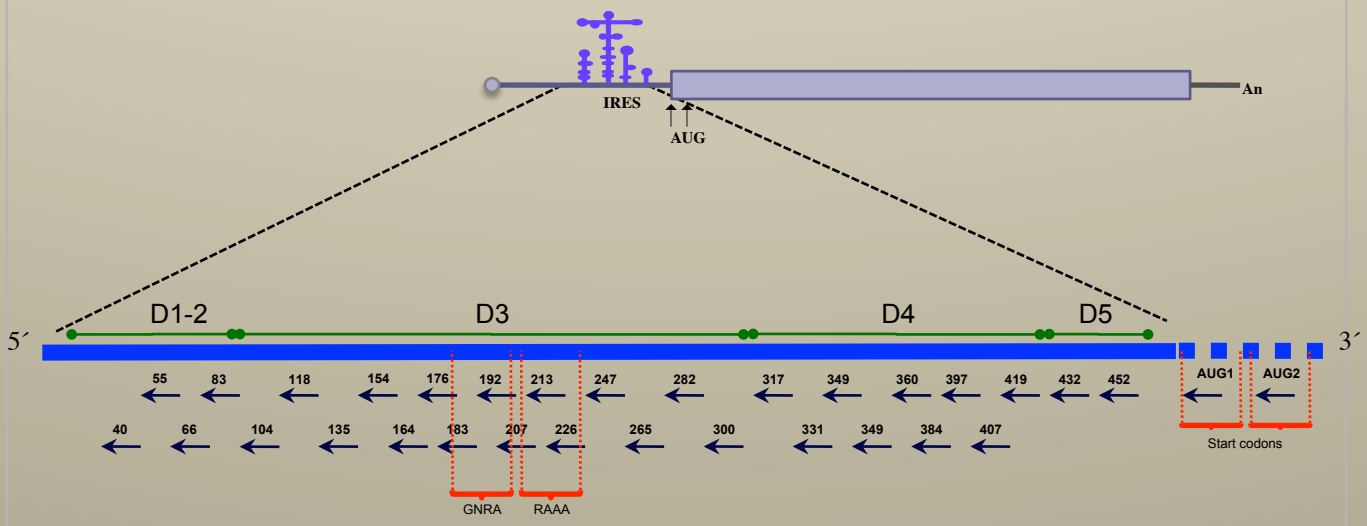

Teodoro, Jr. Fajardo Mallari

Departamento de Biología Molecular
Facultad de Ciencias
Universidad Autónoma de Madrid
Julio, 2011

Universidad Autonóma de Madrid

Facultad de Ciencias

Departamento de Biologia Molecular

Picornavirus IRES:
Accessibility and Inhibition of Viral Gene Expression

Memoria presentada por

Teodoro, Jr. Fajardo Mallari

Para optar al grado de Doctor en Ciencias

por la Universidad Autónoma de Madrid

Centro de Biología Molecular ¨Severo Ochoa¨

Facultad de Ciencias

Madrid, Julio, 2011

Dedication

This research work is wholeheartedly dedicated to:

Ligaya, my mother, who has guided me truly, I dearly love and miss her.

Her love and care, I cannot compare.

Teodoro, my father, whose never-ending support is a source of my strength

to continue on my journey.

Proud as ever, typical of a father.

With great achievements follow humility.

The fulfillment of this work was made possible through the help of Agencia Española de Cooperacion Internacional para el Desarollo of the Ministerio de Asuntos Exteriores y Cooperacion. This work was accomplished through the stewardship of my thesis adviser and mentor, Dr. Encarnación Martinez-Salas, of the Centro de Biologia Molecular ¨Severo Ochoa¨, Universidad Autonoma de Madrid-CSIC.

Acknowledgement

Purihin ang Ama!

I wish to thank all the people who accompanied me on my journey to achieve my vision. I also acknowledge those who had been instrumental, in any way, for the realization of this great endeavor. To all of you, my deepest gratitude.

Specifically, I would like to acknowledge the following:

My parents, for bringing me this world so I can appreciate the beauty of the things that surround me. The source of my hope and inspiration, Ligaya and Teodoro, I am forever grateful.

My brothers, sisters, pamangkins (nieces and nephews) and members of my extended family. Never a single day had passed that I was not thinking of you. To my family, my earnest appreciation and thank you for having you always beside me.

Susan Simon, who persistently pushed me to apply for the scholarship program of the AECI. She was instrumental to my existence in Madrid. To Susan, my sincerest admiration.

Dr. Encarnacion Martinez-Salas, through her guidance and wisdom, I learned intelligently. My thesis would not be possible if not for her patience, advices and support. I reckon ¨learn from your own experiments¨, she often says, and so I will remember this dictum on my way. To Encarna, my genuine regard.

To my tutor, Dr. Jose Antonio Lopez or JAL, for taking time to review this research work despite his busy schedule. To JAL, my genuine appreciation.

To my colleagues in CBMSO and to the present and past members of the laboratorio 309, my heartfelt admiration. We may take different paths but still our minds as one will meet and still our hearts as one will beat. When we part ways, success may be with us all days.

Thanks to David and Noemi, the two doctors in the lab, for sharing their knowledge when I needed to learn a new procedure or protocol, I really appreciate it.

My appreciations for Alfonso, Nuria, Helena, Noemi (Garcia) and to all my pals in CBMSO, coffee-break buddies and my confidants, who love to grab a bite of every Filipino food I make, a salute to you!

To Jorge, who have taught me the nitty-gritty of every procedure in the lab, and who always crave for Asian cuisine of rice noodles (pancit), dim sum and spring rolls, my appreciation for his assistance.

To Liza and Javier, the neophytes in the lab, thank you for the companionship. Follow where your heart will lead you and take the opportunity to learn something new.

To the people outside of the magical world of lab 309, who showed me that life outside the laboratory is as wonderful as it can be. Especial thanks to:

My second family in Madrid, to the members of the ¨Bahay ni Kuya¨ or Big Brother´s House (Weng, Minerva, Desiree, Tyne, Suzette, Lea, Anne, Jem, Letty, Levie, Sheryl, Doris, Millet, Jaz and ate Letty), who share my emotions, laughters, tears, joys and sorrows. Hurrahs to all of you.

To the members of the laboratory 308, Zaida, Sofia, Joana, Sergio, Vicky, Cely, Marta, Bene and Maripaz, who belong to the family of Encarna and Crisanto, thanks for the comradeship.

To Ivan, Fermin and to our circle of friends, who have showed me that there is another world outside my world of science. Thank you for the companionship, warmth congeniality, camaraderie and moments of sharing wonderful stories. To you, my veneration.

I may have forgotten to mention the names of people who came across my path, to them, my sincerest thanks.

The defense of a thesis is not the end, but rather, the beginning. It signals the start of something new, the commencement of a new era in our life. We are the next in line.

I will always reminisce and cherish the time I spent with all of you. Those unfading and precious memories will ever shine in my heart forever.

Table of Contents

DEDICATION

ACKNOWLEDGEMENT

LIST OF ABBREVIATIONS

SUMMARY

INTRODUCTION **15**

I. The protein Synthesis Process 16

I.I Cap-dependent translation initiation 16

I.II Alternative Translation Initiation Mechanisms 18

II. The Foot-and-mouth Disease Virus viral genome 19

III. Picornavirus IRES RNA-protein interactions 23

IV. The FMDV IRES is a self-acting RNA element 20

V. IRES structure 26

VI. Antisense oligoribonucleotides and inhibition of gene expression 27

VII. ASO based antiviral agents 29

OBJECTIVES **31**

MATERIALS AND METHODS **33**

I. Constructs 34

I.I In-vitro transcription 35

II. 2 O´-methyl Oligoribonucleotides 36

III. Pre-annealing of antisense oligoribonucleotides with the IRES and In-vitro translation 36

IV. Cells lines 39

IV.I Transfection of RNA annealed with ASO 39

IV.2 PFU inhibition assay 40

V. Western blot analysis 40

VI. Electrophoretic Mobility Shift Assay 41

RESULTS **42**

I. Interference of IRES-dependent translation in-vitro 43

I.I Modification of bicistronic RNA translation efficiency by ASO 43

I.II IRES-dependent translation efficiency is affected by ASO targeting domain 1-2 45

I.III Apical and proximal region of the central domain are differentially susceptible to ASO interference 46

I.IV ASO complementary to domains 4 and 5 effectively down-regulated

translation of bicistronic RNA 49
I.V Control of FMDV gene expression in-vitro 50
I.V.I AUG1 is the most potent inhibitory ASO in-vitro 50
I.VI Differential response of domain 2, 3, and 4 to ASOs 52
I.VII The domain 5 region is susceptible to inhibition by ASO 53
II. Control of FMDV genome gene expression in cultured cells 50
II.I ASO targeting AUG1 and AUG2 are inhibitory in tissue culture cells 54
II.II Interference of ASO complementary to domain 1-2 on translational efficiency in-vivo 56
II.III Effects of ASO targeted to domain 3 differs in-vivo and in-vitro 57
II.IV Domain 4-5 behave differently in the presence of the ASO in-vivo 59
II.V Inhibition of viral translation at an extended time 59
III. Accessibility of IRES to ASO 61
III.I Differential accessibility of the FMDV AUG region 62
III.II IRES domains 1-2 and 4-5 exhibit differences in accessibility 63
III. III IRES central domain accessibility 64
III.III Accessibility of domain 3 suggests flexibility relative to the entire IRES 66
III.IV The integrity of the GNRA and RAAA motifs play an important role in IRES accessibility 67
DISCUSSION **71**
I. IRES as a tool in controlling gene expression 72
II. Differential responses of the two AUGs to ASOs depend on its secondary structure 73
III. IRES accessibility and its correlation to inhibition of protein synthesis 75
III.I Potent inhibitory ASOs and accessibility to its target sequence 75
III.II Relationship between accessibility and inhibition in the IRES conserved motifs 80
III.III The 5´side of the GNRA and RAAA stem loop are candidate targets to inhibition of ASOs 83
IV. The apical region of the IRES central domain adopts a flexible structure 83
V. Concluding remarks 85
CONCLUSIONS **87**
REFERENCES **89**

List of Abbreviations

ATP	Adenosine Triphosphate
ASO	Antisense Oligoribonucleotide
BSA	Bovine Serum Albumin
CAT	Chloramphenicol Acetyl Transferase
cDNA	complementary DNA
Ci	Curie
cpm	Counts per minute
cre	Cis-acting replication element
DMEM	Dulbecco´s Modified Eagle Medium
DMS	Dimethyl Sulfate
dNTP	Deoxynucleotide triphosphate
DTT	Dithiothreitol
eIF	Eukaryotic Translation Initiation Factor
EMCV	Encephalomyocarditis Virus
eRF	Eukaryotic Translation Release Factor
FCS	Fetal Calf Serum/Fetal Bovine Serum
FMDV	Foot-and-mouth Disease Virus
GNRA	Motif present in the FMDV IRES (N is any nucleotide and R is any purine)
GTP	Guanosine Triphosphate
GUAG	Mutation in the GNRA motif carrying a single nucleotide substitution ($G_{178}UAA_{181}$ to $G_{178}UAG_{181}$)
h	Hour
HAV	Hepatitis A Virus
HCV	Hepatitis-C Virus
HIV	Human Immunodeficiency Virus
hpi	Hours pos-infection
hpt	Hours post-transfection
HRV	Human Rhinovirus
IRES	Internal Ribosome Entry Site
ITAF	IRES trans-acting factor
kDa	Kilodalton
Lpro	L-protease of the Foot-and-mouth Disease Virus
Luc	Luciferase protein
Met-tRNAi	Methionyl initiation t-RNA
min	Minutes
mRNA	Messenger RNA
Mw	Molecular Weight Marker

NMIA	N-methylisatoic anhydride
nt/nts	Nucleotide/s
ORF	Open Reading Frame
PABP	Poly(A)-binding protein
PAGE	Polyacrilamide Gel Electrophoresis
PBS	Phosphate buffered Saline
PCBP	Poly (rC)-binding protein
PFU	Plaque Forming Units
Poly(A)	Poly-Adenine Tract
Poly(C)	Poly-Cytidine Tract
PTB	Polypyrimidine tract-binding protein
PV	Poliovirus
PVDF	Polyvinyledene flouride
RAAA	Motif present in the FMDV IRES (R is any purine)
rpm	Revolution per minute
rNTPs	Ribonucleotide Triphosphate
RRL	Rabbit Reticulocyte Lysates
rRNA	Ribosomal RNA
RRM	RNA Recognition Motif
SARS	Severe Acute Respiratory Syndrome
Scr	Scrambled sequence
SD	Standard Deviation
SDS	Sodium Dodecyl Sulfate
SDS-PAGE	Sodium Dodecyl Sulfate- Polyacrilamide Gel Electrophoresis
SHAPE	Selective 2´Hydroxyl Acylation analyzed by Primer Extension
TBS	Tris-Buffer Saline
TMEV	Theiler´s Murine Encephalomyelitis Virus
tRNA	Transfer RNA
UTR	Untranslated Region
WB	Western Blot
Wt	Wildtype

SUMMARY

PICORNAVIRUS IRES:

ACCESSIBILITY AND INHIBITION OF VIRAL GENE EXPRESSION

Picornavirus protein synthesis is controlled by the Internal Ribosome Entry Site (IRES), a cis-acting element that recruits the translation machinery without the need for m^7GpppN cap on the mRNA. In Foot-and-mouth disease Virus (FMDV) RNA, protein synthesis starts at two AUGs, AUG1 and AUG 2, as soon as the viral genome enters the cell cytoplasm. Factors necessary for protein synthesis recognize specific motifs in the IRES element, which is organized in domains 1-5. RNA probing and Selective 2´Hydroxyl Acylation analyzed by Primer Extension (SHAPE) reactivity showed that the central domain is a self-folding region that contains the conserved GNRA and RAAA motifs organized in loops. Differences in the RNA organization of the IRES have been observed by *in vivo* footprint assays relative to the RNA probing observed *in vitro*, indicating conformational changes in the RNA structure that may be important for IRES activity.

We have used *in vitro* and *in vivo* translation assays to explore the accessibility of the FMDV IRES structure to 32 overlapping sequences of 2´O-methyl antisense oligoribonucleotides (ASO) to analyze the capacity of ASOs to interfere viral gene expression. *In vitro* transcribed RNAs of the form CAT-IRES-Luciferase or the FMDV RNA genome were annealed with ASO complementary to different IRES regions. ASOs complementary to luciferase AUG, FMDV RNA AUG1 and AUG2 regions and a scrambled sequence were used for control purposes.

The luciferase AUG ASO was inhibitory. However, FMDV RNA AUG1 and AUG2 present different results. AUG2 was more inhibitory *in vivo* than *in vitro*, while the AUG1 was inhibitory at both conditions.

Results from *in vitro* translation showed that the bicistronic RNA regions sensitive to ASO inhibition are distributed all along the IRES while in FMDV RNA context, regionsinhibited by ASOs were mostly located in the apical region of D3, D5 and AUG1. *In vivo*, each domain of the IRES possesses a region potently inhibited by the ASO through reduction of virus yield. The D3 region of the IRES exhibit different results in *in vitro* and *in vivo*, particularly in the apical region where GNRA and RAAA motifs are located. This could be a result of RNA-RNA or RNA-protein interactions changes in the IRES in solution or inside the cell.

Correlating the accessibility of the IRES in RNA-ASO gel electrophoretic mobility shift assay showed that the more accessible regions in the IRES exhibited the highest inhibitions (with few exceptions). These results revealed the accessible regions of the IRES and demonstrated its property to be optimal targets to inhibit viral gene expression. This could pave the way for the development of new methods of combating this recurrent animal infection.

RESUMEN

PICORNAVIRUS IRES:

ACCESIBILIDAD e INHIBICIÓN DE LA EXPRESIÓN GÉNICA

La síntesis de proteínas de los picornavirus esta controlada por el sitio de entrada interna del ribosoma (IRES), un elemento del RNA que actua *en-cis*, reclutando la maquinaria de traducción sin necesidad de la estructura m^7GpppN en el ARNm. La síntesis de proteínas virales se inicia a partir de dos AUGs, AUG1 y AUG2, tan pronto como el genoma viral entra en el citoplasma de la célula. Los factores necesarios para traducción reconocen motivos específicos del IRES, que están distribuidos en dominios (1-5). Estudios de estructura del ARN y reactividad SHAPE (Selective 2´Hydroxyl Acylation analyzed by Primer Extension) mostraron que el dominio central es una región plegable autónoma que contiene los motivos conservados GNRA y RAAA, organizados en bucles. Diferencias en la organización del IRES se han observado por ensayos de footprints *in vivo* en relación con la estructura del ARN observado *in vitro*, lo que indica cambios conformacionales en la estructura del ARN que pueden ser importantes para la actividad IRES.

Hemos realizado el análisis de traducción *in vitro* e *in vivo* para explorar la accesibilidad de la estructura del IRES del virus de fiebre aftosa frente a 32 secuencias de oligorribonucleótidos antisentido 2´ O-metilo (ASO) con objeto de analizar su capacidad de interferir la expresión del genoma de FMDV. Transcritos obtenidos *in vitro* de RNAs bicistrónicos CAT-IRES-luciferasa o el genoma del FMDV se annillaron con ASO complementarios a las diferentes regiónes del IRES. Los ASOs complementarios al AUG de la luciferasa, a las regiones AUG1 y AUG2 del RNA viral y secuencias aleatorias fueron utilizados como controles.

El ASO AUG de la luciferasa fue inhibitorio. Sin embargo, los AUG1 y AUG2 del RNA FMDV presentaron resultados diferentes. AUG2 inhibió más *in vivo* que *in vitro*, mientras que el ASO AUG1 fue inhibitorio en ambas condiciones.

Los resultados de la traducción *in vitro* del RNA bicistrónico muestra que las regiones sensibles a inhibición se distribuyen en todo el IRES, mientras que ASO inhibidores en el ARN de FMDV se encuentra principalmente en la región apical de D3, D5 y AUG1. En el entorno celular, cada uno de los dominios del IRES posee una región fuertemente inhibida por ASO, medida a través de la reducción del la producción de virus. La región D3 del IRES muestran resultados diferentes *in vitro* e *in vivo*, sobre todo en la región apical donde se encuentran los motivos GNRA y RAAA. Estas diferencias podrían ser el resultado de cambios en las interacciones ARN-ARN o ARN-proteína dependiendo de que el IRES esté en solución o en el interior de la célula.

La correlación de la accesibilidad del IRES en ensayos de retardo en gel mostró que las regiones más accesibles en el IRES se corresponden con las mayores inhibiciones (con pocas excepciones). Estos resultados demostraron la accesibilidad del IRES y su capacidad de servir como dianas para inhibir la expresión de los genes

virales, y podría allanar el camino para el desarrollo de nuevos métodos de lucha contra esta infección animal recurrente.

INTRODUCTION

I. The Protein Synthesis Process

In prokaryotes and eukaryotes, ribosomes are recruited to mRNAs in a sequential, multistep process. Prokaryotes start translation by recruiting the 30S ribosome subunit to the initiation site of the mRNA by base pairing the Shine-Dalgarno (SD) sequence located upstream of the AUG codon to the complementary anti-SD sequence in the 16S rRNA (Sonenberg and Hinnebusch, 2009). However, in eukaryotes an optimal consensus sequence GCCA/GCCAUGG for the AUG start codon, which is called the Kozak sequence, is used to initiate translation (Kozak, 1987; Marintchev and Wagner, 2004). The purine in the position -3 and the G in the position +4 are the most important nucleotides (nts). In addition to proper mRNA initiation sequence, a large number of factors, termed translation initiation factors (eIFs) are required to recruit the ribosomal subunits and start the translation process.

I.I Cap-dependent translation initiation

Typically, eukaryotic mRNAs contain 5´ untranslated regions (UTR), about 100nt, characterized by possessing an m^7GpppN residue at the 5´end (termed cap). The 3´UTR however, are variable in length and polyadenylated. The process of translation initiation (Fig. 1) begins with the production of free 40S and 60S subunits separated from post-termination complexes (post-TCs) (Jackson et al., 2010). This complexes, which is comprised of the 80S ribosome still coupled to mRNA, P-site deacylated tRNA and the eukaryotic release factor 1 (eRF1), are dissociated into subunits. After the dissociation, the 40S subunit is still bound to mRNA and tRNA, and eIF1 helps in the release of the tRNA while eIF3j promotes the dissociation of mRNA. Hence, in the recycling of the 80S into 60S and 40S subunits, the factors eIF3, eIF1 and eIF1A are recruited to promote the dissociation while the eIF2-GTP-Met-tRNAi attaches to the 40S bound to eIF3, eIF1 and eIF1A, forming the 43S complex (Hinnebusch, 2006; Jackson et al., 2010; Pestova et al., 2001).

The ternary complex (TC), comprising eIF2, GTP and Met-tRNAi, binds to the free 40S subunit facilitated by eIF1, eIF1A, eIF5 and eIF3, producing the 43S pre-initiation complex (PIC). The eIF4F, a complex of eIF4G, eIF4E and eIF4A, binds to the cap structure of the mRNA through eIF4E and interacts with the 43S PIC assisted

by the poly (A)-binding protein (PABP) bound to the poly (A) tail and eIF3. The eIF4F accomplish the binding to PABP and eIF3 through eIF4G, which, aside from binding to eIF4E, has additional binding sites for the ATP-dependent RNA helicase eIF4A and for eIF3. The eIF4G C-terminal domain is in contact with eIF3 while its N-terminal is responsible for its interaction with eIF4E.

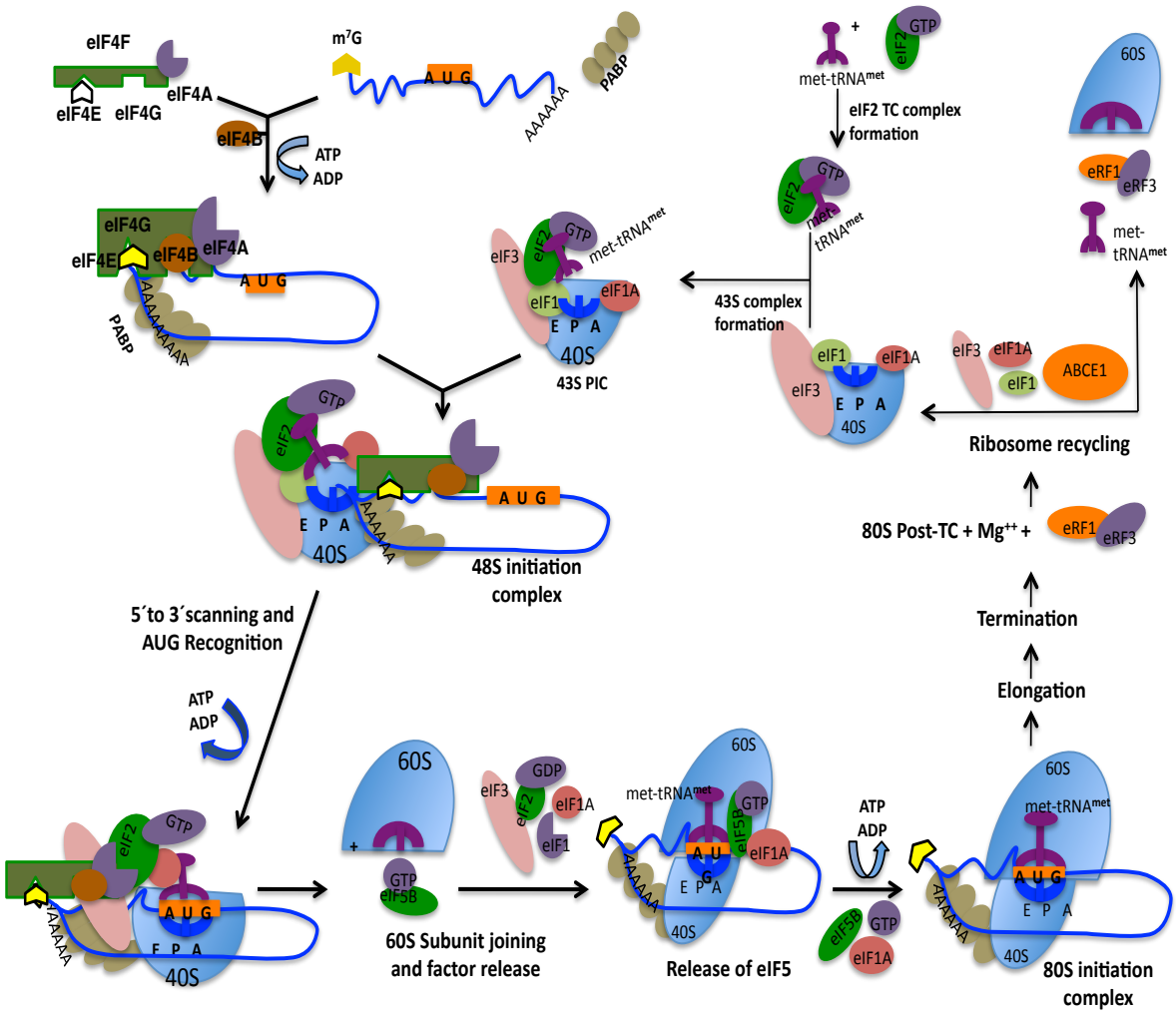

Figure 1. Model of eukaryotic translation initiation. The process of protein synthesis is discussed in the text (modified from Jackson, 2010).

The 43S PIC scans the mRNA until an AUG start codon is found; this process is stimulated by eIF1, eIF1A and eIF4G, and also requires eIF4A, its cofactor eIF4B and ATP hydrolysis when secondary structure occurs in the mRNA 5´UTR. Recognition of

AUG releases eIF1 from its location near the P-site, enabling the 48S PIC to assume a closed conformation incompatible with scanning and triggering Pi release. In the final step, which may occur simultaneously with eIF2-GDP dissociation, the 60S ribosomal subunit is joined to the 40S subunit containing the Met-tRNAi and mRNA to form the 80S initiation complex in a reaction stimulated by GTP-bound eIF5B. The eIF2-GDP must be recycled to eIF2-GTP for a new round of initiation, and this GDP-GTP exchange reaction is catalyzed by eIF2B (Hinnebusch, 2006).

The GTP bound to eIF2 in the scanning complex is hydrolyzed to GDP in an eIF5-dependent manner; however, release of Pi from eIF2 is prevented by eIF1 until an AUG start codon enters the ribosomal P-site and base-pairs with the anti-codon of Met-tRNAi. eIF2-GDP is then thought to dissociate, leaving the Met-tRNAi in the peptidyl (P) site of the 40S ribosomal subunit base paired with the AUG codon. The release of the Pi from the 43S and mRNA complex depends on the presence of an AUG codon. Translation usually starts with the 5'-most AUG codon until it encounters the stop codon at the 3´end of the open reading frame. After translating the ORF and encountering the stop codon termination starts by the attachment of eRF1 and eRF3 to the 80S and the process of post-TCs recycling begins.

I.II Alternative Translation Initiation Mechanisms

A subset of eukaryotic mRNAs can circumvent the scanning process by way of specialized sequences, termed Internal Ribosome Entry Site or IRES, originally discovered in the genome of picornaviruses (Pelletier and Sonenberg, 1988). Infection from these viruses modifies the cellular translation machinery inhibiting cap-dependent translation (Fig. 2). In the case of the foot-and-mouth disease virus (FMDV), the L protease cleaves eIF4G early in infection, leading to the shut-off of cap-dependent protein synthesis (Devaney et al., 1988). The carboxy-terminal end of eIF4G, a cleavage product of the L protease, binds eIF3 and eIF4A and is necessary for full activity of picornavirus IRES (Lopez de Quinto and Martinez-Salas, 2000) (Fig. 2). IRES elements have also been found in cellular mRNAs translated during conditions of cap-dependent inhibition (Baird et al., 2006). It is also a common feature of *Picornaviridae*, *Flaviviridae* (Pestivirus, hepatitis C virus [HCV]), *Retroviridae*

(Lentivirus) (Balvay et al., 2009; Buck et al., 2001) and *Dicistroviridae* RNAs (Kieft, 2009; Roberts and Groppelli, 2009).

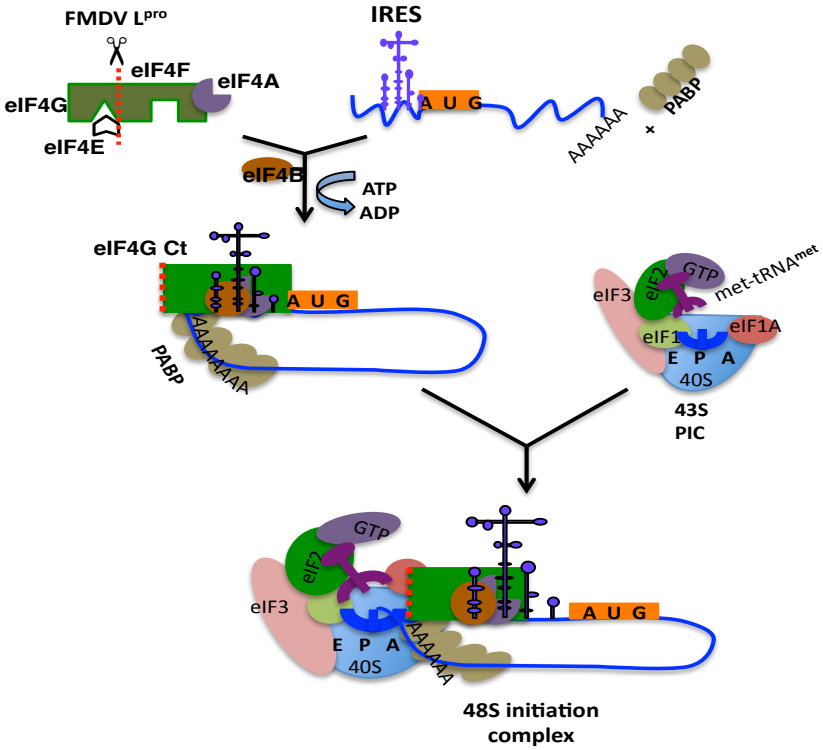

Figure 2. Model of FMDV translation initiation. The mRNA shows the location of the IRES; the broken line on eIF4G shows the FMDV L-protease cleavage.

II. The Foot-and-Mouth Disease Virus genome

The FMDV, the prototype of the aphthovirus genus of the *Picornaviridae* family, contains a positive sense single-stranded RNA genome of about 8500 nts (Fig. 3). Seven serotypes exists, A, O, C, Asia1, SAT1, SAT2, and SAT3 (Knowles and Samuel, 2003). Vaccination with one serotype does not confer immunity with other serotypes as cross-protection is not shared between serotypes. The viral genome consists of a 5'UTR, a single open reading frame (ORF) coding a polyprotein, and a poly(A) tail at its 3'UTR. The 5'UTR is about 1,300 nt, significantly longer than the 5'UTR of most cellular mRNA's which are typically 50-100 nt. In comparison with other picornavirus RNAs, the poliovirus (PV) and the encephalomyocarditis virus (EMCV) 5´UTR is 740 and 830 nt, respectively.

The FMDV 5'UTR comprises the S fragment, the poly(C) tract, a region folding

in several pseudoknots, the *cis*-replication element (*cre*) and the IRES, that recruits the translational machinery for initiation of protein synthesis in the viral RNA (Belsham and Martínez-Salas, 2004). The 3'UTR consists of two components, a region of about 100 nt of heterogenous sequence and the poly (A) tail. It has been shown that the 3'UTR can stimulate the IRES activity (Lopez de Quinto et al., 2002; Serrano et al., 2006) and participates in the viral RNA replication (Saiz et al., 2001).

Replication of the virus occurs in the cytoplasm of infected cells (Domingo et al., 2002). Upon entry into the cell, the viral ORF is translated into a polyprotein of about 2330 amino acids that are co- and post-translationally cleaved by virus-encoded proteases into several precursors. This cleavage finally generate 15 different mature structural and non-structural proteins, including 2 forms of the Leader (L) protein and 3 different copies of VPg (3B) (Fig. 3) (Carrillo et al., 2005; Grubman and Baxt, 2004). The FMDV genome does not contain the cap structure (m^7GpppN) typically present in cellular mRNAs at its 5' end. Instead, it contains a covalently-linked Viral Protein (VPg). Upon uridylylation to VPgpU (pU), each of the 3 copies of VPg can be used by the virus encoded 3D RNA polymerase as a primer for viral replication (Nayak et al., 2005).

Translation initiation of the polyprotein starts at two in-frame AUG codons separated by 84 nt and is directed by an IRES element that is located several hundred of nt downstream from the 5´ end of the RNA. Although both AUGs can be used as start codons for viral protein translation, the second one is preferentially utilized as starting site (Cao et al., 1995; Lopez de Quinto and Martinez-Salas, 1999). Initiation of protein synthesis at two AUGs produces two forms of the L protease with common COOH termini, Lab^{pro} and Lb^{pro} (about 200 and 170 amino acids, respectively). The L protease co-and post-translationally self-cleave from the rest of the polyprotein (Forss et al., 1984).

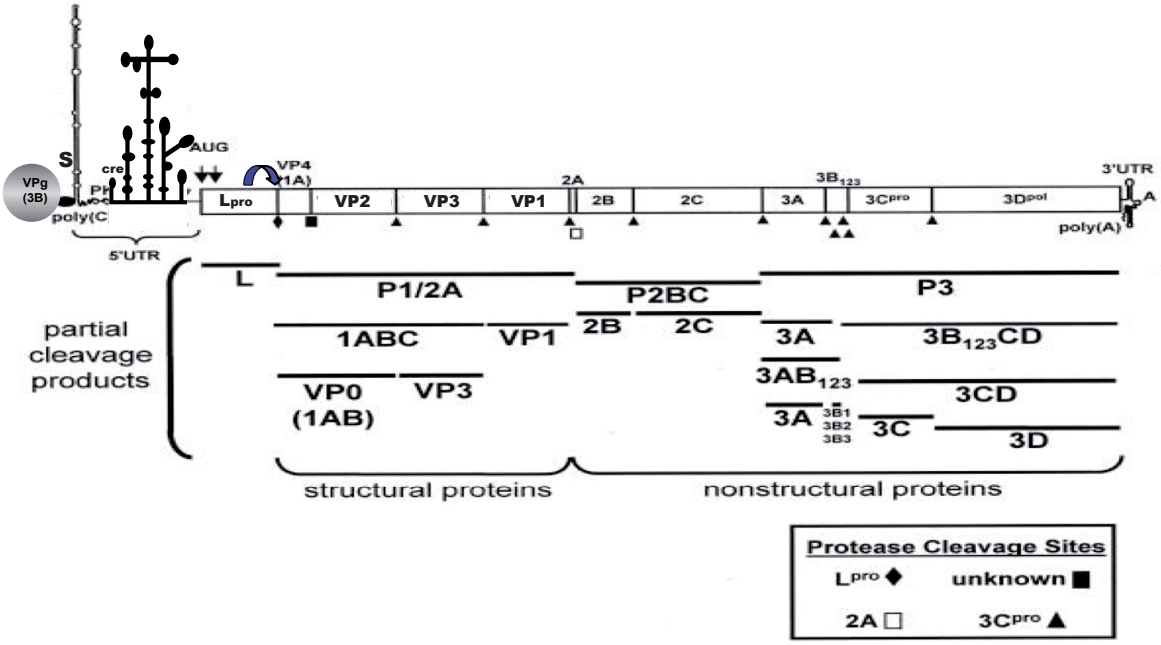

Figure 3. **Schematic map of the FMDV genome**. The diagram shows the location of VPg, the functional elements of the genome, S region, poly C, pseudoknot, cre, IRES, functional AUG, coding region and the 3´UTR. The open reading frame shows the structural and non-structural protein, and sites of the cleavage of the proteases. (Modified from Grubman, 2004).

III. Picornavirus IRES RNA-protein interactions

For many years, the only accepted view to initiate translation was the cap dependent mechanism. In 1988, this dogma was challenged by experiments performed by the groups of N. Sonenberg and E. Wimmer, that proved the existence of cap-independent initiation of translation in picornavirus RNAs mediated by IRES elements (Jang et al., 1988; Pelletier and Sonenberg, 1988).

Picornavirus IRESs are relatively long (~460 nt) *cis*-acting elements that recruit the 40S ribosomal subunits to the mRNA with the help of cellular *trans*-acting factors, independent of the presence of upstream AUG codons or stable RNA structures (Martinez-Salas et al., 2008). The IRES element is a regulatory region that is absolutely required for successful picornavirus infection (Pilipenko et al., 1992).

Different types of IRES exist in picornavirus mRNAs and the need for canonical eIFs depends on each type (Martinez-Salas et al., 2008). In Type I (poliovirus), and Type II (FMDV, EMCV) IRESs, eIF4GCt, eIF4A, eIF3, and eIF2 are needed to start

translation (Fig. 2 and 4). Type III IRESs (HAV) is the only picornavirus RNA that needs the help a complete eIF4G, while eIF3 and eIF2 are only needed by Type IV (HCV like) IRES elements (Belsham, 2009).

Host factors other than the canonical eIFs also play a role in modulating the activity of picornavirus IRESs for proper functioning. These IRES *trans*-acting factors (ITAFs) may act as RNA chaperone that stabilizes the IRES conformational structure prior or during the translation process for proper recognition by the translational machinery. Each picornavirus IRES, including those who share similar secondary structure, may require different set of RNA-binding proteins (Pilipenko et al., 2000).

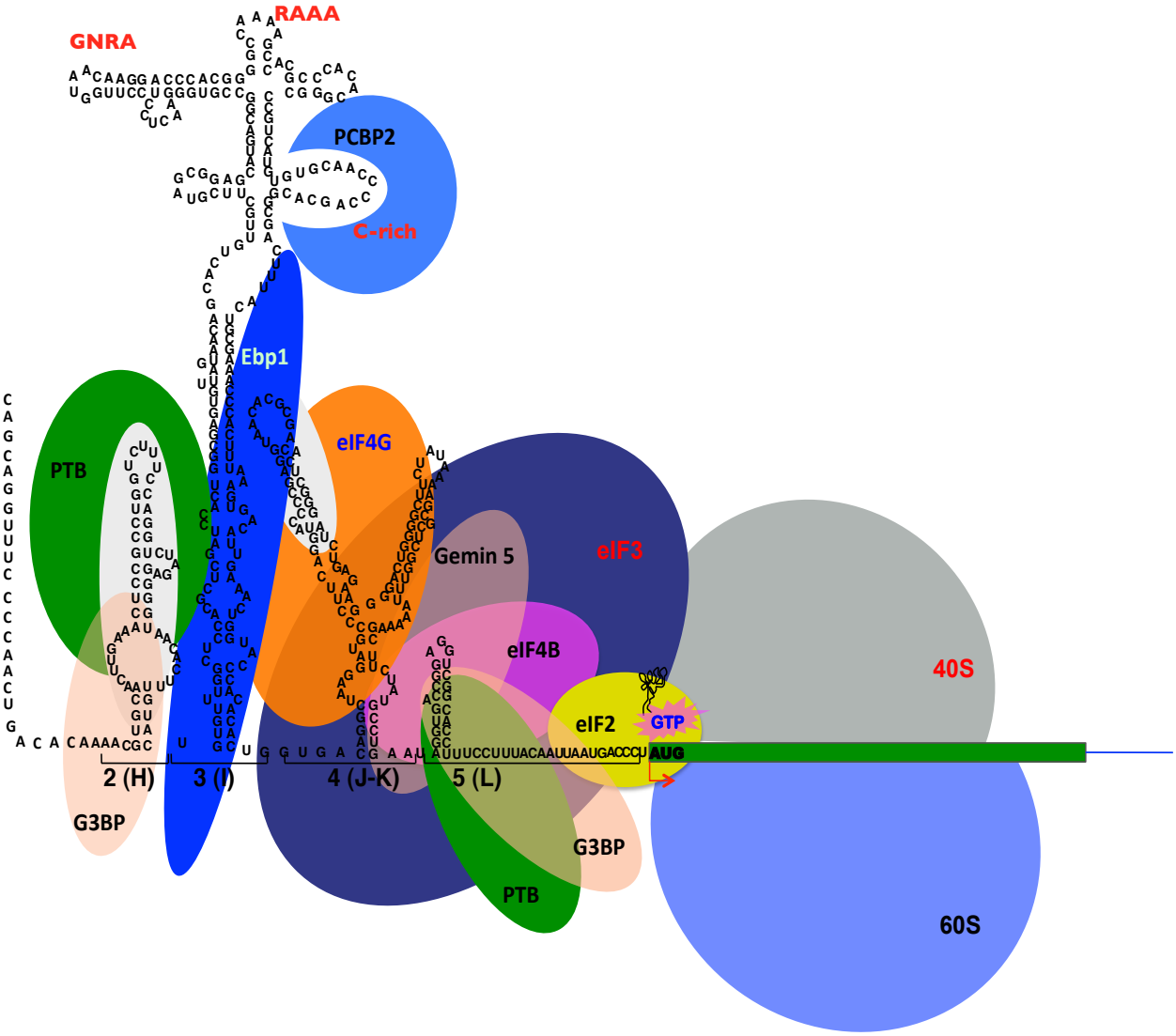

Figure 4. Binding sites of eIFs and ITAFs binding sites in the FMDV IRES. The IRES is arranged in domains 1-5 or H-L.

The polypyrimidine tract-binding protein (PTB) that binds to unpaired bases of pyrimidine-rich regions stimulates the function of FMDV, EMCV, TMEV, PV, HRV and HAV IRESs (Table 1) but not in HCV (Brocard et al., 2007). Other host proteins with IRES stimulatory function are poly (rC)-binding protein 2 (PCBP2) required for translation initiation and RNA replication of poliovirus (Blyn et al., 1997), the upstream of N-ras protein (unr) which binds to HRV IRES (Anderson et al., 2007) and is necessary for both HRV and PV translation (Boussadia et al., 2003); the La autoantigen and SRP20 are essential for PV translation (Costa-Mattioli et al., 2004; Semler and Waterman, 2008). The requisite for erbB-3-binding protein (Ebp1/ITAF45) was also reported in FMDV translation (Andreev et al., 2007; Pilipenko et al., 2000; Yu et al.) but not EMCV (Monie et al., 2007). Other ITAFs identified by proteomics (Pacheco et al., 2008) may function as downregulators of translation (Gemin5 and DRBP76:NF45) (Martinez-Salas and Ryan, 2010; Pacheco et al., 2009) (Table 1).

Table 1. *Trans*-acting factors interacting with picornavirus and HCV IRES.

Protein	IRESs	RNA-binding motif	Effect
PTB	FMDV, EMCV, TMEV, PV, HRV, HAV, HCV*	RRM	Stimulation
PCBP2	PV, HRV, HAV, CBV, FMDV*, EMCV*, HCV	KH	Stimulation
Unr	PV, HRV	CSD	Stimulation
Ebp1/ITAF45	FMDV, EMCV*	Lys-rich	Stimulation
DRBP76:NF45	HRV	dsRBD	Repression
La	PV, EMCV, HAV, HCV	RRM, SBM	Stimulation
Gemin5	FMDV	WD, coiled-coil	Downregulation
SRp20	PV	RRM, RS	Stimulation

* IRES where no effect was observed with the protein

IV. The FMDV IRES is a self-acting RNA element

The FMDV IRES, encompasses 462 nts distributed in five domains (Fig. 5). Domains 1 and 2 consist of 84 nt, with the first 21 nt recognized as the continuation of the *cre* element (Mason et al., 2002). Sequences in domain 2 include a polypyrimidine tract (UCUUU) that is a binding site of PTB (Luz and Beck, 1991).

The Domain 3, consisting of 210 nts, the most apical region of which is arranged

as a cruciform structure (Fig. 5), plays a crucial role in RNA-RNA interactions (Ramos and Martinez-Salas, 1999). The proximal part is organized as a base-paired structure interrupted with bulges that includes several non-canonical base pairs and a helical structure essential on IRES activity (Martinez-Salas et al., 1996).

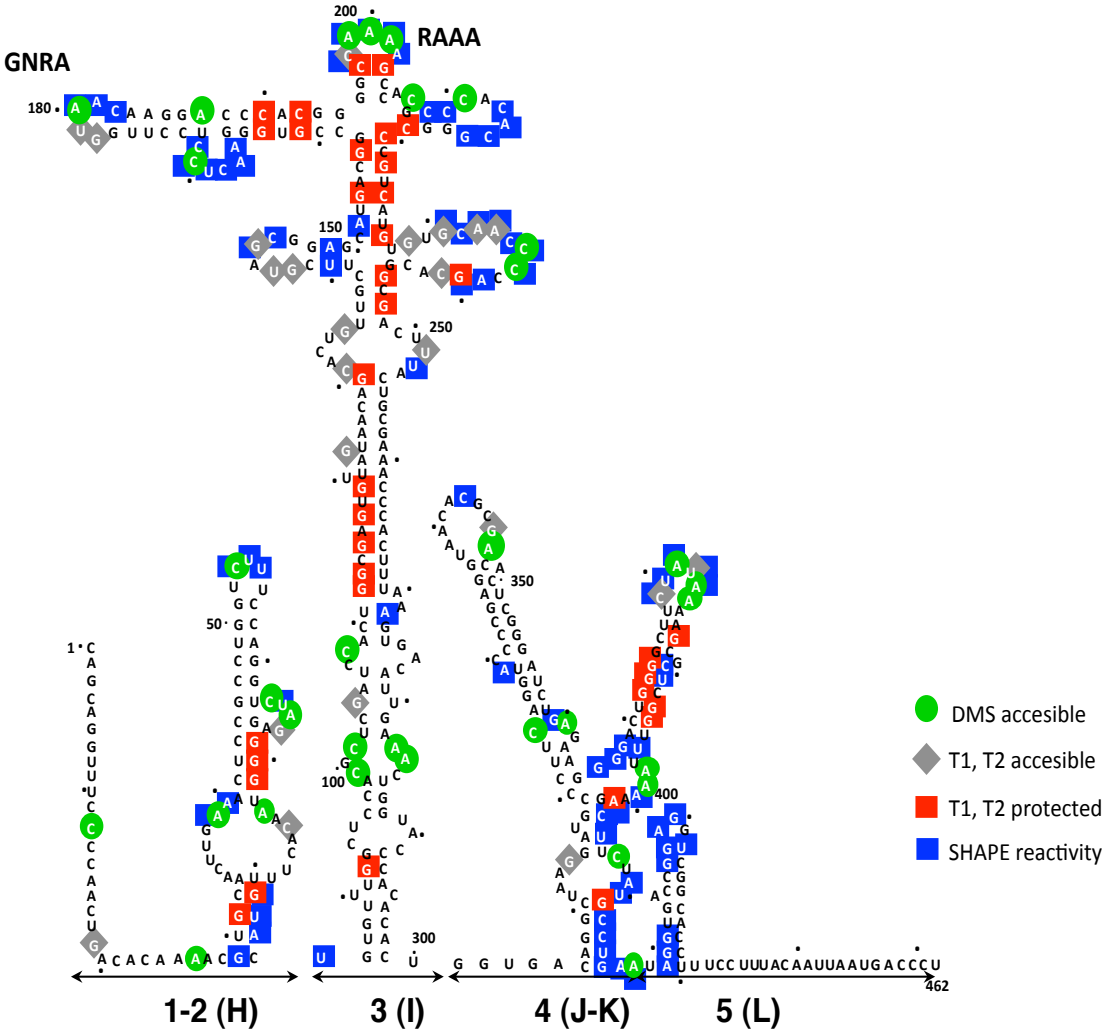

Figure 5. Secondary structure of the FMDV IRES. Arranged in domains 1-5 (H-L), the RNA structure shows accessible and protected nt by RNA probing (DMS), T1, T2 RNase and SHAPE reactivity. The domain 3 shows the conserved motifs GNRA and RAAA. Every ten nts are marked with a dot.

Domain 4 has two hairpin loops, with two A-rich internal bulges (Fig. 5) conserved in all field isolates of FMDV as well as EMCV. This domain is responsible for the interaction with eIF4G (Fig. 4) (Kolupaeva et al., 1998; Lopez de Quinto and Martinez-Salas, 2000), an essential step in the IRES-dependent translation initiation.

Domain 5 is composed of a conserved hairpin-loop with a pyrimidine-rich tract preceding the first functional AUG codon (Fig. 4). Specific motifs spread in domains 2, 4 and 5 are responsible for the interaction with cellular proteins PTB, eIF4G, eIF3 and eIF4B (Lopez de Quinto et al., 2001) (Fig. 4).

Organization in stable stem-loop is a typical attribute of IRES elements (Fernandez-Miragall et al., 2009; Martinez-Salas, 2008). The FMDV IRES RNA structure is phylogenetically conserved. RNA structural studies show that the FMDV, EMCV and PV IRESs GNRA motif adopt a tetraloop conformation at the tip of a stem-loop (Du et al., 2004; Fernandez-Miragall and Martinez-Salas, 2003; Phelan et al., 2004). The central domain, termed D3, contains the conserved GNRA, RAAA and C-Rich motifs (Fig. 5). The purine-rich GNRA and RAAA motifs are important in FMDV IRES activity (Fernandez-Miragall and Martinez-Salas, 2003) and do not tolerate nt substitution, deletions or insertions (Lopez de Quinto and Martinez-Salas, 1997). Maintenance of the GNRA conserved motif was also reported to be important for EMCV IRES activity (Robertson et al., 1999).

Picornavirus IRES activity depends on the coordination of RNA structure and RNA-protein interactions. It was proposed that Domain 3 plays an important role in the proper functioning of the FMDV IRES translation but its specific role is yet to be discovered. Only a few interactions are found between D3 and host proteins in comparison to domain 5 (Pacheco et al., 2008). Hence, it is proposed that this domain may play an important role in the organization and functional conformation of the FMDV IRES (Martinez-Salas et al., 2008). The organization of the RAAA stem-loop was dependent on the local RNA structure determined by GNRA-dependent interactions (Fernandez-Miragall et al., 2006). It is thought that these conserved motifs may facilitate RNA–RNA or RNA–protein interactions required to maintain the tertiary structure needed for proper recognition of the IRES element by the translational machinery. In agreement with this hypothesis, strand specific long-range RNA-RNA interactions have been shown to occur between the central region of the FMDV IRES (Ramos and Martinez-Salas, 1999).

Under appropriate conditions, structured RNA molecules undergo a transition to a three-dimensional fold in which the helices and the unpaired regions are precisely organized in space (Westhof E, 2000).

To date, no high-resolution structures or cryo-EM reconstructions of picornavirus IRES is available. Distantly related IRES elements do not share primary sequence and they appear to be organized in distinct RNA structures (Filbin and Kieft, 2009; Martinez-Salas et al., 2008). Comparison of the biophysical characteristics of the IRES present in the dicistrovirus intergenic region, and FMDV IRES RNAs shows that the amount of inherent folded structure in the unbound IRES RNA is inversely correlated with the need for ITAFs and eIFs.

V. IRES structure

RNA probing of the FMDV IRES showed significant differences in the accessibility *in vitro* and *in vivo* of domain 3 to dimethyl sulfate (DMS), a reagent that reacts with unpaired bases in the RNA structure and is used to measure accessibility to C and A bases (Fernandez-Miragall and Martinez-Salas, 2007). The region spanning the apical region of domain 3 was accessible to DMS modification *in vivo* and *in vitro* but six nts were accessible only *in vivo*. The differences in the accessibility of the IRES to DMS suggest that the central region of the IRES adopts a different conformation *in-vivo* or *in vitro*. A decreased attack of residues *in vivo* suggests a potential interaction with cellular proteins.

Similarly, results of UV-cross linking with AMT-psoralen showed a local reorganization of RNA structure (Fernandez-Miragall and Martinez-Salas, 2007). Further structural analysis explored the reactivity of the IRES to a novel method called Selective 2´Hydroxyl Acylation analyzed by Primer Extension (SHAPE) through modification of the susceptible 2´-OH ribose using N-methylisatoic anhydride (NMIA). This technique shows the flexible nts in the RNA (Wilkinson et al., 2006). RNA SHAPE reactivity using the wild type IRES and domain 3 transcripts suggests that the GNRA tetraloop could be involved in tertiary interactions within the IRES D3 (Fernandez et al., 2011). D2 and D4 were highly reactive to NMIA indicating the presence of flexible regions with hairpin loops and relatively large internal bulges, clustered in motifs (Fig. 5).

IRES accessibility was also looked at through pairing of the fluorescent-labeled transcript D3 or the entire IRES with complementary DNA oligoribonucleotides

printed on the microarray (Fernandez et al., 2011). Results from this experiment showed similarities between the accessibility of the D3 region uncovered by microarray and SHAPE reactivity. Taken as a whole, the accessible D3 regions in the microarray were also reactive to SHAPE probing, except for some nts in the apical region. Key differences in the SHAPE reactivity and accessibility by the microarray showed that SHAPE reactive nts 181-183 and 209-216 were not accessible to their complementary DNA oligoribonucleotides (Fernandez et al., 2011).

SHAPE and RNA accessibility comparison in the mutant GUAG supported the idea of a change in RNA conformation affecting distant regions in the secondary structure of the FMDV IRES, a result which is consistent with the fact that GNRA tetraloops are often involved in RNA folding (Correll and Swinger, 2003). SHAPE reactivity also provides information that domain 3 is a self-folding RNA module and suggest that GNRA motif is most likely the main player in the tertiary interactions, probably involving mechanisms other than complementary base pairing.

VI. Antisense oligoribonucleotides and inhibition of gene expression

Antisense Oligonucleotide (ASO) are single stranded (~20 nts) sequences (usually synthetic ribonucleotide or deoxyribonucletide) complementary to the target mRNA that forms a hybrid via Watson-Crick base pairing. The resulting hybrid can block gene expression by various mechanisms, depending on the chemical make-up of the oligonucleotide (Fig. 6A) and location of the hybridization. The strength and stability of interactions between the ASO and mRNA depends on factors such as thermodynamic stability, the secondary structure of the target mRNA, and the proximity of the hybridization site to functional motifs on the designated transcript such as translational start site (Chan et al., 2006).

A.

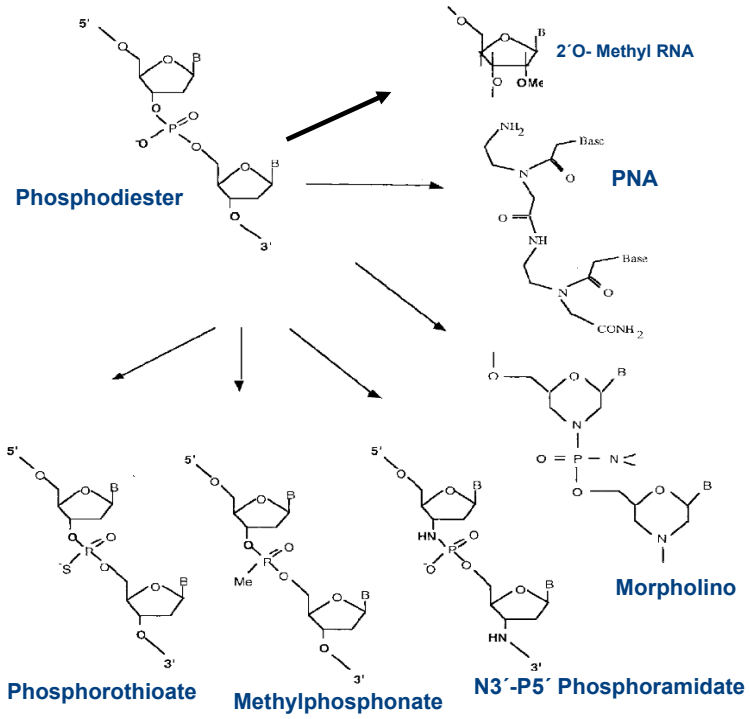

B.

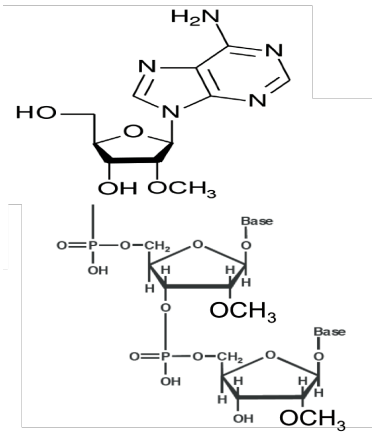

Figure 6. Antisense Oligoribonucleotides A. Examples of chemical modifications of oligonucleotides. **B**. Diagram showing the arrangement of a 2´O-Methyl oligoribonucleotides. The 2'-OH residue of the ribose molecule is replaced by an O-alkyl group (methyl).

Unmodified oligonucleotides are unstable *in vivo* due to rapid nuclease degradation (Helene and Toulme, 1990). To increase stability, several modifications have been carried out. One of the second-generation ASO carries 2´-O-sugar modifications (Fig. 6B), which increases the stability of duplexes with complementary

RNA. The addition of a methoxy group to the C2' position of the sugar provides enhancement of nuclease resistance and increases the affinity of an oligomer for mRNA (Yoo et al., 2004) (Fig. 6B). The 2´O-methyl oligoribonucleotides (2´O-methyl RNA) which replaces the 2'-OH residue of the ribose molecule by an O-alkyl group (methyl) shows the same behavior as DNA. It is resistant to degradation by cellular nucleases, stable to hydrolysis by strongly alkaline solutions, and hybridize specifically to the target mRNA with higher affinity than phosphodiester or phosphorothioate. These oligoribonucleotides form high melting heteroduplexes with targeted mRNA, more stable than RNA:RNA or RNA:DNA duplex, and induce antisense effect by a non-RNaseH-dependent mechanism (Dias and Stein, 2002).

Inhibition of gene expression may occur by at least two mechanisms. First, through steric or physical blocking of mRNA which prevents or inhibits the progression of splicing, the physical block to binding of the initiation complex, scanning of the 5' leader by the 40S subunit or the assembly of a functional 80S complex at the AUG initiation codon, or elongation steps of translation. Second, through RNase H-dependent event, which degrades its target by cleaving the RNA-DNA duplex region of the mRNA preventing translation. RNase H is a ubiquitous enzyme that hydrolyzes the RNA strand of an RNA/DNA duplex. RNase H-dependent ASO can inhibit expression when targeted to any region of the mRNA while 2´O-methyl is efficient when targeted to the 5´UTR or AUG initiation codon region (Cotten et al., 1991).

VII. ASO based antiviral agents

Several studies have been done employing antisense RNA as antiviral or therapeutic agents by inhibiting translation, either by steric blocking of the translational machinery or activation of the RNase H to induce RNA cleavage (Haasnoot et al., 2007). Antisense RNA as a strategy for antiviral control has also been demonstrated to specifically suppress RNA viruses in cell cultures either by inhibiting viral translation or replication. Studies have been done to investigate the use of antisense RNA transcript to inhibit FMDV viral gene expression directed against each of the two functional FMDV AUG (Gutierrez et al., 1993), 3´UTR (Gutierrez et al.,

1994) and to both, the 5´and 3´UTR (Bigeriego et al., 1999; Rosas et al., 2003). On the other hand, antisense RNA with morpholino modifications (Fig. 6A) inhibit viral gene expression of FMDV with high efficacy and specificity (Vagnozzi et al., 2007).

Researchers have developed similar approaches to use antisense RNA or its modifications as antiviral agents such as the use antisense RNA to inhibit HCV viral translation (Gonzalez-Carmona et al., 2010; Wakita et al., 1999); phosphorothioate-based antisense RNA for cytomegalovirus (Vitravene, 2002); morpholino-modified RNA for West Nile virus (Deas et al., 2005), Ebola virus (Enterlein et al., 2006) (Warfield et al., 2006), influenza A (Ge et al., 2006), dengue virus (Kinney et al., 2005), severe acute respiratory syndrome coronavirus (Neuman et al., 2005), equine arteritis virus (van den Born et al., 2005) and HIV virus (Gu et al., 2006); locked nucleic acid-based antisense RNA for HCV (Laxton et al., 2011), among others.

Other approaches to use RNA and non-RNA based antiviral were also undertaken. For instance, the use of small interfering RNA (siRNA) to induce RNAi mediated cleavage of the mRNA was used to inhibit FMDV (Chen et al., 2004; Cong et al., 2010; Kahana et al., 2004; Lv et al., 2009; Pengyan et al., 2008), EMCV (Jia et al., 2008) and PV (Gitlin et al., 2002). Ribozyme, on the other hand, is used to enhance RNA cleavage, ligation reactions and peptide bond formation. The ribozyme-based antiviral was developed in gene therapy settings (Haasnoot et al., 2007) as anti HIV (Li et al., 2003; Macpherson et al., 2005).

The results provided by the studies done to inhibit several pathogenic viruses showed the potential use of antisense RNA based therapeutic agents to answer the growing problem of viral infection control. In addition, although differences exists in chemical properties and modifications of antisense oligonucleotides as antiviral agent, their common aim is to point to one target, that is, the successful inhibition of replication of human and animal pathogenic viruses.

OBJECTIVES

- To interfere IRES function by blocking susceptible sequences of the FMDV IRES critical for gene expression, leading to altered translation in bicistronic and FMDV RNAs and reduced viral replication of FMDV RNA.

- To reveal the accessible and protected motifs of the IRES by its hybridization with the 2´OH-modified antisense oligoribonucleotides in appropriate condition.

- To determine the correlation between IRES accessibility to ASOs and inhibition of gene expression in bicistronic RNA and FMDV RNA context.

MATERIALS AND METHODS

I. Constructs

The plasmid pBIC AvrII-NotI (Lopez de Quinto et al., 2002) expresses the IRES of FMDV C-S8c1 inserted between the chloramphenicol acetyltransferase (CAT) and firefly luciferase (Luc) genes, under the control of T7 promoter (Fig. 5). In this bicistronic RNA, translation of the CAT gene is cap-dependent while that of the firefly luciferase is IRES-dependent.

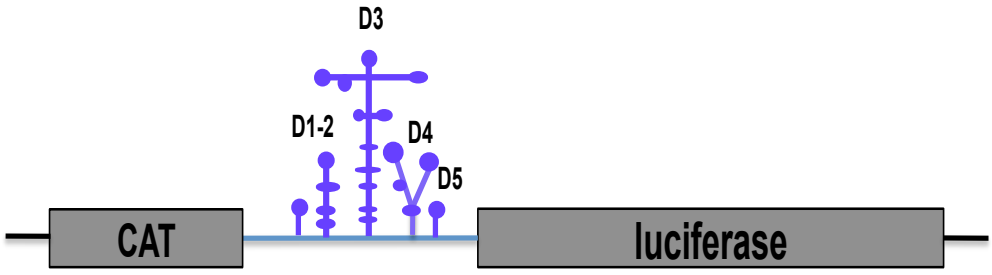

Figure 7. Schematic representation of the bicistronic RNA construct.

The plasmid pMT28, encoding a cDNA copy of FMDV C-S8c1 genome inserted into pGEM-1 under the control of the SP6 promoter was described previously (Garcia-Arriaza et al., 2004). Transcription of the cDNA clone of pMT28 with SP6 RNA polymerase yields an RNA of 8115 nts.

Based on its secondary structure, the IRES (nts 1-462) was subdivided into 5 domains, with nts 1-85 for domain 1-2 (H), nts 84-297 for domain 3 (I), and nts 306-462 comprising the domains 4 (J-K) and 5 (L) (Ramos and Martinez-Salas, 1999). The constructs for transcribing a monocistronic RNA of the FMDV IRES extended to the second initiator AUG was described in (Lopez de Quinto and Martinez-Salas, 1999). The construct expressing domain 3 was described in (Ramos and Martinez-Salas, 1999). The construct of IRES D3 carrying the mutation in the GNRA ($G_{178}UAA_{181}$ to $G_{178}UAG_{181}$) and RAAA ($A_{199}AAAG_{203}$ to $C_{199}GCCC_{203}$) motifs was detailed in (Lopez de Quinto and Martinez-Salas, 1997).

I.I *In vitro* transcription

The bicistronic RNA (Fig. 7) was synthesized *in vitro* by using pBIC AVRII-NotI linearized with Not1. About 800 ng of plasmid was linearized with 15U of NotI, for 2 hours at 37ºC. Following deproteinization with phenol-chloroform, the DNA was precipitated using 0.1 M NaCl and 2.5 volumes of absolute ethanol, washed with 70% ethyl alcohol, dried and resuspended in RNase free water. The purity of the linearized DNA was checked in a 1% agarose gel electrophoresis. *In vitro* transcription was carried out by adding T7 RNA polymerase buffer, 50 mM DTT, 2.5 mM rNTPs, 10U of RNase inhibitor and 5U of T7 RNA polymerase to 0.80 μg of DNA template and incubated for 1 hour and 30 min at 37ºC. After transcription, 1U of DNase RQ1 was added and incubated for 30 min at 37ºC to digest the template DNA. Example of pBIC RNA construct transcribed *in vitro* is shown in Fig. 8.

To synthesize RNA of plasmid pMT28, linearization was carried out with 10U of Nde1. The linearized pMT28 was transcribed with SP6 RNA polymerase buffer, 50 mM DTT, 2.5 mM rNTPs, 10 U of RNase inhibitor and 5U of SP6 RNA polymerase. Shown in Fig. 8 is an example of the pMT28 RNA transcribed *in vitro*.

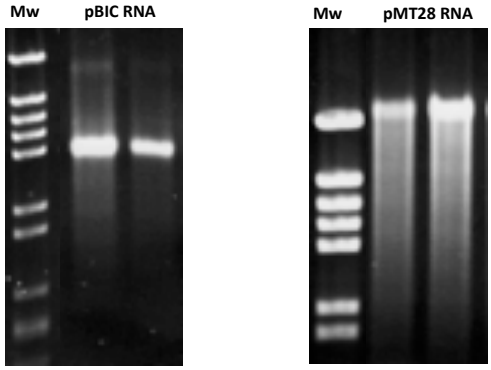

Figure 8. pBIC and pMT28 RNAs synthesized *in vitro*. Representative example of an ethidium bromide stained agarose gel showing the *in vitro* transcribed RNA of pBIC (bicistronic CAT-IRES-luc) and pMT28 (FMDV RNA).

The FMDV IRES construct extended to the second AUG was linearized with 16U of Bbu1 (Andreev et al., 2007). Plasmids encoding central domain (D3wt), D3 $GUAG_{181}$ and D3 $C_{199}GCCC_{203}$ were linearized with 10U of Sma1, deproteinized and purified. Transcriptions of the plasmid were done with 5U of T7 RNA polymerase in the presence of RNase inhibitor.

The integrity of the RNA transcript and the efficiency of the synthesis were checked in 1% agarose gel electrophoresis, visualized by ethidium bromide staining. The newly synthesized RNA was stored at -70ºC.

II. 2´O-methyl Oligoribonucleotides

Antisense oligoribonucleotides (ASO) sequences, ranging from 14 to 19 nt, with 2´O-methyl instead of the 2´OH of the ribose in the four flanking nucleotides are shown in Table 1. ASOs are numbered by the position of the nt at its 5´end.

Thirty-two antisense sequences were designed to hybridize with the IRES RNA, including the luciferase AUG, or AUG1 and AUG2 of FMDV RNA (Table 1 and Fig. 9). A scrambled sequence of 16 nt, with 50% G/C content, was included as specificity control. The scrambled nucleotide sequence was checked with NCBI-BLAST software to prevent any possible match in the IRES or the host cellular RNAs.

Mfold program and oligo analyzer was used to predict the secondary structure of each antisense oligonucleotide to prevent self-dimerization, formation of stable hairpins, and to optimize its hybridization to the IRES avoiding perfect hairpin targets.

ASO were stored in concentration of 60 μM RNase free water at -70ºC.

III. Pre-annealing of antisense oligoribonucleotides with the IRES and *in vitro* translation

Optimization of the assay was done by annealing the AUG and Scr ASO (1, 10, 30 and 60 μM) to 250 ng of bicistronic RNA for 20 min at room temperature, 37ºC, 42ºC or 65ºC and, then, added in rabbit reticulocyte lysates (RRL) mixture to a final reaction volume of 10 μl. After determining the optimal condition for the translation of bicistronic RNA in the presence of the ASO, subsequent assays with the rest of the ASO were done with 25 ng of RNA, 60 μM ASO, annealed at 37ºC for 20 min.

Table 2. 2´O-methyl Antisense Oligonucleotides

Oligo name	nt length	IRES Target Region (nt)	Sequence	% GC	Tm ºC
40	15	D2 5´ stem 40-26	mUmUmCmAAGTTGCAmCmGmUmU	40	47
55	16	D2 5´hairpin 55-40	mAmAmGmACCAGGCGGmAmGmUmU	56	57
66	16	D2 3´hairpin 66-51	mCmUmAmGACCTGGAAmAmGmAmC	50	46
83	15	D2 3´stem 83-68	mUmAmCmAAAGUGUUmAmCmCmC	40	47
104	19	D3 5´ base 104-85	mCmGmAmGCGTGGAGCCAAAmCmAmCmA	60	60
118	14	D3 5´stem 118-105	mAmCmUmCGCCAGTmGmGmAmU	57	59
135	18	D3 5´stem 135-118	mAmCmAmGTGCTGTTACTmAmAmCmA	39	55
154	18	D3 5´ bulge 154-138	mUmCmAmUGCTCCGCTACmGmAmAmG	56	58
164	14	D3 5´ stem 164-150	mCmCmAmCGGCCGTmCmAmUmG	71	54
176	14	D3 5´ bulge 176-163	mAmAmGmGAGGAGTmUmCmCmC	57	56
183	17	D3 5´ GNRA 183-167	mUmGmUmUACCAAGGAGmGmAmGmU	47	46
192	15	D3 3´ GNRA 192-178	mGmUmGmGGTCCTTGmUmUmAmC	54	46
207	17	D3 5´RAAA 207-191	mGmUmGmGCTTTTGGCCmCmCmGmU	65	64
213	15	D3 3´ RAAA 213-199	mGmUmGmGGCGTGGCmUmUmUmU	60	53.4
226	17	D3 loop 226-210	mAmUmGACGGGCCCGTmGmUmGmG	71	58
247	16	D3 C-rich 247-233	mUmCmGmCCGTGCTGGmGmGmUmU	69	61
265	17	D3 3´stem 265-249	mUmGmGmGTTTCGCAGTmAmAmAmG	47	56
282	18	D3 3´stem 282-265	mUmCmAmATGTCACTTTAmAmAmGmU	27	45
300	17	D3 3´ base 300-284	mAmGmUmGTGTGGGTACmCmAmGmU	53	62
317	17	D4 5´ base 317-301	mAmUmCmCTTAGCCTGTmCmAmCmC	53	62
331	16	D4 5´J domain 331-317	mGmGmGmUACCTGAAGmGmGmCmA	63	60
349	18	D4 J domain 349-334	mAmGmUmGTCGCGTGTTAmCmCmUmC	56	61
360	18	D4 3´ J domain 361-344	mUmCmAmGATCCCGAGTGmUmCmGmC	61	63
384	18	D4 K domain 384-367	mUmUmAmUAGAAGCCCCAmGmUmCmC	50	56
397	18	D4 K domain 397-378	mAmAmCmCGAGCGCTTTTmAmUmAmG	44	53
407	16	D4 K domain 407-392	mGmAmAmGCTTTTTAAmAmCmCmG	38	44
419	17	D 4 5´stem n419-404	mUmAmUmUCAGGCATAGmAmAmGmC	41	49
432	17	D5 hairpin 432-415	mCmCmUmCCGGTCACCTmAmUmUmC	59	59
452	19	D5 Single Stranded 452-433	mUmUmGmUAAAGGAAAGGUmGmCmCmG	47	48
AUG	18	luciferase AUG	mCmUmUmCCATTTTACCAmAmCmAmG	39	49
AUG1	19	FMDV AUG1	mCmAmGmTTGTATTCATAGmGmGmTmC	42	52
AUG2	18	FMDV AUG2	mGmAmAmUTCCATTTTTCmCmUmGmC	39	52
SCR	16	Random sequence	mUmGmCmAGCTGACAGmUmGmUmA	50	57

Nucleotides with 2-O´methyl modifications are designated with a letter ¨m¨. GC, percentage of guanine and cytosine pairs. Tm, melting temperature.

The same pre-annealing conditions were used for the translation of the viral polyprotein in RRL using pMT28 RNA.

In vitro translation was done by adding the RNA annealed with ASO to a reaction mix containing 6.5 μl of nuclease-treated rabbit reticulocyte lysates (RRL) (Promega), 1 μl (1 mM) amino acid mix minus methionine and 0.5 μl (6 μCi) ^{35}S-methionine in a final volume of 10 μl.

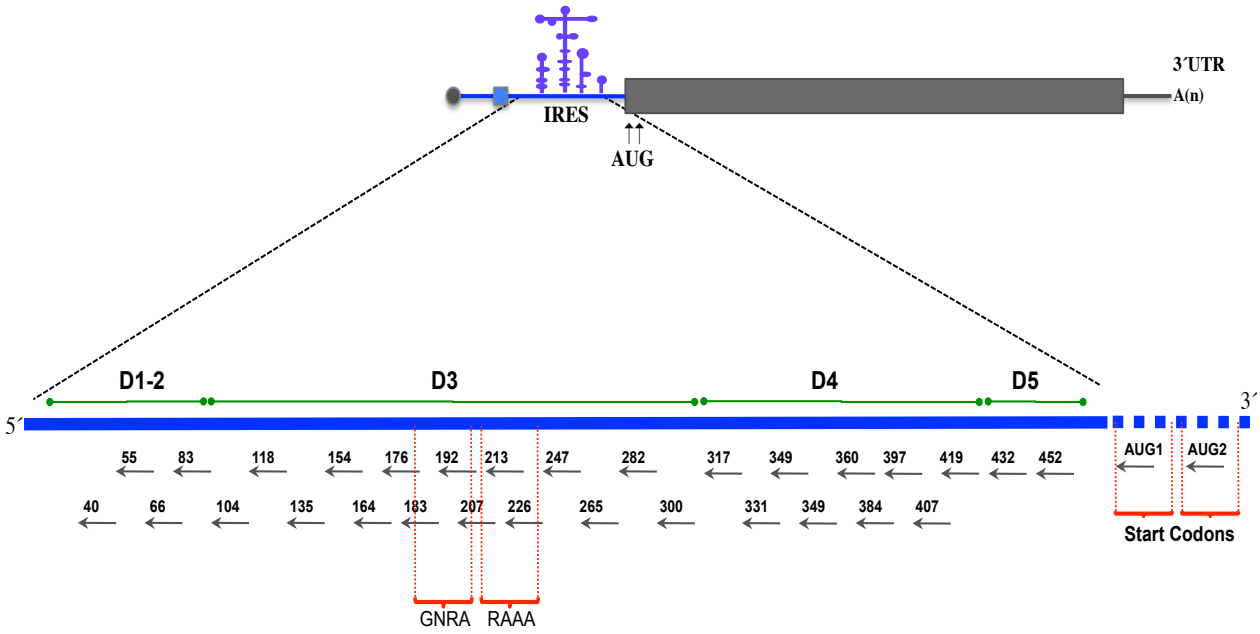

Figure 9. Target region of the ASOs. The FMDV genome is represented showing the location of IRES. The solid blue line symbolizes the IRES element. Green line shows the division of the IRES in 5 domains. Arrows symbolize each of the 32 ASO below their target region, the position of GNRA and RAAA motifs is indicated. AUG1 and AUG2 start codons location is shown in blue broken line.

Translation reaction was carried out at 30ºC for 60 min. The reaction was treated with 1 μl of RNase A, incubated for 10 min at room temperature prior to addition of 5 μl SDS-loading buffer and fractionated in polyacrylamide gel with sodium dodecyl sulfate (SDS-PAGE) immediately, or stored at -70ºC (Lopez de Quinto and Martinez-Salas, 1999).

Bicistronic RNA translation samples (2 μl) were analyzed by autoradiography of 15% SDS-PAGE, while pMT28 RNA translation products were analyzed in 12% SDS-PAGE. Gels were stained with commassie blue, destained with a mixture of

10% methyl alcohol and 10% acetic acid before being vacuum dried and exposed for autoradiography into a 13x18cm radiographic film.

To determine the capacity of the ASO to inhibit IRES activity, the intensity of the ^{35}S-labeled proteins from three independent experiments, luciferase (62.5kDa) and CAT (26 kDa) in bicistronic RNA, or viral polypeptides for pMT28 RNA, were measured in a densitometer (BioRad). The efficiency of IRES inhibition was determined as the ratio of luciferase intensity over the CAT intensity in the same gel lane, relative to the value observed in the sample without ASO.

Inhibition of viral polypeptides in translation of pMT28 RNA was calculated by dividing the value of total polypeptides translated in the presence of the ASO to that of the control RNA without ASO.

IV. Cells lines

BHK-21, derived from Syrian golden hamster kidney cells, was used for transfection of pMT28 RNA. IBRS-2 derived from Swine kidney, for titration of virus yield (Martin-Acebes et al., 2008). Both cell lines were grown in Dulbecco´s modified Eagle´s medium (Gibco-BRL) supplemented with 5% fetal calf serum (FCS), 50 mg Gentamicin, 200 mg P-hydroxybenzoic Acid Butyl Ester (antimycotic agent) and 44 mM amino acids.

IV.I Transfection of RNA annealed with ASO

Prior to transfection, 50 pg of pMT28 RNA was annealed with 10 nM of each ASO for 20 min at 37ºC, and added to a mixture of lipofectin reagent. Triplicates of BHK-21 cells grown in 35 mm well dishes (80% confluency), washed three times with DMEM, were transfected with the mixture of RNA pre-annealed with each ASO and lipofectin in 0.5 ml of DMEM. This time point is considered as the first hour. Three hours post-transfection (hpt), the cells were washed with DMEM three times, and 2 ml of fresh DMEM with 4% FCS was added. At 24 hpt, 200 μl supernatant was collected from each of the 35 mm duplicate dish, immediately put on ice and stored at -70ºC. A 200 μl supernatant from 48 hpt was also collected and stored.

Cell extracts were prepared for the determination of VP1 viral protein from 24 h and 48 h transfected cells with 100 μl of 50 mM Tris-HCl, pH 7.8, 120 mM NaCl, 0.5% NP40 centrifuged at 14,000 RPM for 5 min to remove cellular debris. Transfection experiments were repeated at least 3 times.

IV.II PFU inhibition assay

Virus yield from three independent assays were titrated in swine epithelial cells IBRS-2 to determine the capacity of the ASO to inhibit plaque forming units (PFU) formation. Monolayer of IBRS-2 cells were grown at 85-90% confluency in 35 mm dish, washed three times and infected with serial dilutions of the supernatant taken from transfected BHK-21 cells. One hour after adsorption, the viral inoculum was removed and the cells were washed three times, overlaid with DMEM medium with 0.5% agar supplemented with 2% FCS. Virus titer (PFU/ml) was scored 24 hours post-infection (hpi) by fixing the cells with 2% formaldehyde solution and stained with 0.3% crystal violet in 2% formaldehyde solution.

The viral titer (PFU/ml) from the 24 and 48 hpt supernatant was determined by counting the lysis plaques that developed after 24 hpi (Sobrino et al., 1983). The virus yield inhibition was calculated as the mean of PFU/ml of three independent assays of pMT28 RNA transfected BHK-21 cells with each ASO relative to the PFU/ml of pMT28RNA transfected without ASO.

V. Western blot analysis

Cell extracts from pMT28 RNA transfected BHK-21 cells were resolved in 10% SDS-PAGE, transferred to a PVDF membrane in a semidry condition (Bio-rad) and blocked with 6% milk-TBS overnight at 4ºC or 4 h at room temperature. After three washing with PBS-1%Tween for 10 min, VP1 protein was detected using the SD6 mouse monoclonal antibody (1:1000) in PBS-BSA for 2 h at room temperature and washed with PBS-1%Tween. The PVDF membrane was then incubated with the goat-antimouse secondary antibody coupled to horseradish peroxidase in PBS-BSA for 1 h at room temperature. The VP1-antibody complex was detected by enhanced

chemiluminescence (ECL, GE Healthcare). To make sure that amount of protein sample loaded on the membrane are of the same quantity in each sample in every gel, the same membrane was used to detect α-tubulin as the loading control.

VI. Electrophoretic Mobility Shift Assay

To assess the accessibility of the FMDV IRES to the ASO, RNA-ASO interactions were analyzed by gel shift assay using transcripts encompassing the whole IRES extended to the 2nd AUG, the wildtype domain 3 alone (nts 84 to 297), domain 3 with GUAG mutation in the GNRA motif ($G_{178}UAA_{181}$ to $G_{178}UAG_{181}$) and domain 3 with CGCCC mutation in the RAAA motif RAAA ($A_{199}AAAG_{203}$ to $C_{199}GCCC_{203}$).

ASO (1μM) were 5´end labeled with 10 μCi (γ-^{32}P)-ATP, 10 U T4 polynucleotide kinase in 50 mM Tris-HCl, 10 mM $MgCl_2$ and 5 mM DTT. Unincorporated γ-^{32}P was removed by exclusion chromatography (Microspin G-25 column, GE Healthcare). Labeled ASO were purified, ethanol precipitated and stored in RNase free water.

Prior to RNA-RNA interactions, unlabeled RNA was denatured at 80ºC for 1 minute, immediately put on ice and then mixed in 50 mM sodium cacodylate pH 7.5, 100 mM KCl and 10 mM $MgCl_2$. RNA-RNA interaction was performed with 0, 10 and 100 ng of RNA annealed with 100 nM of γ-^{32}P labeled ASO in binding buffer in a final volume of 10 μl (Ramos and Martinez-Salas, 1999).

RNA-RNA complex was allowed to form for 20min at 37ºC and immediately analyzed by electrophoresis in native acrylamide gels supplemented with 2.5 mM $MgCl_2$. The complexes were run in 4% native acrylamide gels at 4ºC for 60 min. 150V in TBM buffer (45 mM Tris, pH 8.3, 43 mM boric acid, 0.1 mM $MgCl_2$) (Fernandez-Miragall and Martinez-Salas, 2003). The gel was dried and exposed by autoradiography.

The intensity of the retarded complexes and the free probe were analyzed in a densitometer. The RNA accessibility was calculated as the percentage of the intensity of the retarded complex relative to the intensity of the labeled ASO (free probe).

RESULTS

I. Interference of IRES-dependent translation *in vitro*

Information on the secondary structure of FMDV IRES was available, primarily done by chemical and enzymatic probing (Fernandez et al., 2011; Fernandez-Miragall et al., 2009). Studies were also conducted to inhibit FMDV replication by hybridizing in the 5´UTR and 3´UTR of the genome sense and antisense transcripts (Gutierrez et al., 1994; Rosas et al., 2003) or a short morpholino antisense RNA (Vagnozzi et al., 2007), both of which proved to be inhibitory. However, little information was available regarding the relationship of the IRES accessibility and its capacity to affect translation efficiency. This work attempts to determine the capacity of 2´O-methyl modified ASO to inhibit viral gene expression *in vitro* and *in vivo*, to establish a correlation between IRES accessibility and inhibition of translation, and to reveal information on the susceptibility of the IRES structure against interfering factors.

To perform its function in protein synthesis, the IRES must adopt a proper conformation suitable for the recruitment of the translational machinery (Belsham and Sonenberg, 1996; Martinez-Salas et al., 2008). This is achieved by the contribution of the entire IRES sequence. Arranged into 5 domains, the central domain (D3) contains structural elements needed for proper IRES activity while most host proteins bind to domains 1-2 and 4-5 (Fernandez-Miragall et al., 2009).

I.I Modification of translation efficiency of bicistronic RNA by ASO

To obtain information on the capacity of the ASO to interfere with IRES activity, a bicistronic RNA of the form CAT-IRES-Luc was used (Fig 7). Different concentrations (0.1 to 6 μM) of 2 ASO (AUG which is complementary to the luciferase AUG codon and Scrambled (Scr), a randomized sequence of 16 nt) (Table 2 and Fig. 10) were annealed with the bicistronic RNA prior to incubation with rabbit reticulocyte lysates (RRL). The relative IRES activity in the presence of ASO was measured as the ratio of the intensity of luciferase to CAT produced from the two cistrons, normalized to the ratio of these proteins translated in the absence of any ASO.

As evidenced by the effect of different concentrations of AUG ASO in the relative IRES activity, concentrations of 3 μM and 6 μM annealed to bicistronic RNA

were the most inhibitory (Fig. 10A,B), with a relative IRES activity of 40% and 26%, respectively. On the other hand, the bicistronic RNA annealed to Scr ASO showed no inhibition in any of the concentrations used.

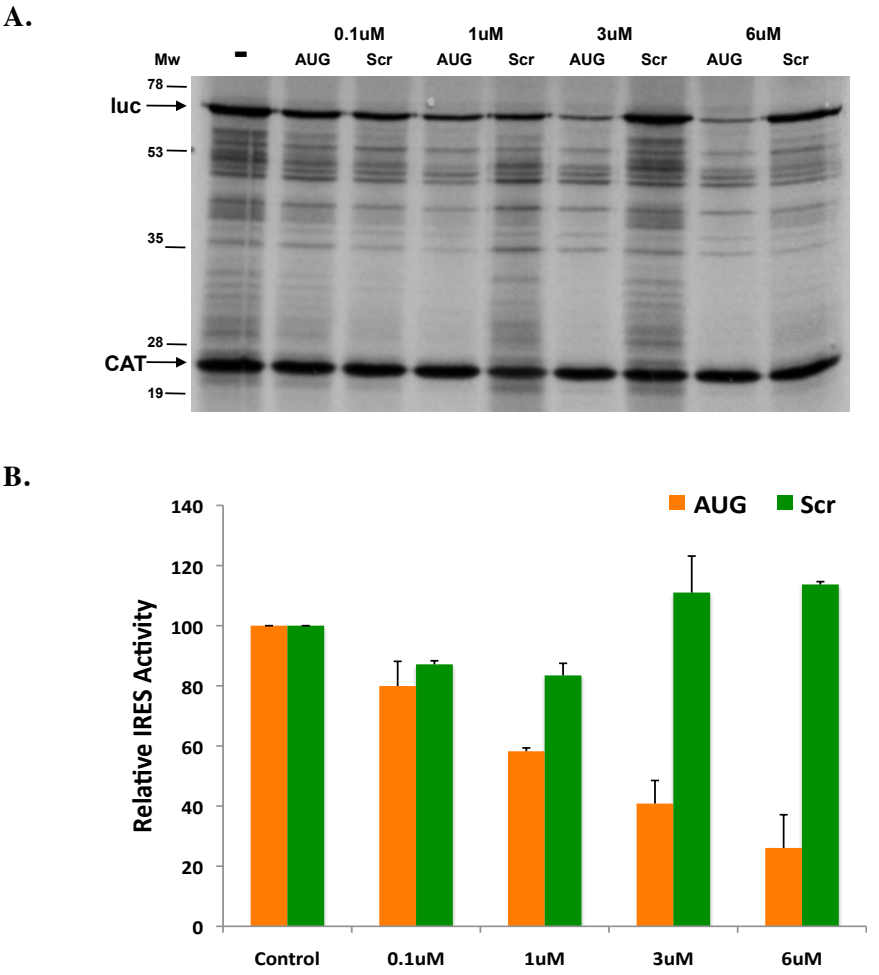

Figure 10. Effect of ASO concentration on bicistronic RNA translation A. Autoradiogram of the *in vitro* translation assay showing the translation products of 250 ng bicistronic RNA in the presence of AUG and Scr ASOs. Luc-luciferase (62.5 kDa), CAT- Chloramphenicol Acetyltransferase (26 kDa), Mw-Protein Marker. -, no ASO **B.** IRES-dependent translation by different concentration of oligonucleotides, control (no ASO). The luciferase intensity is normalized to the value of CAT intensity.

Varying annealing temperatures showed different inhibitory pattern on the bicistronic RNA translation, with the most inhibitory pre-annealing temperature obtained at 37ºC (Fig. 11). The results obtained in the optimization experiments have showed that the inhibitory effect of the ASO is dose and temperature dependent.

Thus, succeeding assays were carried out with 6 μM concentration of ASO, annealed 20 min at 37ºC, prior to *in vitro* translation.

The inhibition of IRES-dependent translation of the bicistronic RNA in the presence of the AUG ASO demonstrated the capacity of the ASO to down-regulate translation if annealed to a critical region**.** The non-inhibitory effect of the Scr ASO compared to translation of the control RNA without ASO, demonstrated that the ASO effects were specific. This information encouraged us to proceed to assess the effect of a panel of customized ASO in gene expression if annealed to different IRES region prior to translation.

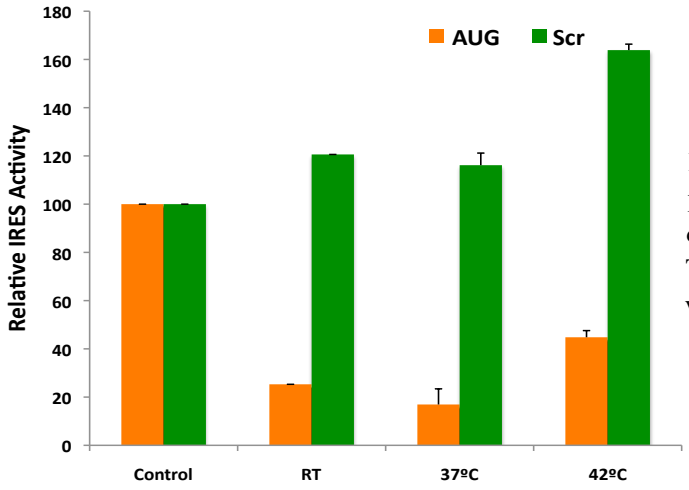

Figure 11. Effect of annealing temperature of ASO on bicistronic RNA translation. Inhibition of IRES-dependent translation in the presence of AUG and Scr ASO at different temperature, for 20 minutes. The luciferase is normalized to the value of CAT.

I.II IRES-dependent translation efficiency is affected by ASO targeting domain 1-2

Overlapping regions of the FMDV IRES were tested with 30 ASO sequences, between 14 to 19 nt in length, annealed to the bicistronic RNA and translated *in vitro*, using the RRL system. ASO targeting the bicistronic RNA AUG codon and Scr sequence were always carried out in parallel for control purposes.

To evaluate the effect of ASO in IRES efficiency, bicistronic RNA was pre-annealed to 4 different ASO complementary to domain 1-2 of the FMDV IRES, prior to *in vitro* translation. These ASOs (40, 55, 66, and 83) inhibited IRES activity to various extents (Fig. 12A,B)**.** In all cases, the inhibition was below 60%, with ASO 83 exerting the lowest IRES efficiency (25%), ASO 55 at 35%, ASO 66 at 40% and ASO 40 at 55%. The *p*-value for each ASO, including the AUG and Scr, $p<0.05$

demonstrated that the translation efficiency at 60% and below differed significantly from the control. Therefore, it was considered that translation efficiency below 60% is inhibitory while those above 60% is adjudged non-inhibitory.

The domain 2 of the IRES folds as a stem-loop with the pyrimidine-rich motif located at the loop (Fernandez-Miragall et al., 2009). The pyrimidine-rich tract provides binding site of PTB, proposed to act as a chaperone for the stabilization of the IRES structure in a suitable conformation for proper recognition by the translation machinery (Fernandez-Miragall et al., 2009; Kafasla et al., 2010). The decrease in the efficiency of IRES-dependent translation in the presence of the ASO indicated the presence of a critical region in this domain needed for the proper functioning of the IRES. This result correlated with the mutational analysis done on this region that proved to be lethal for the IRES function (Fernandez-Miragall et al., 2009).

The inhibition of IRES activity by ASO 40, 55, 66 and 83 may suggest that disruption of the RNA structure in this domain induced by the ASO is not tolerated by the IRES. Additionally, the negative effect on translation of ASO targeted to domain 2 can be explained by the interference in the RNA-protein interactions affecting the appropriate functioning of the IRES.

I.III Apical and proximal regions of the central domain are differentially susceptible to ASO interference.

The inhibitory pattern of domain 1-2 in the presence of the ASO provided critical information on how ASOs affect IRES activity. To test if the same effect can be observed in domain3, a set of 15 ASOs were designed to hybridize to overlapping sequences covering the entire central domain (ASOs 104, 118, 135, 154, 164, 176, 183, 192, 207, 213, 226, 247, 265, 282 and 300) (Table 2).

In vitro translation of bicistronic RNA in the presence of ASOs displayed differences in their inhibitory patterns (Fig. 12A,B). The differences were noted in the most apical region where inhibition of IRES function was detected in sequences complementary to ASOs 164, 192, 207, 213 and 247 where translation efficiency fell below 60%. Lack of inhibition, on the other hand, was observed in ASOs 176, 183 and 226.

A.

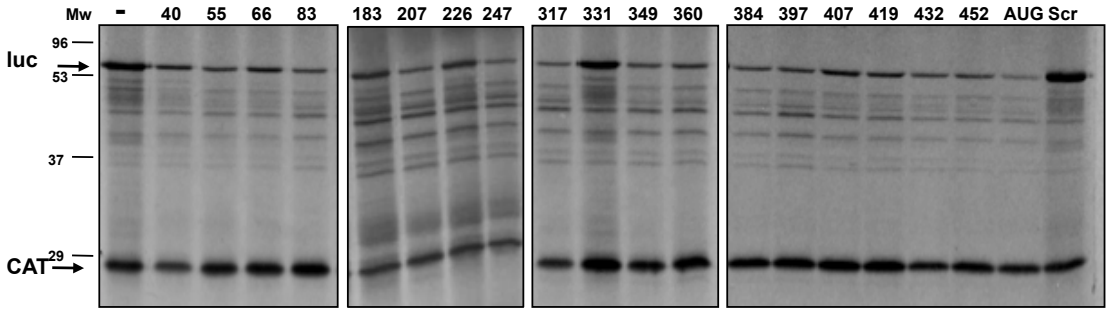

B.

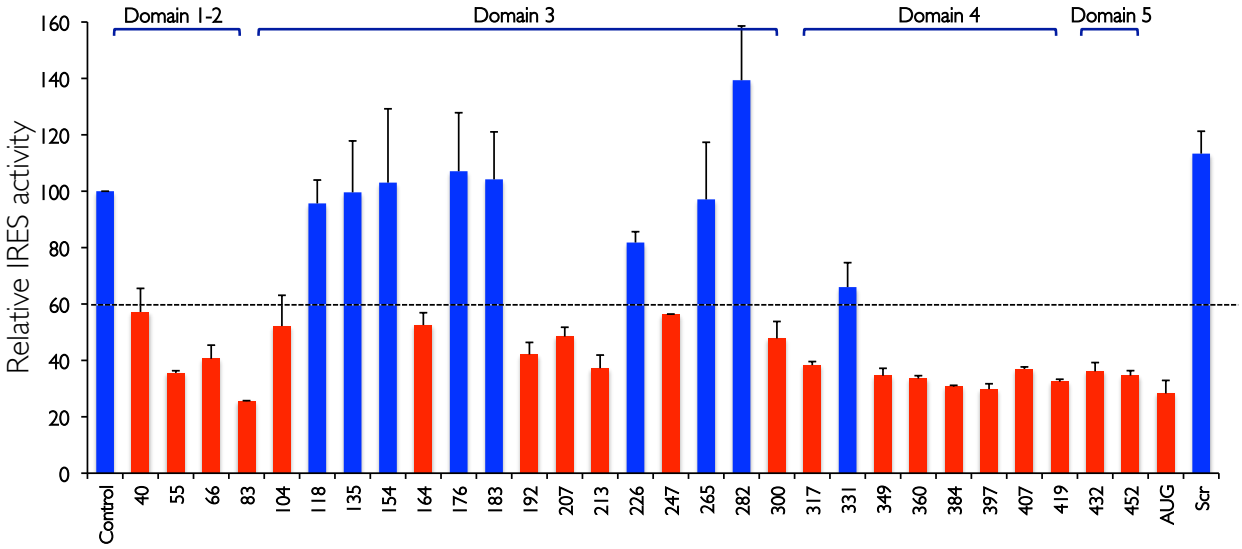

C.

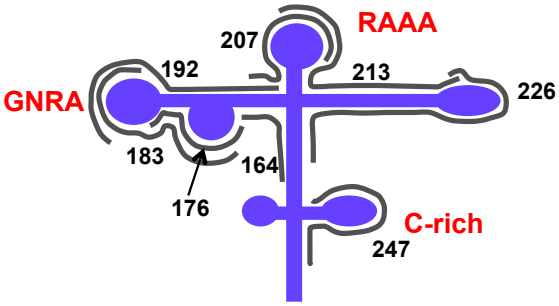

Figure 12. RNA translation efficiency *in vitro* in the presence of ASO. A. Autoradiogram of the *in vitro* translation assay showing the translated proteins, luciferase and CAT, using 250ng of pBIC RNA annealed to 60µM each ASO, at 37ºC for 20min. The numbers above the gel correspond to each ASO **B.** Relative IRES activity calculated as the percentage of IRES-dependent translation in the presence of ASO. AUG and Scr were used as controls. The intensity of the luciferase and CAT was measured in a densitometer in three independent assays. The p-value ($p \leq 0.05$) indicated that relative activities below 60% are statistically different from the control. **C.** Schematic of apical region of the central domain showing the ASO target sequences.

As mentioned before, the domain 3 is a self-folding region that contains the conserved GNRA, RAAA and C-Rich motifs, organized in loops (Fernandez-Miragall and Martinez-Salas, 2003), with the most apical region arranged as a cruciform structure. The structural organization of FMDV IRES involves tertiary interactions determined by GNRA-dependent interaction that dictates the stability of the domain 3 structure (Fernandez et al., 2011; Fernandez-Miragall and Martinez-Salas, 2003).

As reflected by the relative IRES activity, targeting the three conserved motifs of the central domain affected the IRES function if interfered by ASO. The two RAAA motif ASOs (Fig. 12C) registered a reduction in the translation efficiency of 48% for 207 and 37% for 213. The GNRA motif ASO, 192 (Fig. 12C)**,** that targets the GNRA motif from its 3´ end, reduced the IRES efficiency to 42% while the ASO 247 targeting the C-rich (Fig. 12C) reduced the translation to 56%. This reduction signals the vulnerability of these regions to structural disturbance of the ASO in altering IRES function.

It is important to mention that this region contains loops with experimentally proven accessible nucleotides (Fernandez-Miragall et al., 2009) (Fernandez et al., 2011). Interestingly, ASO 183, that targets the GNRA motif from its 5´ end led to 104% efficiency of translation, a clear difference from ASO 192. The opposite inhibitory results of ASOs targeting the GNRA hairpin indicate that this region responds differently to external factors. Another region of the central region not affected by ASO are the sequences of the GNRA hairpin complementary to ASO 176, which registered 106% efficiency, demonstrating the resistance of this IRES region to withstand the blocking effect of ASO. However, a moderate reduction (52%) was observed in ASO 164, covering the stem of the apical region.

The proximal region of D3, is organized as a base-paired structure interrupted with bulges that includes several non-canonical base-pairing (Serrano et al., 2009). Lack of inhibition was noted by more than 60% translation efficiency in ASO 118, 135, 154, 265 and 282 (Fig. 12A,B). The lack of inhibition can be attributed to the double-stranded structure in this region rendering it inaccessible to pairing with the ASO.

While the ASO complementary to the stem were not inhibitory, the ASOs complementary to the proximal base reduced IRES translation efficiency. ASOs 104 and 300 reduced the translation efficiency to 52% and 47%, respectively (Fig. 12A,B). These regions contain spacer sequences between domain 1-2 to 3 and domain 3 to 4. The reduction in the efficiency could have been induced by the partial blocking of the spacer that destabilizes the D3 structure, or blocking the helical structure occurring in the stem 3, in agreement with the need of a helical region for IRES activity (Martinez-Salas et al., 1996).

Overall, the inhibition observed as a consequence of the pairing of ASO to D3 may suggest that this domain mediates the accurate RNA conformation critical for IRES function.

I.IV ASOs complementary to domains 4 and 5 effectively down-regulated translation of bicistronic RNA

Conserved structural elements present in the domains 4 and 5 of the FMDV IRES are responsible for binding of eIFs (Kolupaeva et al., 2003) (Lopez de Quinto et al., 2001). To extend the IRES inhibition analysis in the bicistronic RNA, domains 4 and 5 were hybridized to ASOs prior to *in vitro* translation. Results of the RRL assays revealed that most ASOs annealed to domains 4 and 5, effectively decreased IRES activity below 40% (Fig. 12A,B). However, the J-domain resisted the effect of ASO 331, resulting to a 66% IRES activity, probably owing to its double-stranded structure. Inhibitory ASOs 317, 349, 360, 384, 397, 407, 419 complementary to domain 4, and ASOs 432 and 452 in domain 5, impaired IRES activity *in vitro* presumably disturbing the ability of this region to bind with translation factors.

Domain 4 is a conserved region essential for IRES activity; mutational analysis revealed lack of IRES activity as a result of the impairment of the eIF4G binding (Lopez de Quinto and Martinez-Salas, 2000). Likewise, domain 5 provides the binding site for eIF4B, eIF3 and PTB (Lopez de Quinto et al., 2001). Inhibition by ASO targeting domains 4 and 5 could be due to the disturbance of the correct RNA organization or impairing its ability to perform RNA-protein interactions.

I.V Control of FMDV gene expression *in vitro*

I.V.I AUG1 is the most potent inhibitory ASO *in vitro*

Initiation of viral polyprotein synthesis occurs in two in-frame AUG triplets in aphthovirus (Belsham, 1992), 84 nt apart, with a strong preference to initiate translation in the second AUG (Lopez de Quinto and Martinez-Salas, 1999). Translation starting at AUG1 or AUG2 gives rise to two different forms of L protease (Lab and Lb, respectively) (Cao et al., 1995; Sangar et al., 1987).

To measure the ability of the ASO to inhibit translational activity in the context of a complete FMDV genomic RNA that translates into a complete viral polyprotein, AUGs and Scr ASO were incubated with the *in vitro* transcribed FMDV RNA (pMT28 RNA) under the same condition used in the inhibition assay of the luciferase protein. In the FMDV RNA *in vitro* translation, the AUG ASO used to block the luciferase protein in the bicistronic RNA, was replaced by two ASO complementary to AUG1 and AUG2 of the FMDV genome, transcribed from the pMT28 plasmid.

Initial assay of the pMT28 RNA entailed the use of the AUG1, AUG2 and the Scr ASO in parallel to RNA without ASO. Analysis of the synthesized polyprotein revealed a considerable difference in translation efficiency of pMT28 RNA in the presence of the two AUG ASOs. The capacity of the ASOs to inhibit polyprotein synthesis by blocking the first AUG was significantly greater than that of the AUG2 (Fig. 13A). The translational efficiency in the presence of the AUG1 ASO (15%) was well below 60%, chosen as the threshold between the inhibitors and non-inhibitors based on *p*-values ($p<0.05$). Translation in the presence of the AUG2 ASO still continued with moderate efficiency (75%), while FMDV RNA protein synthesis was not affected by the Scr ASO (Fig. 13A, C). It is noteworthy to mention that the AUG2 is located in a double-stranded region (Fernandez-Miragall et al., 2009) whereas the AUG1 is located in a single stranded region downstream of the IRES domain 5.

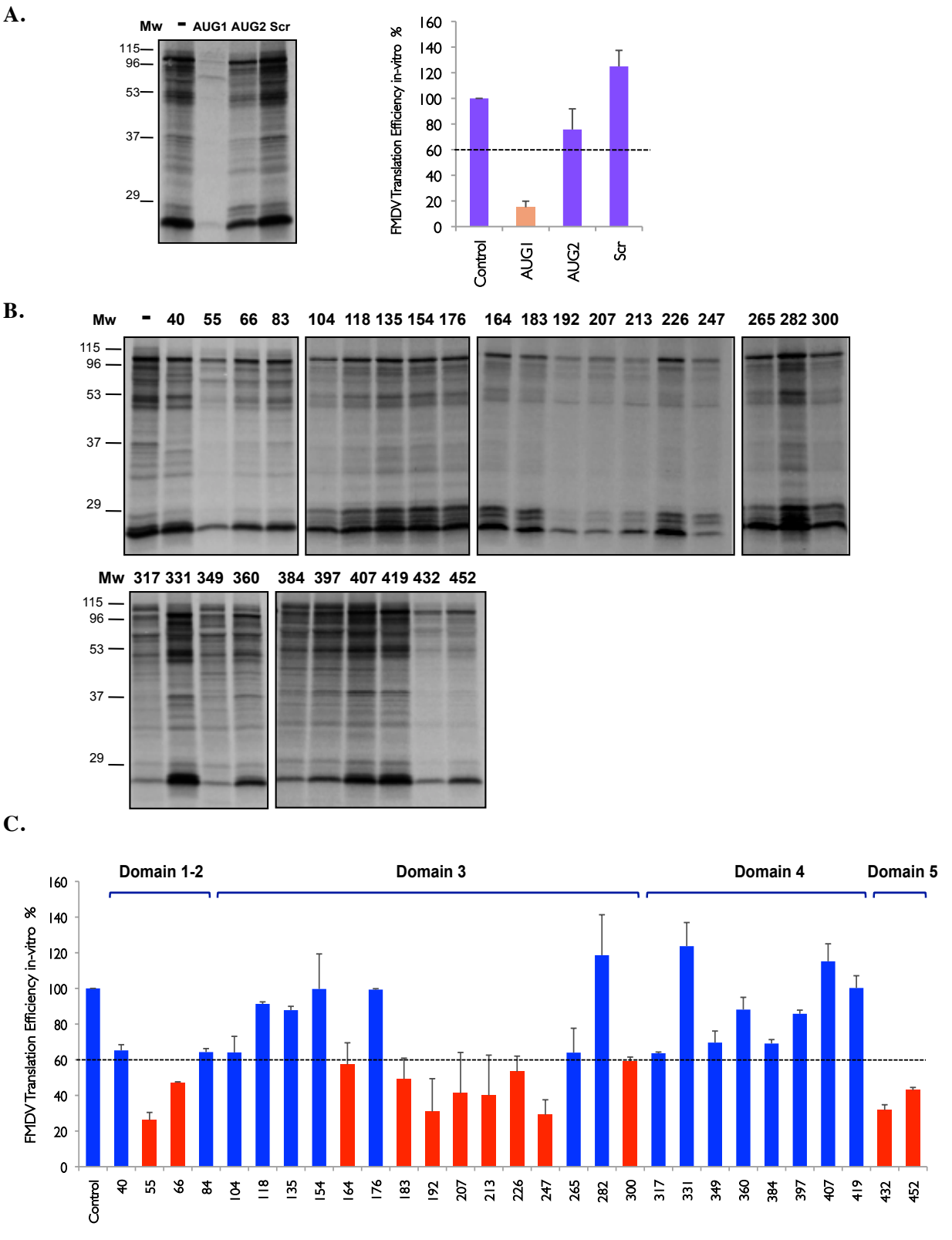

Figure 13. Inhibition of FMDV RNA translation efficiency *in vitro* in the presence of ASO. A. Autoradiogram showing the products of pMT28 RNA translation with AUG1, AUG2 and Scr ASO using 250 ng of RNA annealed to 60μM each ASO at 37ºC for 20min. **B.** Autoradiogram of the *in vitro* translation assay showing the viral proteins. The numbers above the gel correspond to each ASO. **C.** Efficiency of pMT28 RNA translation in the presence of ASO. The intensity of the viral polypeptides were measured in a densitometer in three independent assays. The p-value ($p \leq 0.05$) indicates that the inhibition below 60% is statistically different from the control.

I.VI Differential response of domain 2, 3, and 4 to ASOs

After revealing the capacity of the ASO to down-regulate IRES activity in using the AUG1 and AUG2 ASO, this work has also sought to uncover the competence of the ASO to intervene in the role of the IRES in a full length FMDV genome. To accomplish this task, the FMDV RNA was annealed with each of the 30 overlapping ASO (Table 2) under the same condition of AUG1, AUG2 and Scr ASO prior to progressing the RRL translation.

The polyprotein translation inhibition due to the different ASO annealed to the full length FMDV RNA varies depending on each ASO (Fig. 13 B, C). Consistent with the results obtained in the bicistronic RNA, the ASOs that hybridize to the loop of domain 2 (ASO 55 and 66) were inhibitory with translation efficiency of 26% and 47%, respectively. In contrast to the inhibition observed in the bicistronic RNA, the stem was able to withstand the presence of ASOs 40 (65%) and 83 (64%). The observed variations in the loop and stem of this domain may be explained by interference by the ASO in the binding site of PTB.

The result of the 15 ASOs targeting the central domain of the IRES is comparable to that of the domain 1-2. Variations were similarly observed with most of the inhibitions were noted in ASOs complementary to the D3 apical part while ASOs complementary to stems were mostly non-inhibitory. Inhibitions of IRES activity were eminent in all of the conserved motifs of the central domain. Translational efficiency were reduced by two ASOs used to block the GNRA motif (183 at 49% and 192 at 30%); two ASOs for RAAA motif (207 at 41% and 213 at 39%); and in the ASO for the C-rich motif (247 at 29%). Additionally, weak down-regulation was observed in ASO 226 (53%) and 164 (57%), both of which are located in the apical region. Inhibition was also shown by the ASO 300 (59%), located in the right proximal region of domain 3. In contrast, the ASOs complementary to the stem were mostly non-inhibitory, ranging between 64% (104) to 118% (282). The ASO inhibitions in the central domain, particularly in the apical region, reflect the susceptibility of the IRES conserved regions, and reveal the crucial role of the central domain in the translation process.

These results revealed some differences with the bicistronic RNA, the two ASO

that binds GNRA motif (183 and 192) were both inhibitory in FMDV RNA while in bicistronic context, only the 192 ASO was able to reduce translation activity. This inhibition may indicate that in the FMDV RNA context, ASO disturbance in the GNRA motif is not tolerated. Similarly, the RAAA motif could not tolerate the interference of the ASO either in the 5´or the 3´ end, as this motif is inhibitory in the presence ASO 207 and 213.

A striking result was noted in the inhibitory pattern exhibited by the ASOs hybridizing to the domain 4. In the FMDV RNA, most domain 4 ASOs values were above the 60% level, as shown by 317 (63%); 349 (69%); 360 (88%); 384 (69%); 397 (85%); 407 (115%) and 419 (100%) (Fig. 13 B, C) shifting from inhibitory in the bicistronic to non-inhibitory in the FMDV RNA. ASO 331, however, maintained its non-inhibitory pattern in the bicistronic RNA. The shift of the inhibitory pattern in this domain may be attributed to the tolerance to ASO due to the protection offered by the proteins binding to this domain in FMDV RNA context.

Differences observed in the stem of domain 1-2 (40 and 83), in the GNRA motif (183), and in domain 4 (317, 349, 360, 384, 397, 407, 419) may also suggest conformational IRES changes, dependent on its interaction with other *cis*-acting RNA elements in the full length FMDV RNA (Serrano et al., 2006).

I.VII The domain 5 region is susceptible to inhibition by ASO

The disruption of domain 5 caused by the ASO was not tolerated as reflected by the reduced polyprotein synthesis in the presence of the ASO complementary to the hairpin (432) and the single-stranded region (452) (Fig. 13 B, C). Values of the translation efficiency fell below the non-inhibitory threshold (432 at 31% and 452 at 42%). The inhibition of domain 5 had similarities in the inhibition noted when ASOs bind to other loops (domain 1-2 or the apical domain 3). However, double-stranded regions in domain 1-2, and domain 3 were not affected by the presence of the ASO.

In concordance with the bicistronic RNA, binding of the ASO to domain 5 may interfere with its ability to bind host factors, such as eIF4B and PTB. Another reason for the inhibition in this domain is the steric blocking caused by the ASO in the single-stranded region of the domain 5, interfering the landing site of the translational

machinery, effectively down-regulating the initiation of translation.

II. Control of FMDV genome gene expression in cultured cells

II.I ASO targeting AUG1 and AUG2 are inhibitory in tissue culture cells

To investigate the capacity of the ASO to block viral polyprotein translation in the competitive environment of the cellular cytoplasm, AUG1 and AUG2 ASO, targeting the two AUG start codons of the viral genome, were first tested. The Scr ASO was included for control purposes. To determine the optimal amount of pMT28 RNA for virus yield analysis, different quantities of RNA (25 pg to 2 ng) were transfected in BHK-21 cells and virus yield of the supernatant at 24 hpt was titrated in IBRS-2 cells. 50 pg of FMDV RNA yielded 16 x 10^2 pfu per ml at 24 hpt. Then, different concentrations (1-20 nM) of AUG1, AUG2 and Scr ASO were annealed to 50 pg of pMT28 RNA for 20 min at 37ºC and transfected in BHK-21 cells. Virus yield was determined 24 hpt to ascertain the optimal inhibitory ASO concentration (Fig. 14).

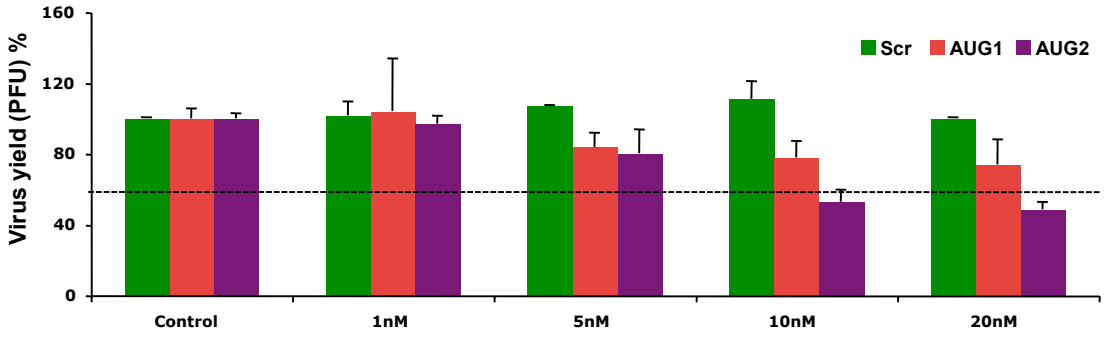

Figure 14. Virus yield inhibition. A. 50pg of pMT28 RNA was annealed with 10nM AUG1, AUG2 and Scr ASO, for 20min at 37ºC, prior to lipofectin transfection in BHK-21 cells. Virus yield was determined as the number of PFU in the supernatant 24 hpt, made relative to the control RNA without ASO.

Expression of the viral genome was inhibited in the presence of these ASOs. However, the inhibition caused by the AUG2 (22%) was more pronounced than that of AUG1 (60%) (Fig. 15A,B). Thus, in contrast to the inhibitory results observed *in vitro* where AUG1 was more inhibitory, the AUG2 is 3 times more inhibitory than AUG1 *in vivo*, indicating that the best target for inhibition of viral replication is by

blocking the AUG2 region. In accordance with this results, the selection of the AUG2 as the starting point of translation is favored over the AUG1 (Lopez de Quinto and Martinez-Salas, 1999). These results also showed that ASO Scr exhibit no effect on the translation of FMDV RNA (Fig. 15A,B). This provides us information that the ASO used were sequence specific as neither the *in vitro* nor the *in vivo* assay showed inhibition with Scr ASO.

To confirm the inhibition of viral protein synthesis in the presence of the AUG1 and AUG2 ASO, a western blot was done to detect the VP1 structural protein synthesized in BHK-21 cells (Fig. 15C). The reduced intensity of VP1 band compared to the control without ASO and Scr confirmed that there was, indeed, an inhibition of viral gene expression in the presence of the ASO.

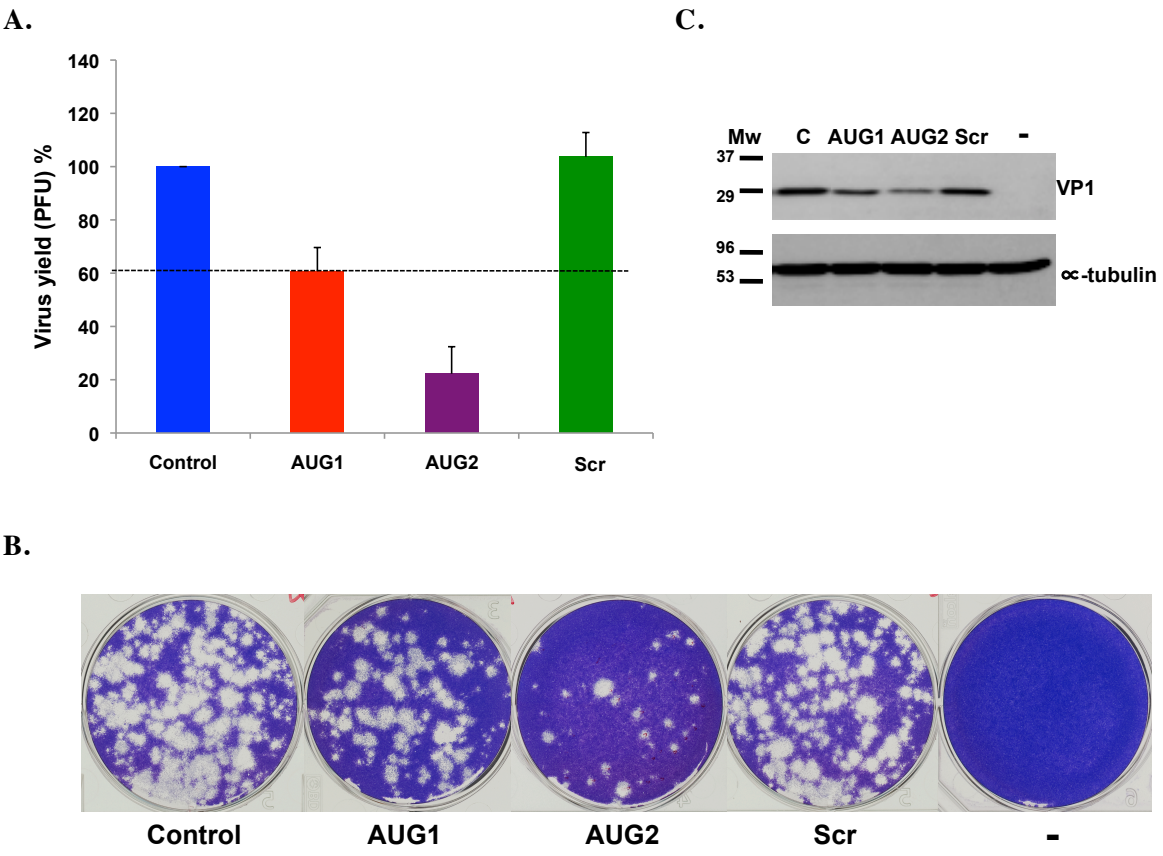

Figure 15. Virus yield inhibition by ASO AUG1 and AUG2. A. Virus yield titrated from 24 hpt supernatant (PFU/ml) using 50pg pMT28 RNA annealed to ASO AUG1 and AUG2 for 20min at 37ºC. **B.** Representative examples of viral plaques**.** Titration was done on monolayer of IBRS-2 cells cultured in 0.5% agar, with 4% FCS. **C.** Western blot of BHK-21 cell extract showing the VP1 protein. α-tubulin was used as loading control. Control (no ASO), (-) no pMT28 RNA.

II.II Interference of ASO complementary to domain 1-2 on translational efficiency *in vivo*

The domain 1-2 of the IRES in the context of the FMDV RNA was also probed *in vivo* to investigate if the ASO bound to this domain has the capacity to inhibit viral plaque forming units. Surprisingly, changes were observed when virus yield is compared with the *in vitro* translation. A significant change was noted in the proximal region where virus yield in the presence of the ASO 40 fell at 20%, compared to the 65% translational activity *in vitro* (Fig. 16A,B).

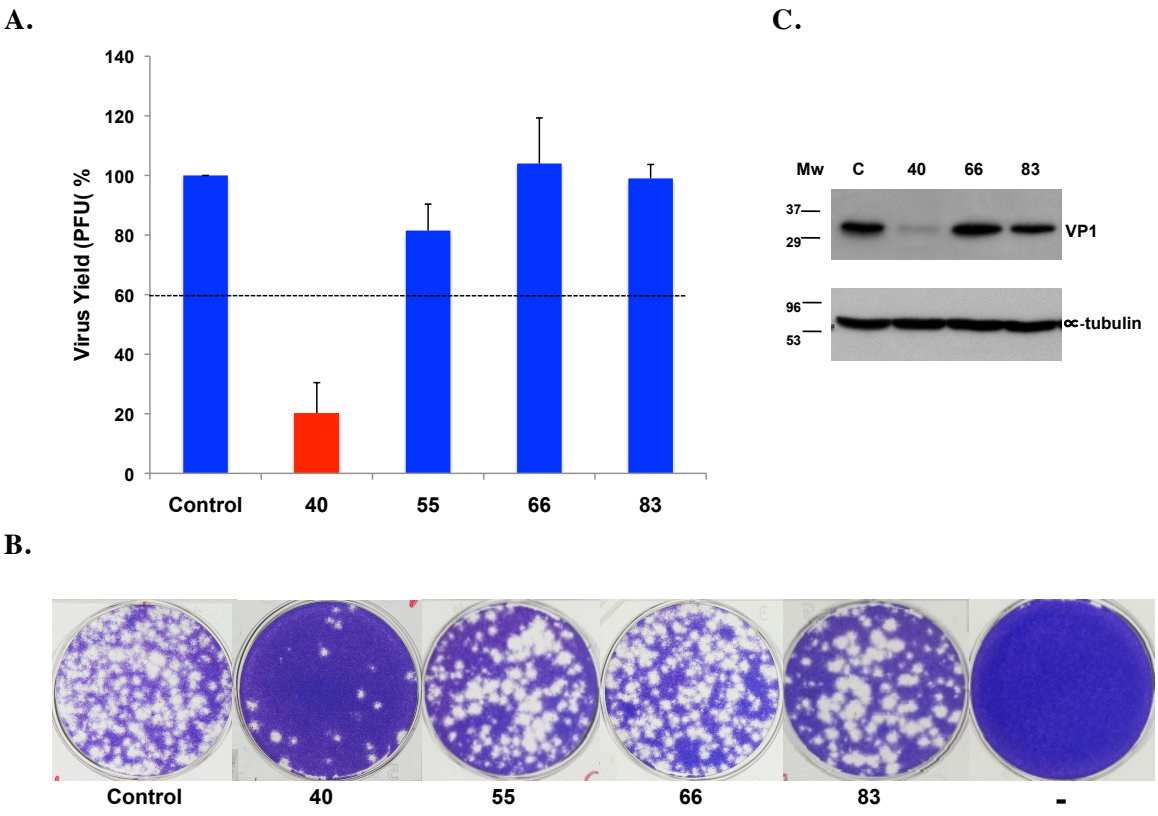

Figure 16. Virus yield inhibition by ASO complementary to domain 1-2. A. Virus yield (percentage of PFU) titrated from 24 hpt supernatant (PFU/ml) using 50pg pMT28 RNA annealed to domain 1-2 ASOs. **B.** Representative examples of viral plaques formed from supernatant of 24 hpt in **(A),** numbers correspond to each ASO**. C.** Western blot of BHK-21 cell extract showing the VP1 protein. α- tubulin was used as loading control.

The change from the inhibitory activity of ASO 40 from non-inhibitory *in vitro* to inhibitory *in vivo* may be attributed to the pairing of the ASO to the proximal part

of the domain 1-2 which is contiguous to *cre*, an element necessary for viral replication (Belsham and Martínez-Salas, 2004; Mason et al., 2002). An opposite change was observed in the distal region of this domain, 55 and 66 ASO at 81% and 104% virus yield *in vivo* was a change from 26% and 47% *in vitro* translational activity, respectively. ASO 83, however, was still non-inhibitory (Fig. 16A, B**).** These results were confirmed by the reduction of VP1 in the western blot (Fig. 16C**).**

The difference in the inhibition observed in the ASO complementary to domain 1-2 in the *in vitro* and *in vivo* may be attributed to the different concentration and presence of various cellular proteins, such as PTB, that may protect the loop (55 and 66) while rendering the stem vulnerable to ASO attack (40).

II.III Effects of ASO targeted to domain 3 differs *in vivo* and *in vitro*

The virus yield inhibition by ASO 183 and 207 demonstrated a reduction to 40% and 39%, respectively **(**Fig. 17A,B**),** consistent with the reduction in the *in vitro* translational efficiency. However, ASO complementary to the sequences upstream of the GNRA motif did not affect virus yield (164 at 78% and 176 at 100%). Likewise, the 3´region of these motifs were resistant to the effect of ASO, reflected by the high virus yield of ASOs 192 (96%) and 213 (71%) **(**Fig. 17A,B**)**. Another conserved motif, the C-rich showed resistance to ASO 247 with virus yield of 91%, in contrast to the results *in vitro*. Differences in the efficiency of protein synthesis were confirmed by western blot **(**Fig. 17C**).**

ASOs complementary to the stem of domain 3 also produced a significant change from *in vitro* results. ASOs 265 and 282 were non-inhibitory *in vitro* translation but shifted to become inhibitory (36% and 39%). The ASO 300, that targets the 3´ proximal stem, registered inhibition of virus yield at 52%, in agreement with its result in RRL. In agreement with the virus yield analysis, the VP1 translated protein detected by western blot confirmed the non-inhibition noted in ASOs 282 **(**Fig. 17 C) and 300 (not shown).

No inhibitory effect was detected in pMT28 RNA translation *in vivo* in ASO 104 (71%), 118 (107%), 135 (99%), and 154 (90%). It is important to consider that the complementary regions of these ASO were located in the stem of domain 3.

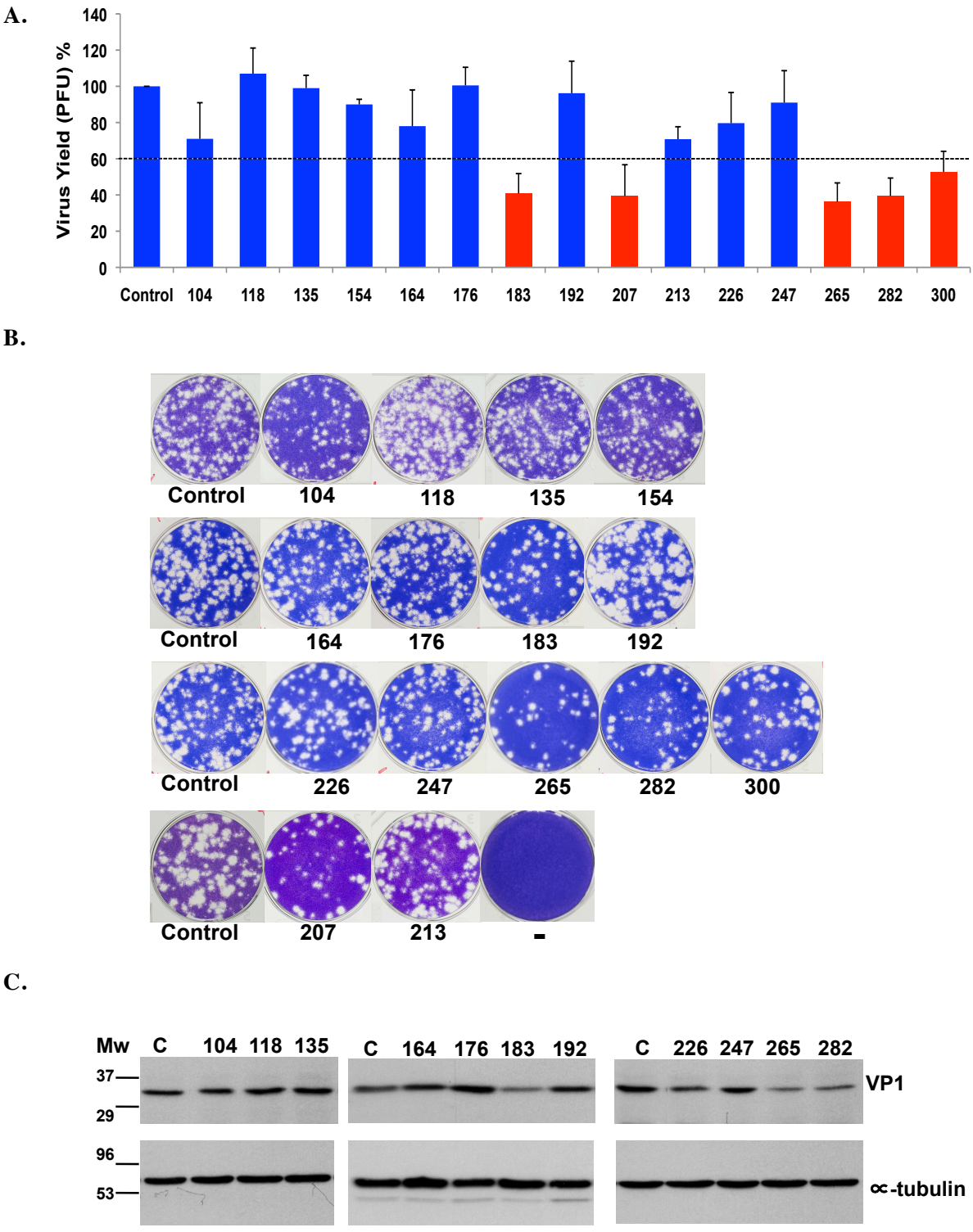

Figure 17. Virus yield inhibition by ASO complementary to domain 3. A. Virus yield titrated from 24 hpt supernatant (PFU/ml) using 50pg pMT28 RNA annealed to domain 3 ASOs **B.** Representative examples of viral plaques formed from supernatant of 24 hpt in **(A),** numbers correspond to each ASO**. C.** Western blot of BHK-21 cell extract showing the VP1 protein. α- tubulin was used as loading control.

The inhibition of observed in ASO targeting domain 3 demonstrated the differences in the activity of the IRES in *in vivo* as compared with the *in vitro* in the context of a full length FMDV RNA, especially in the apical region where the conserved GNRA and RAAA motif is located.

II.IV Domain 4-5 behave differently in the presence of the ASO *in vivo*

The effect of the ASO complementary to domains 4 and 5 in *in vivo* assays revealed that domain 4 was not affected by the interference of the ASO. An exception was the 349 ASO, where a severe decline in virus yield (23%) was noticed (Fig. 18). As regard to other ASO in domain 4, the virus yield results of ASOs 317, 331, 360, 384, 397, 407 and 419 were all above 60% (Fig. 18A,B), indicating that the IRES activity is not affected if ASO are pre-annealed to this region, similar to the pattern of inhibition in the *in vitro*.

Domain 5, however, behaved different from domain 4. Similar to the inhibitory results obtained *in vitro*, this domain did not tolerate the disruption caused by the ASO. More specifically, the inhibition was more pronounced in the hairpin (432, 24%) than in the single stranded region (452, 32%) (Fig. 18A,B).

II.V Inhibition of viral translation at an extended time

The capacity of ASOs to inhibit viral polyprotein synthesis was also investigated by extending the incubation up to 48 hpt in BHK-21 cells. The virus yield inhibitions compared to control FMDV RNA revealed that 5 ASO (40, 183, 349, 432 and AUG2) were able to extend their inhibitory capacity until 48 hpt (Fig. 19). It is important to mention that these 5 ASO showed the highest potency in inhibiting the viral multiplication at 24 hpt, with a virus yield average below 40%. The inhibition until 48 hpt indicates the potency of the ASO to remain inhibitory and the ASO capacity to inhibit viral replication in the presence of an increasing quantity of viral particles.

A.

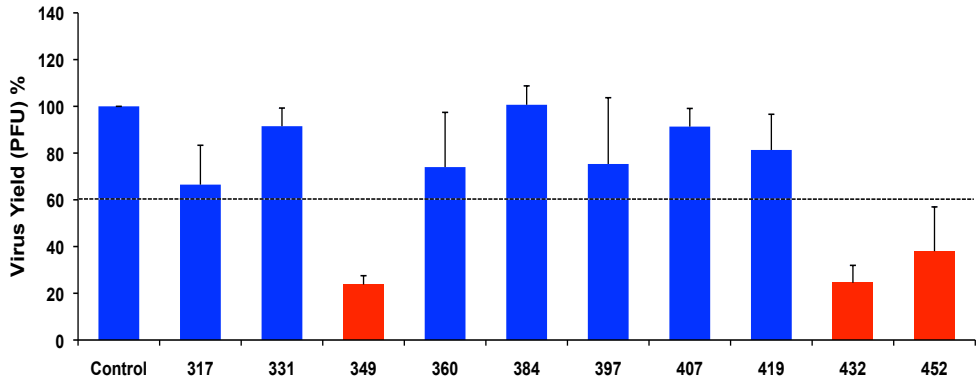

B.

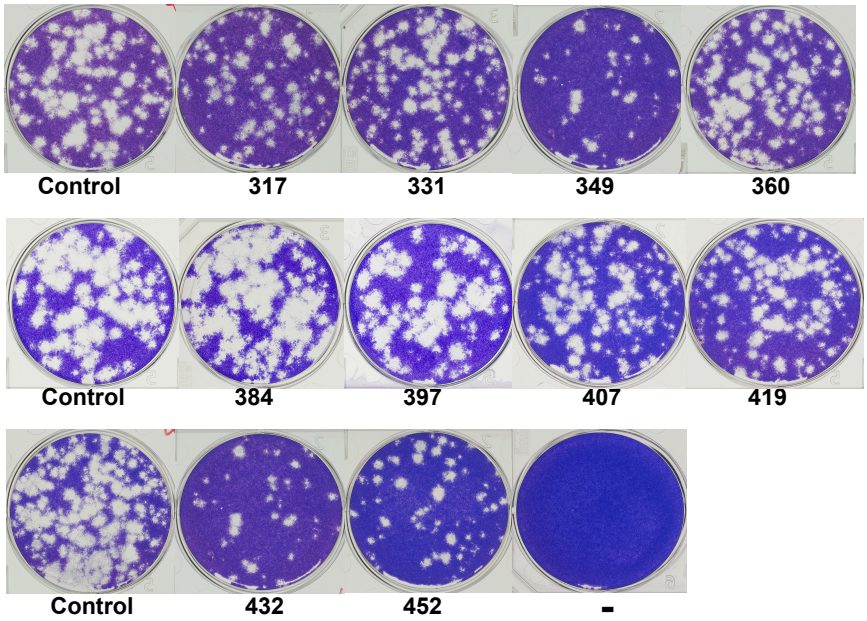

C.

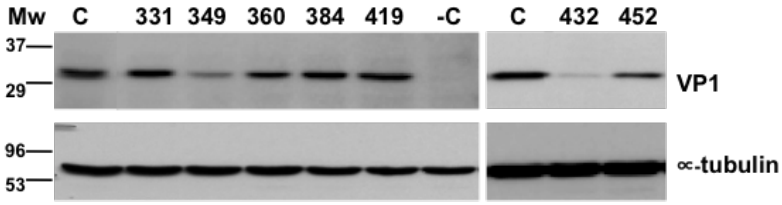

Figure 18. Virus yield inhibition by ASO complementary to domains 4 and 5 A. Virus yield titrated from 24 hpt supernatant (PFU/ml) using 50pg pMT28 RNA annealed to domains 4 and 5 ASOs. **B.** Representative examples viral plaques formed from supernatant of 24 hpt in **(A),** numbers correspond to each ASO. **C.** Western blot of BHK-21 cell extract showing the VP1 protein. α- tubulin was used as loading control.

The data from the inhibition of the AUG regions of bicistronic and the FMDV RNA denotes that ASO can interfere gene expression. The inhibition demonstrated by ASOs complementary to the different domains of the IRES clearly suggests the critical role this RNA element is playing in translation of the whole mRNA. Each IRES region inhibited by their complementary ASO also revealed susceptible sequences in the IRES critical to internal initiation.

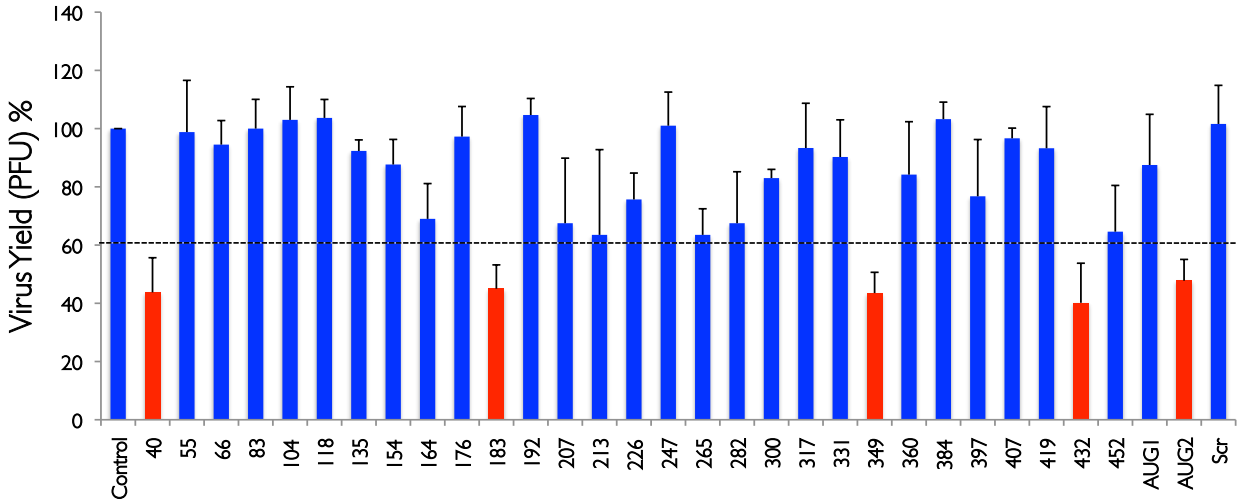

Figure 19. Extended inhibition of virus yield by ASO. Virus yield (percentage of PFU) titrated from 48 hpt supernatant (calculated as PFU/ml) using 50pg pMT28 RNA annealed to ASO.

III. Accessibility of IRES to ASO

To obtain a deeper understanding on the relevance of IRES accessibility to translation, a RNA electrophoretic mobility shift assay was performed in the context of a full length IRES. This study also aimed to reveal possible changes in the IRES accessibility in the context of a wild type domain 3 alone, and mutant RNAs carrying a substitution in the GNRA motif ($G_{178}UAA_{181}$ to $G_{178}UAG_{181}$) and replacement of the RAAA motif ($A_{199}AAAG_{203}$ to $C_{199}GCCC_{203}$). To achieve this objective, FMDV IRES sequence extended up to second AUG was annealed with labeled ASO and analyzed in native PAGE. To compare changes in accessibility between the full length RNA and D3 wildtype, IRES D3 alone, GUAG and CGCCC mutants were annealed to the labeled ASO in identical conditions to the full length IRES. Labeled ASO capable of

binding to its complementary region in the IRES will form a retarded complex visible in the autoradiography of native acrylamide gel. IRES accessibility to labeled ASO was measured as the ratio of the retarded complex to the free probe, expressed in percentage. Percentage of retarded probe above 5% was regarded as accessible, while 5% to 3% was considered moderate to low accessible and falling below 2% was non-accessible.

III.I Differential accessibility of the FMDV AUG region

Accessibility of the IRES to 2´O-methyl ASO offered information on the AUG region (Fig. 20)**.** Accessibility measured as the percentage of the retarded complex unveiled that the most accessible region is located in the AUG1, with 44% of retarded probe, consistent with the fact that this region is located in a single stranded region (Fernandez-Miragall et al., 2009). Likewise, translation was inhibited by AUG1 ASO *in vivo*, indicating its successful pairing to its complementary region.

A.

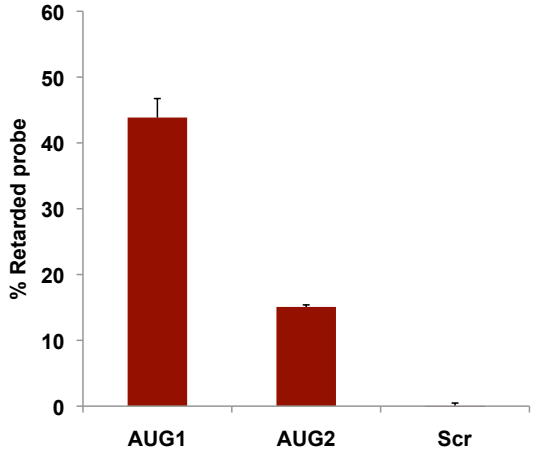

B.

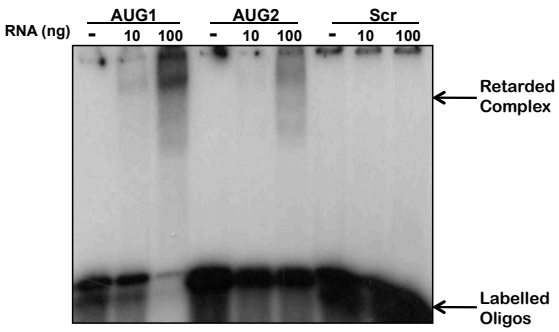

Figure 20. FMDV IRES RNA AUG-ASO complex formation A. Percentage of retarded probe from interaction of FMDV IRES RNA extended to 2nd AUG (100 ng) and γ-^{32}P labeled AUG ASOs. **B.** Autoradiogram of the retarded complex using 10 and 100ng RNA and 100nM of γ-^{32}P labeled AUG ASOs for 20min at 37ºC, analyzed in a 2.5mM $MgCl_2$ 4% acrylamide native gel run in TBM buffer with 0.1mM $MgCl_2$ at 4ºC.

AUG2, on the other hand was accessible to a lower degree, with 15% of retarded probe. Positioned in a region preceded by A-rich sequences, the AUG2 is located in a double stranded region (Andreev et al., 2007) explaining the lesser ASO accessibility. However, this does not affect the capacity of the ASO to inhibit gene expression *in vivo*, in agreement with previous data showing that AUG2 is preferred over the AUG1 in infected and transfected cells (Lopez de Quinto and Martinez-Salas, 1999). The binding of the ASO to the region just before the AUG2 (ASO blocks nt position -9 to +9 with respect to A as +1) might have a negative effect on the assembly of the 80S complex resulting to reduced translation.

III.II IRES domains 1-2 and 4-5 exhibit differences in accessibility

Inter-domain contacts have been observed between domain3 and other domains (domains 1-2 and 3 and domains 4-5 and 3) (Ramos and Martinez-Salas, 1999). The PTB, one of the host factors that interact with the FMDV IRES was also proven to interact with the polypyrimidine-rich tract of the domain 2 (Luz and Beck, 1991) while specific sequences in domains 4-5 provides the binding site for eIF4G, eIF3 and eIF4B (Lopez de Quinto et al., 2001). Accessibility observed in domains 1-2 and 4-5 varies depending on the secondary structure depicted in Fig 5. Nucloetides located on single stranded sequences and bulges were more accessible than that of the sequences in a double stranded structure (Fig. 21A, B). ASOs 40 (23%), 331 (17%), 349 (11%), 360 (11%), 432 (25%) and 452 (25%), had a higher accessibility owing to their secondary structures located either in a single stranded sequences or in bulges and loops. Accessibility on these regions were also noted by RNA probing (Fernandez-Miragall and Martinez-Salas, 2007), SHAPE (Fernandez et al., 2011) and microarray (Fernandez-Sanchez, 2010). On the other hand, the less than 5% accessibilities of ASOs 55, 66, 83, 317, 384, 397 and 419 can be attributed to their location in a double stranded structures or other factors such as intra-molecular contacts between IRES domains.

III.III IRES central domain accessibility

Differences in the RNA organization of the IRES have been observed by *in vivo* footprint assays relative to the RNA probing observed *in vitro* (Fernandez-Miragall and Martinez-Salas, 2007), indicating conformational changes in the RNA structure that may be important for IRES activity.

RNA structure of domain 3 has accessible nt in the stem, bulges and loops (Fig. 5). The GNRA and RAAA motifs were accessible to ASO (Fig. 21A,B). Notably, it was observed that accessibility at the 3´end of these motifs was higher than the 5´, as reflected in the capacity of ASO 192 to form retarded complex (32%) compared to the 4% of ASO 183. Likewise, while the ASO 213 led to 33% retarded complex, ASO 207 was only at 9.67% (Fig. 21A, B). The accessibility noted in the ASOs 183, 192, 207 and 213 were all aligned with the results obtained in SHAPE reactivity, microarray accessibility and RNA probing.

Hybridization to oligonucleotides printed in microarrays noted a highly accessible region in the 3´ region of the GNRA motif (Fernandez et al., 2011) and SHAPE reactivity also recorded reactive nts 181-183, 199-203 and 209-216 (Fernandez et al., 2011). RNA probing has similarly noted accessible nts in this region (Fernandez-Miragall et al., 2009). This suggests the presence of hairpin loops and internal bulges that may have hybridized by ASO. Meanwhile, the variations in the accessibility of the conserved motifs suggest that these regions were flexible.

Not to overlook the non-accessible regions, the results also noted non-accessibility in the D3 apical region. ASO 164 and 176, complementary to the stem and bulge upstream of the GNRA motif (Fig. 12C) recorded insignificant accessibility (1.25% and 0.33%, respectively). The lack of accessibility of these regions was however, similar to results of the microarray hybridization, suggesting that these regions may be involved in stable intra-molecular RNA-RNA interactions.

High accessibility was noted on the bulges located on the apical region. The 5´ apical region bulge recorded retarded probe efficiency of 12% (154) while the C-rich bulge has a higher efficiency at 20% (247). An intermediate to low accessibility was noted in the bulge that covers the region 265 (3%), compatible with RNA probing, SHAPE reactivity, and microarray hybridization.

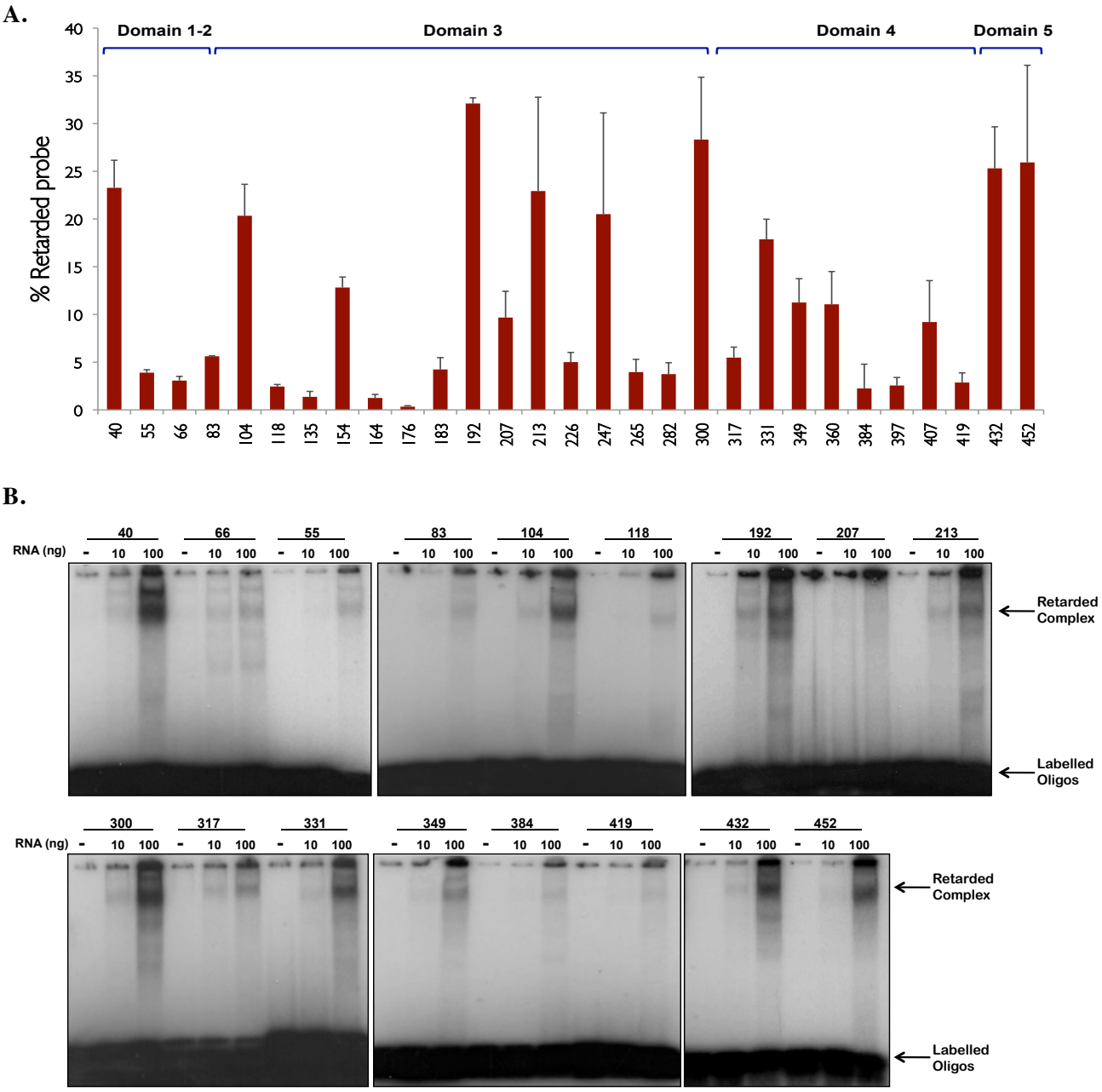

Figure 21. IRES-ASO complex formation. A. Percentage of retarded probe from interaction of FMDV IRES (100 ng) and γ-^{32}P labeled ASO complementary to the different regions of the IRES. Numbers correspond to each ASO. **B.** Representative autoradiogram of retarded complex autoradiogram using 10 and 100 ng RNA and 100nM of γ-^{32}P labeled AUG ASOs for 20min at 37ºC.

The ASO complementary to the stem of domain 3 efficiently formed a retarded complex with the RNA, ASOs 104 (20%) and 300 (28%) (Fig. 21A,B), consistent

with the reactivity showed by SHAPE analysis. This accessibility was presumably caused by unpaired nt in the spacer regions between domains. Very low or non-binders were noted on ASOs 118, 135 and 282, located in the stem of the domain 3.

III.IV Accessibility of domain 3 RNA suggests flexibility relative to the entire IRES.

To further understand the accessibility patterns of the central domain compared to the whole IRES, RNA retardation with labeled ASO bound to a transcript of domain 3 alone were performed under the same condition used in the full length IRES extended to the second AUG.

RNA mobility shift data revealed that the full length IRES and D3 alone showed some differences in accessibility. Notably, there was a 3 fold increase in the capacity to form retarded complex in the most distal parts of D3 with full length IRES in ASO 104 (20% to 66%) and a moderate increase in ASO 300 (25% to 40%) (Fig. 22), possibly a result of the loss of the spacer region between domains 1-2 and 4. This changes may have rendered the D3 more accessible than if it is joined by other domain in a full length IRES.

Another change was the accessibility in the vicinity of GNRA and the RAAA motifs, shifting from being more accessible in the full length RNA to less accessible in domain 3 alone. The change is quite noticeable in ASO 192, with a 3-fold reduction in accessibility (from 32% to 12%) (Fig. 22). Although to a lesser degree, RAAA motif also decreased its accessibility in the domain 3 alone compared to the full length IRES with ASOs 207 (9% to 6%) and 213 (22% to 9%). Meanwhile, in contrast to the decrease in the accessibility of 192, 207 and 213 regions, the ASO 183 had a 3-fold increase in accessibility from 4% to 12% (Fig. 22). The changes in the accessibility of the GNRA and RAAA could have been due to a change in its conformation, likely dependent on the presence of other domains.

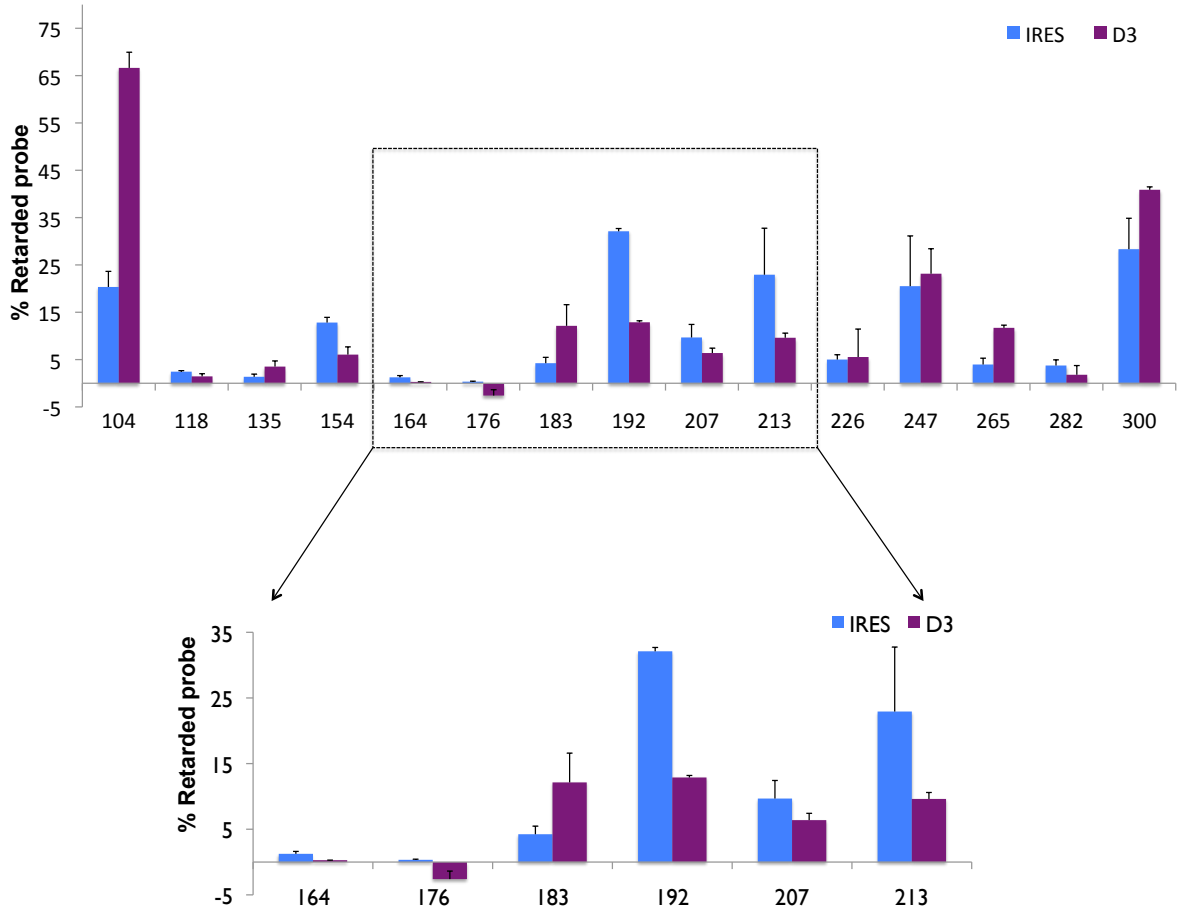

Figure 22. Comparison of accessibility of the whole IRES and domain 3. RNA retarded complexes of IRES RNA or D3 alone with γ-^{32}P labeled ASO. The numbers in the horizontal axis correspond to the ASO. The most apical region of the domain 3 is highlighted in a broken box.

III.V The integrity of the GNRA and RAAA motifs play an important role in IRES accessibility

The GNRA and RAAA motifs play a crucial in the organization of the IRES (Fernandez-Miragall and Martinez-Salas, 2003). Mutations in the GNRA and RAAA motifs were analyzed to understand the effect of a nucleotide change in the sequences of the conserved motifs to its accessibility. These mutations were ($G_{178}UAA_{181}$ to $G_{178}UAG_{181}$) in the GNRA motif and ($C_{198}AAAA_{202}$ to $C_{198}GCCC_{201}$) in the RAAA motif (Fernandez-Miragall et al., 2006) (Fig. 23). RNA complexes with labeled ASO displayed minor changes with ASO targeting the proximal base (104 and 300) as well as ASO 118, 135, 154, 265 and 282, targeting the proximal stem (Fig. 24A,B). These

regions registered similar levels of accessibilities observed both in the domain 3 wildtype and mutated domain 3. The same observation was noted in ASOs 164, 176, 226 and 247.

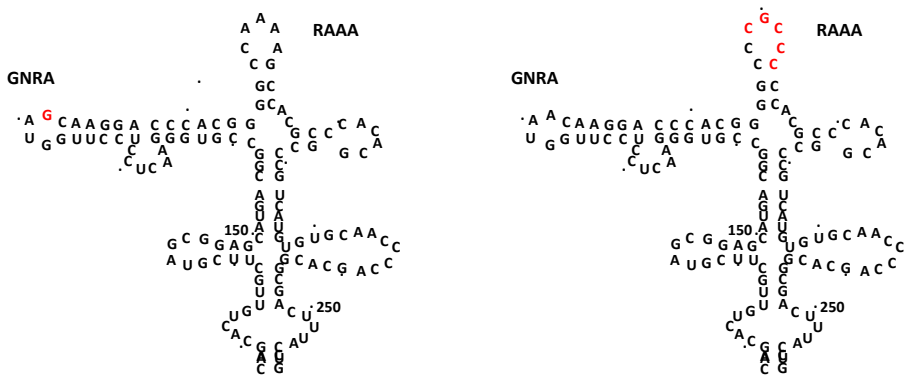

Figure 23. Secondary structure of RNAs carrying mutations in the GNRA and RAAA motifs. Mutations are depicted in red letters.

Significant increase in the accessibility in the domain 3 apical region was noted when ASO 183 and 192 were annealed to an IRES transcript with RAAA mutation. Compared with its accessibility in the wildtype domain 3, a 2-fold increase in accessibility occurred in ASO 192, while an increase (50%) was observed in ASO 183 (Fig. 24A, B). Although the changes that occurred in the GNRA accessibility were not identical in absolute values, the increased accessibility in this region indicates the loosening of RNA structure when the RAAA motif is mutated, making it more accessible to binding by the 183 and 192 ASOs.

Interestingly, the two RAAA ASO exhibited different pattern of accessibility when annealed to a RAAA mutated transcript. As compared with its accessibility in the domain 3, the ASO 213 had a 100% increase in accessibility while a 50% decrease was recorded by the ASO 207 (Fig. 24A,B). This is apparently due to the opening up the apical structure, as a result of the mutation in the RAAA motif, rendering it more accessible to accommodate the ASO (Fig. 23)**.**

A.

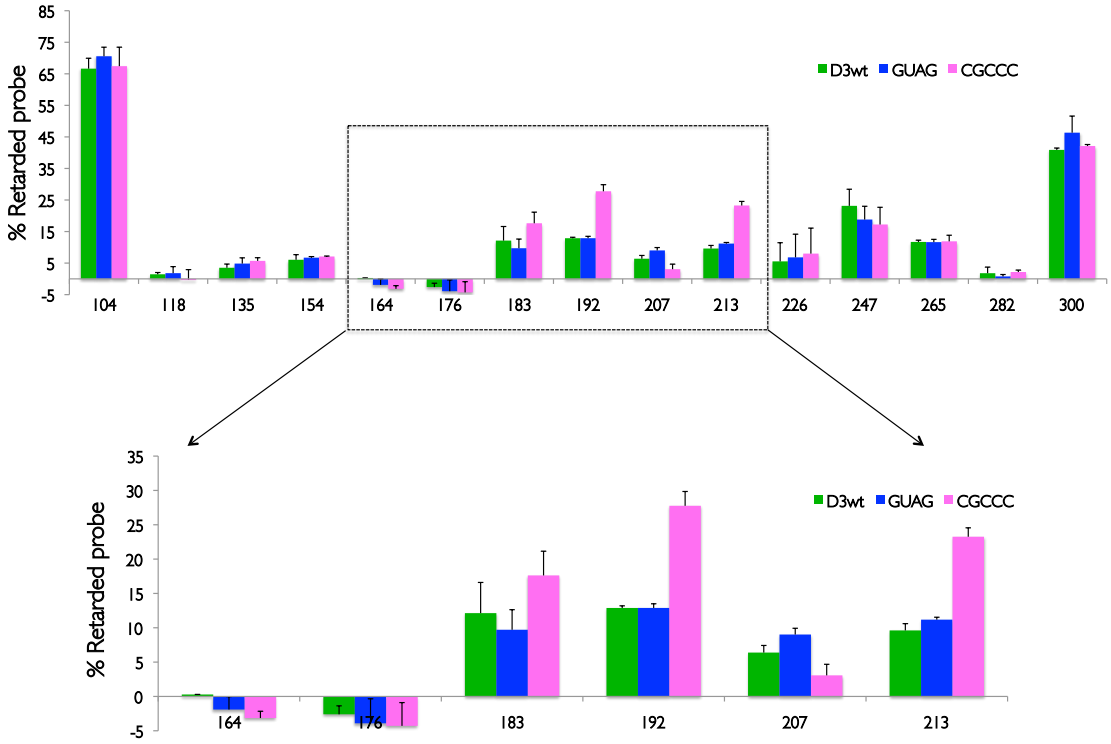

B.

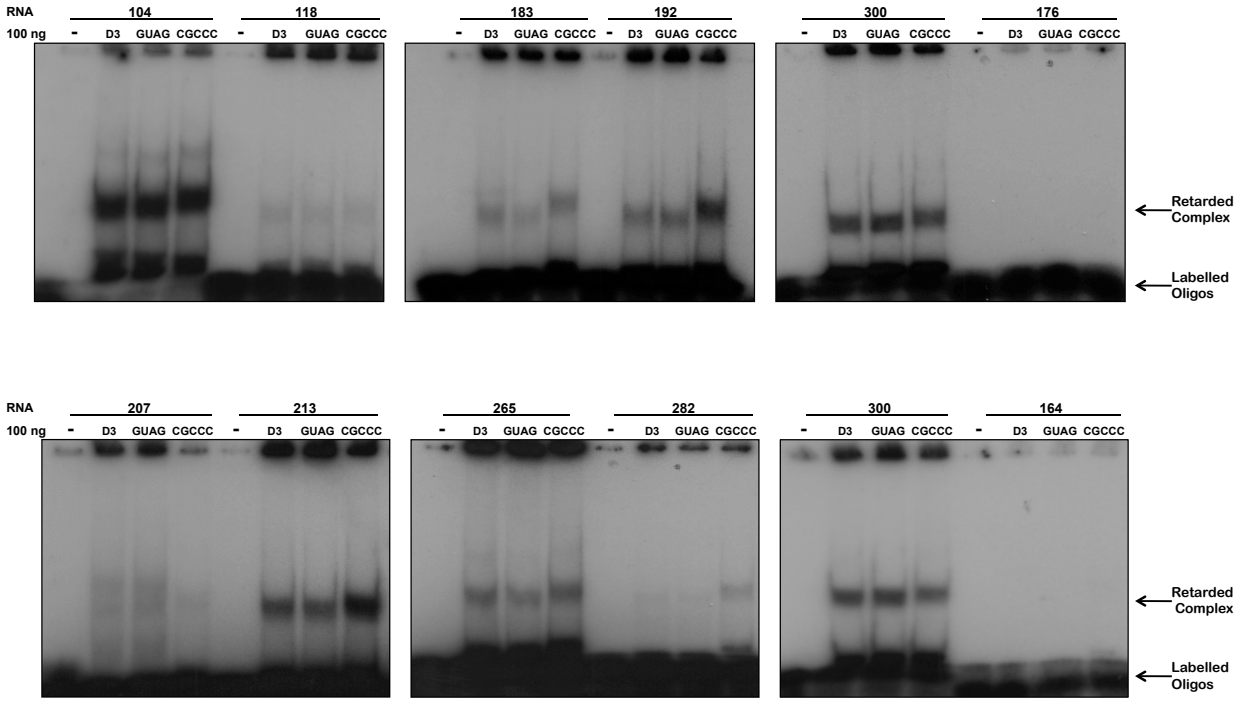

Figure 24. Accessibility of GNRA and RAAA IRES mutants A. Efficiency of RNA retardation of D3 wildtype, D3 GUAG, D3 CGCCC and γ-^{32}P labeled ASOs. **B.** Autoradiogram of retarded RNA complexes of (**A**). The numbers above the gel indicate ASO, and RNAs used.

In the case of the GNRA motif, a single nucleotide mutation in this region instigated a moderate degree of accessibility changes (30% decrease) in the ASO 183 (Fig. 24A,B). In contrast, the two ASO that bind to the RAAA motif increased its accessibility. ASO 207 registered a 50% increase in accessibility while ASO 213 had a 20% increase (Fig. 24A,B). Consistent with the findings of previous researches, this is possibly due opening of the RNA structure in the GUAG RNA making it more accessible (Lopez de Quinto and Martinez-Salas, 1997). Additionally, the changes observed in the accessibilities of the 4 ASO interacting in the mutant apical region of the central domain, 183, 192, 207 and 213 reinforces the relevance of the RNA structure of this region for IRES activity.

Discussion

I. IRES as a tool in controlling viral gene expression

The IRES region proves to be a useful target for antisense RNA and DNA against picornaviruses (Bigeriego et al., 1999; Kahana et al., 2004; Rosas et al., 2003; Stone et al., 2008; Vagnozzi et al., 2007) because this group of viruses depends on the correct conformation of the IRES to initiate translation, the first step of infection. Not to compare with the specificity of chemical or enzymatic methods to explore accessibility, antisense oligonucleotides can detect conformational changes occurring in the IRES relative to its critical role in translation.

The IRES is a complex RNA structure present in the genome of all picornavirus (Belsham, 2009; Martinez-Salas, 2008). Capable of recruiting translational machinery internally without the need for a cap-structure, most picornavirus IRESs possesses conserved motifs despite being organized in 4 types of RNA structure (Belsham, 2009; Fernandez-Miragall et al., 2009). This includes the GNRA motif that adopts a tetraloop conformation and has been proposed to be involved in a tertiary RNA interactions, a C-rich loop (essential for IRES activity in enterovirus and rhinovirus but not aphthovirus and cardiovirus), a RAAA motif (contributes to the correct folding of the EMCV and FMDV IRES) and a polypyrimidine rich tract (12-15 nt in FMDV, EMCV and PV) that lies about 20-25 nts upstream of AUG starting site (Belsham and Sonenberg, 1996; Fernandez-Miragall et al., 2009; Pilipenko et al., 1992).

Secondary RNA structure of the IRES has been mapped previously (Fernandez et al., 2011; Fernandez-Miragall and Martinez-Salas, 2003; Fernandez-Miragall and Martinez-Salas, 2007) but the IRES accessibility in relation to its inhibitory capacity of gene expression seeks further investigation. Inhibition of FMDV RNA translation and using short sequences targeted to the 5´UTR or 3´UTR of the viral genome has been performed with promising results (Rosas et al., 2003; Vagnozzi et al., 2007). Similar works were also done inhibiting viral multiplication by targeting the different region in the FMDV such as VP1 (Lv et al., 2009) (Chen et al., 2004), 2B and 3C (Kim et al., 2008), 2B and 3D (Pengyan et al., 2008) and 3B and 3D (Kahana et al., 2004). Short sequences of RNA also provided support on the possible utilization of antisense as antiviral agent. Poliovirus protein synthesis was inhibited when blocked in the IRES region (Stone et al., 2008) and in the viral capsid or polymerase sequence

(Gitlin et al., 2002) Hepatitis A (Kusov et al., 2006) (Kanda et al., 2004) and coxsackievirus B3 (Schubert et al., 2005) (Yuan et al., 2005; Yuan et al., 2006) viral genome were significantly silenced by short sequences of RNAs blocking critical regions in the ORF. Protein expression and viral replication were likewise reduced when complementary short RNA sequences were used against hepatitis-C virus (Deas et al., 2005; Gonzalez-Carmona et al., 2010; Jopling et al., 2005; Wakita et al., 1999; Zhang et al., 1999).

Similar studies have also been done to inhibit viral replication of many pathogens including Ebola virus (Enterlein et al., 2006), Influenza A (Ge et al., 2006), H5N1 virus (Jin et al., 2011), HIV (Gu et al., 2006; Liu et al., 2011), Dengue virus (Kinney et al., 2005), human papilloma virus (Jiang and Milner, 2002) or SARS virus (Neuman et al., 2005). Inhibitions were performed through the use of antisense RNA or DNA, siRNA, morpholino, phosphodiester derivatives and LNA or DNA chimera as well as high affinity ligands (Darfeuille et al., 2004; Watrin et al., 2009a; Watrin et al., 2009b) targeting different regions of the viral genome.

New approaches taking advantage of the accessibility of the IRES region to inhibit viral replication by blocking genome expression will provide insights on the relationship of RNA structure and function. Early in the RNA reorganization, stable secondary structure form first in the folding process (Sorin et al., 2002) a step critical for the proper conformation of large biologically active RNA sequences (Butcher et al., 1997). Therefore, exploring the IRES accessibility by ASO and further use accessible regions to inhibit viral multiplication provides a useful tool to better understand its overall structure. Rather important also is the unveiling of the RNA accessibility in the context of the viral RNA, the complete IRES sequence as well as transcripts encompassing the central domain alone. In this study, we investigated the accessibility of the IRES region to 2´O-methyl modified ASO and make use of this accessibility pattern to analyze its relationship to the capacity of the ASO to inhibit protein synthesis

II. Differential responses of the two AUGs to ASOs depend on the RNA secondary structure

The capacity of the ASO to inhibit translation was first explored using the bicistronic RNA CAT-IRES-luciferase translated *in vitro* in the presence of AUG and Scr ASO. Similarly, we have analyzed the inhibitory potential of the ASO to affect *in vitro* translation of RNA, encoding a cDNA copy of FMDV genome. We have observed that the inhibitory capacity of the AUG1 and AUG2 ASOs is in accordance with the inhibitory pattern of FMDV infection by targeting this viral region using antisense DNA or RNA (Gutierrez et al., 1994; Vagnozzi et al., 2007).

Although the mechanism of how the ribosome recognizes the two start codons to initiate translation is under debate, the results we obtained here is fully consistent with data demonstrating that by blocking the AUG1 and AUG2 start codons, the progress of FMDV viral synthesis can be halted (Gutierrez et al., 1994; Rosas et al., 2003; Vagnozzi et al., 2007). This is similar to protein synthesis inhibition of other RNA viruses when targeted at their main AUG starting site, such as HCV (el-Awady et al., 2006; Hanecak et al., 1996), alphavirus (Paessler et al., 2008), influenza virus (Hatta et al., 1998), coxsackievirus B3 (Yang et al., 1997) and HIV (Inagawa et al., 2002; Park et al., 2000). In addition, it is shown here that the AUG2 is the critical starting site, as shown by a low virus yield in the presence of the AUG2 ASO (Fig. 15). This occurs in spite of its lower degree of accessibility compared with AUG1 (Fig. 20). Consistent with this observation, AUG2 has been shown to be the preferential starting site of protein synthesis (Andreev et al., 2007; Cao et al., 1995; Lopez de Quinto and Martinez-Salas, 1999). Despite AUG1 starting site shows higher accessibility in the mobility shift assay, and thus could have higher potential of being blocked by the ASO, the results showed a higher virus yield in the presence of its complementary ASO, denoting that the translation mechanism keeps using the AUG2 as starting site when AUG1 is blocked.

On the other hand, in the *in vitro* translation, the FMDV polyprotein is continually synthesized in the presence of the AUG2 ASO, suggesting a shift of translation to start at AUG1 when the AUG 2 is disturbed (Fig. 13A, C), consistent with previous studies (Vagnozzi et al., 2007). The use of AUG1 triplet has been demonstrated *in vitro* where severe reduction of polypeptides occurred by interference

of the AUG1, despite its higher accessibility (Fig. 13A,B and 20A,B). The higher accessibility of the AUG1 region was in agreement with RNA probing (Andreev et al., 2007) suggesting that the AUG1 is located in a single stranded region (Fig. 25). In contrast, the continued translation of viral polyprotein *in vitro* in the presence of AUG2 ASO may be due to its poor accessibility (Fig. 20A,B), being located in a double stranded region (Fig. 25) (Fernandez-Miragall et al., 2009).

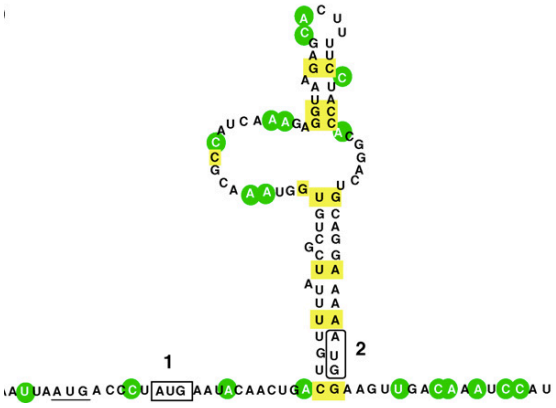

Figure 25. Secondary structure of the FMDV translation initiation region. The positions AUG1 and AUG2 are depicted by rectangles. DMS attacks are depicted by green circles, and yellow boxes depict nucleotide covariation (Fernandez-Miragall et al., 2009).

III. IRES accessibility and its correlation with inhibition of protein synthesis

The inhibition of IRES activity *in vitro* provided deeper understanding on its structure and role in protein translation. IRES regions blocked by the ASOs proved the need for an interaction either with RNA sequence within the IRES (inter and intra-domain), with other RNA regions within the whole genome, as well as disruption of RNA-protein interactions. Moreover, the two AUG regions have proven their important role in translation manifesting the most severe inhibition of protein synthesis. In the whole IRES, however, critical regions also exist as shown by the inhibition of gene expression, some of which had disruption as severe as the AUG.

III.I Potent inhibitory ASOs and accessibility to its target sequence

Protein synthesis inhibition demonstrated several IRES regions susceptible to ASO disruptions distributed in all domains, with domain 5 as the most susceptible

target, both in the bicistronic and FMDV RNA. Moreover, of the 9 ASOs inhibitory *in vivo*, only 4 were potent inhibitors at an extended time in BHK 21 cells with comparable inhibition to AUG ASOs (Fig. 19). Non-inhibitory targets, on the other hand, are dispersed all along the IRES region.

A.

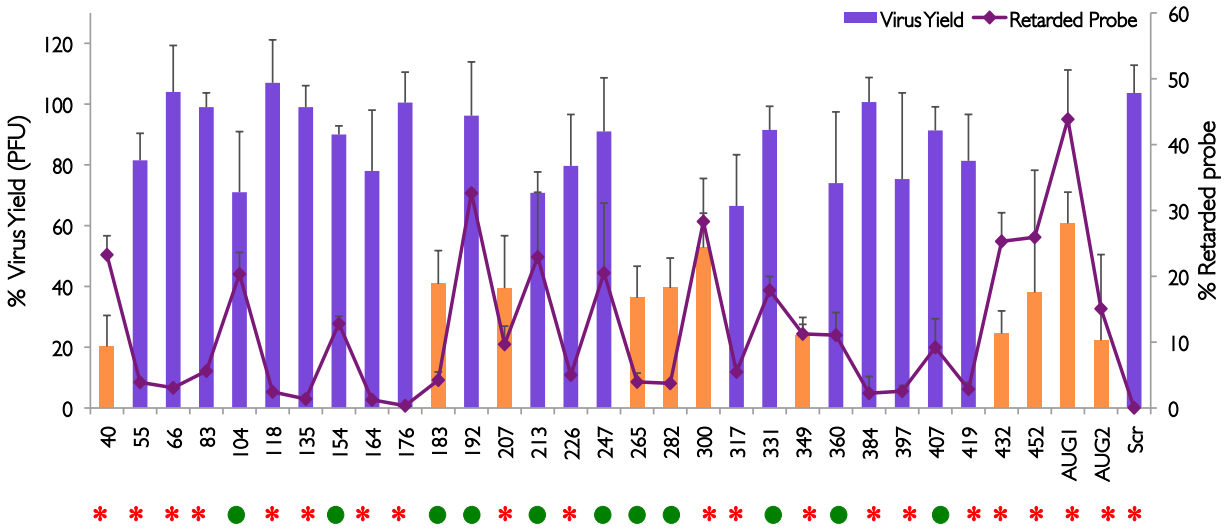

B.

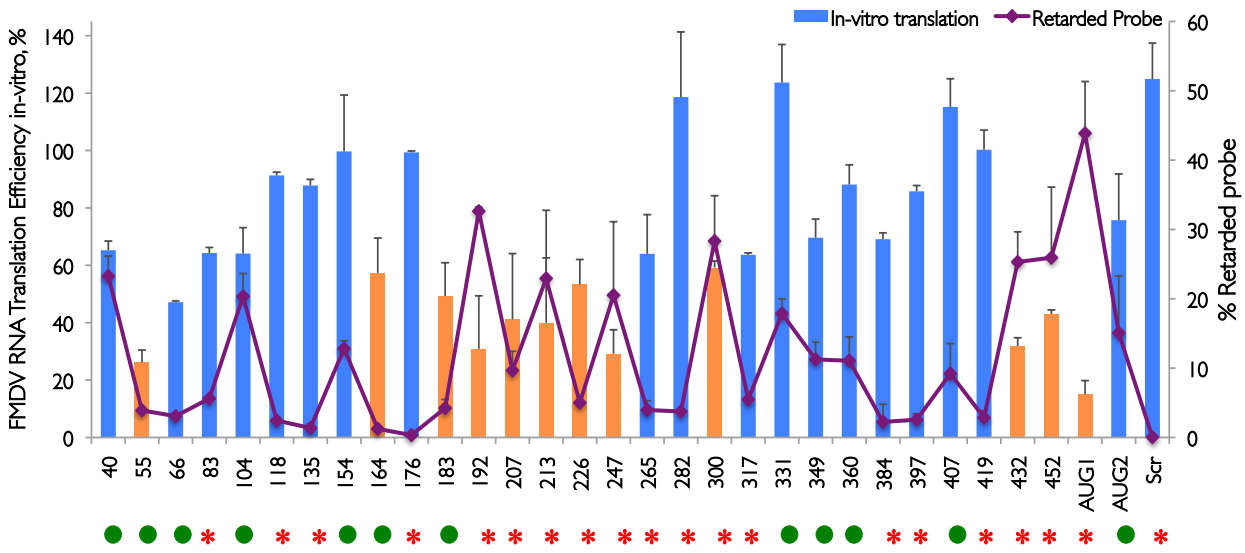

Figure 26. Correlation of IRES accessibility to ASO and RNA translation *in vitro* and *in vivo* A. Correlation of IRES accessibility to ASO and inhibition of viral yield. Green circle depicts direct relationship between accessibility and inhibition while red asterisk depicts inverse relationship. **B.** Correlation of IRES accessibility to ASO and inhibition of RNA translation *in vitro*. Orange bars are the inhibitory ASOs.

A strong inhibitor of protein synthesis in the cellular environment, comparable to the AUG2 ASO, was ASO 40 complementary to domain 1-2 (ASO 40) (Fig. 26). The extended inhibition *in vivo* suggests the presence of a sequence in the proximal region of domain 2 critical for RNA-RNA interactions or protein binding, sensitive to the interference of the ASO 40. *In vitro* however, the translation of FMDV RNA with this ASO was less inhibitory, with values close to 60% (Fig. 26). It is important to note that ASO 40 is complementary to the 15 nucleotides at the 5´proximal region of the IRES domain 1-2, which is also the continuation of the *cre* element, essential for viral replication of FMDV (Mason et al., 2002), PV (Goodfellow et al., 2000; Paul et al., 2000; Rieder et al., 2000) and HRV (Gerber et al., 2001; McKnight and Lemon, 1998). Pairing of the ASO 40 to its complementary sequence in the domain 1-2 may have halted viral replication, thus, resulting to a reduced virus yield, which was not possible to observe in the *in vitro* translation.

Regarding the inhibitory effect of ASO 40, the mobility shift assay showed a highly accessible region in the left proximal region of domain 1-2 and a lower accessibility in the hairpin and right proximal part (Fig. 21), congruent with the RNA accessibility displayed in microarray and RNA probing (Fernandez et al., 2011; Fernandez-Miragall et al., 2009). The higher accessibility of domain 2 left proximal region showed an inverse relationship with *in vivo* inhibition of viral gene expression and a direct relationship with *in vitro* translation, while the lower accessibility of the hairpin and right proximal sequence and higher protein translation suggests an inverse relationship (Fig. 26). This discrepancy between accessibility and inhibition may be explained by the interaction of PTB host factors, needed for internal initiation (Luz and Beck, 1991).

A significant observation was similarly noted in regions where ASOs anneal to domains known to bind host proteins. FMDV and bicistronic RNA protein synthesis was potently halted *in vitro* and *in vivo* when domain 5 anneal to its complementary sequence with ASO 432 and 452. Likewise, blocking of domain 4 by the ASO 349 has significantly inhibited translation of the bicistronic RNA *in vitro* and FMDV RNA *in vivo*, indicating that, domains 4 and 5 are critical for IRES function (Fig. 26). The consistency of the two ASO complementary to domain 5 to inhibit translation of both constructs, in solution or inside the cell, stresses its relevance in the global

function of the IRES. Domain 5 is located upstream of the first starting AUG of the viral polyprotein. Thus, the ASOs may have severely affected the assembly of the translational machinery near the AUG triplet. Further, this potent inhibition, extended at a longer time, may connote the presence of a critical region that is susceptible to structural disruption by external factors. This result is in agreement with previous researches, with similar inhibition in this domain observed when blocked by antisense DNA or RNA (Rosas et al., 2003; Vagnozzi et al., 2007).

Comparing *in vitro* and *in vivo* inhibition of translation by ASO complementary to domain 5 relative to IRES accessibility by mobility shift, an inverse relation is noted (Fig. 26). Furthermore, accessibility of domain 5 region by RNA mobility shift confirmed RNA accessibility in microarray and RNA probing (Fernandez-Sanchez, 2010). The efficient binding of the ASO to its complementary RNA sequence could have prevented domain 5 to have contact with host proteins eIF4B, eIF3 and PTB required for IRES-dependent initiation (Lopez de Quinto et al., 2001; Pacheco et al., 2009).

ASO 349, complementary to the J stem-loop of domain 4, defines an efficient target at extended times, an exception with the rest of domain 4 regions (Fig. 26**).** The potent inhibition recorded, in spite of moderate level of accessibility (Fig. 21), indicates the presence of a sequence highly susceptible to external disruption. The ASO may have blocked the binding of eIF4G, resulting in the failure of the protein to recognize its binding region. eIF4G binds the IRES through its RNA recognition motif (Lopez de Quinto and Martinez-Salas, 2000). Accessibility of this region by mobility shift **(**Fig. 21**),** microarray (Fernandez-Sanchez, 2010) and RNA probing (Fernandez-Miragall and Martinez-Salas, 2007) confirmed the ability of the nts in this domain to anneal to its complementary ASO. An inverse relationship can be noted in ASO 349 with the higher accessibility relative to a potent inhibition of virus yield.

Among the IRES regions, domain 4 has the larger number of non-inhibitory ASO in the FMDV RNA (Fig. 26), likely owing to its function as target of cellular proteins (Hellen and Sarnow, 2001; Lopez de Quinto and Martinez-Salas, 2000; Saleh et al., 2001; Yu et al., 2011). Cell free RRL has limited available supply of cellular proteins in comparison to cell cytoplasm. The diverse result of the bicistronic and FMDV RNA translation inhibition can be further explained by differences in the

abundance of host proteins inside the cell that can protect its binding site in the FMDV RNA from inhibition of the ASO. Moreover, inter-domain contacts (Ramos and Martinez-Salas, 1999) can also contribute to the protection observed in the FMDV RNA translation, but not in the bicistronic RNA. On the other hand, high efficiency translation and virus yield in the presence of the ASO complementary to domain 4 showed an inverse relation with the low accessibility by mobility shift assay (Fig. 26) which is in agreement with the low accessibility obtained by RNA probing and SHAPE (Fernandez et al., 2011).

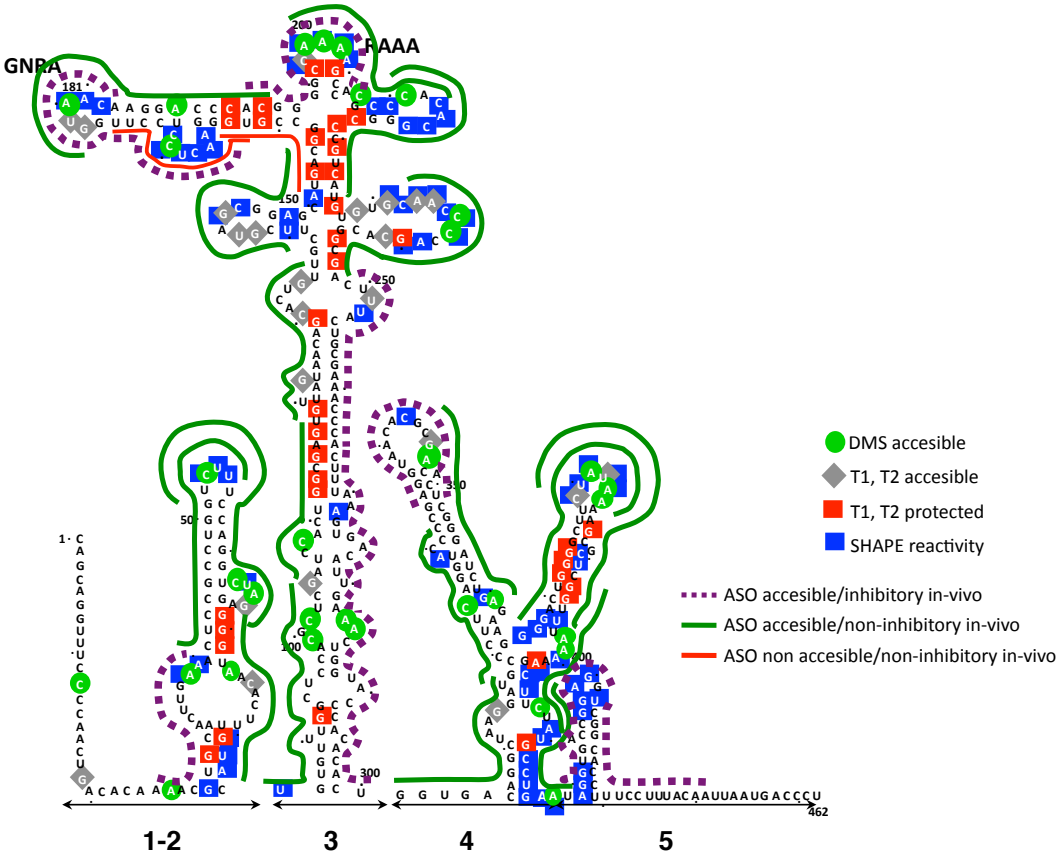

Figure 27. Summary of the IRES secondary structure showing accessibility to ASO *in vivo*.

The non-inhibitory pattern was similarly observed in ASO targeting the double stranded region of the domain 3 (Fig. 27 and 28). This RNA structure may also play a role in the binding of ITAFs as this region is proposed as the binding site of the Ebp1 (Pacheco et al., 2008; Yu et al., 2011). Higher *in vitro* translation activity and virus yield correlates inversely to its lower accessibility, both by mobility shift assay (Fig.

26) and low accessibility in microarray (Fernandez-Sanchez, 2010). In the 3´ proximal sequences, the low virus yield obtained in the presence of the ASO complementary to this region indicated the sensitivity of this area to ASO modification. The reason for the differences between the 5´and 3´region of domain 3 are not known.

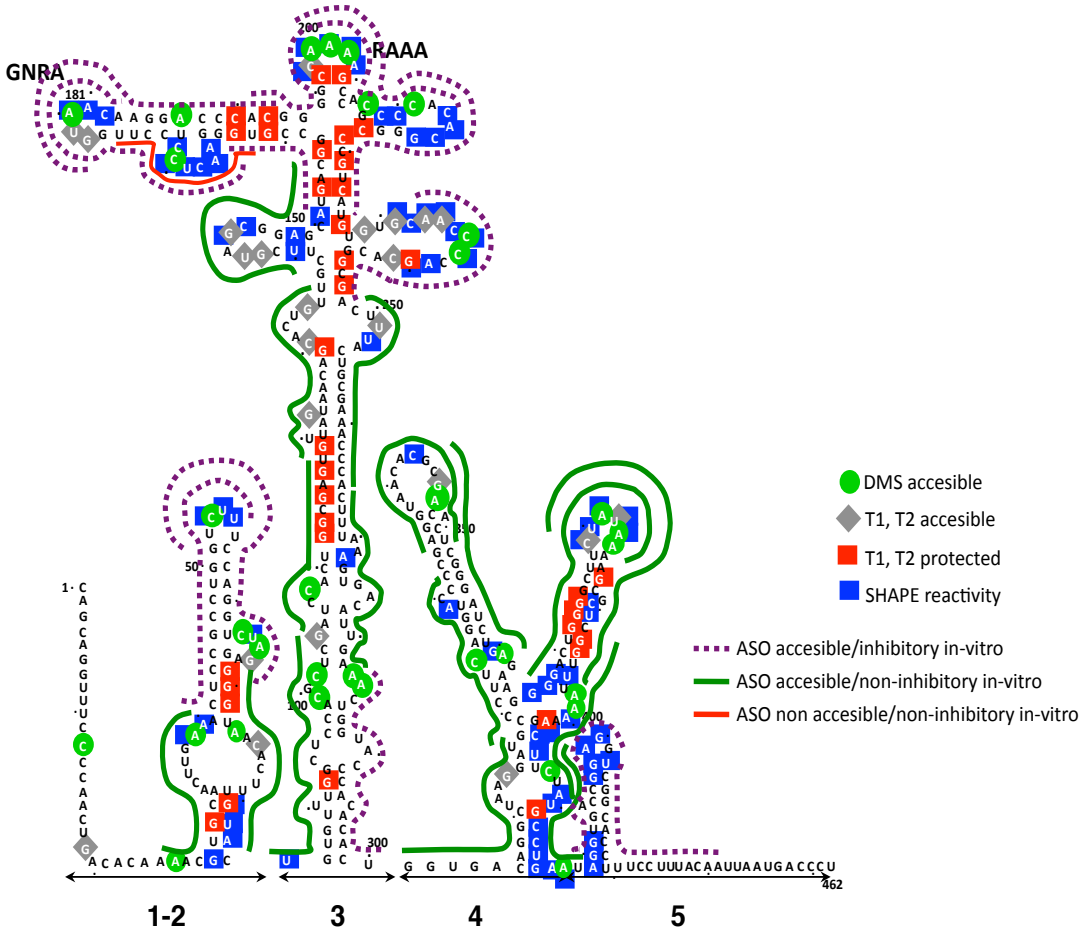

Figure 28. Summary of the IRES secondary structure showing accessibility to ASO *in vitro*.

III.II Relationship between accessibility and inhibition in the IRES conserved motifs

The inhibitions observed when analyzing the central region were mostly from ASO targeting the apical region, where conserved motifs are situated. Inhibition was potent in the region of the GNRA and RAAA motifs, but not in the C-rich motif, both *in vitro* and *in vivo* (Fig. 26). The GNRA motif located in the apical region of the domain 3 is essential for IRES activity (Lopez de Quinto and Martinez-Salas, 1997).

We have found that ASOs complementary to this motif exhibit different inhibitory results. The differential accessibility of the GNRA region was revealed by using two ASO, one is complementary to the GNRA 3´ side (192) while the other is complementary to the GNRA 5´ side (183) (Fig. 26A). The bicistronic RNA translation efficiency was severely affected by the 192 ASO but was not halted by the 183 ASO (Fig. 12). However, in viral RNA, both were able to reduce translation efficiency *in vitro* but only the ASO targeting the 5´side of the GNRA (183) was inhibitory *in vivo* (Fig. 27 and 28). The shift of the response of the ASO 192 from a more inhibitory in *in vitro* to non-inhibitory *in vivo* while maintaining the inhibition of the ASO 183, suggests that differences exist in the local conformation of the apical region. Previous experiments showed that the domain 3 is involved in intra-domain (Fernandez-Miragall and Martinez-Salas, 2003; Fernandez-Miragall et al., 2006), in inter-domain contacts (Ramos and Martinez-Salas, 1999) and in viral 3´ UTR RNA-RNA interactions (Serrano et al., 2006), that can contribute to the differences observed between the bicistronic and the FMDV RNA.

The RNA conformation of the central domain was analyzed by the differences in accessibility to dimethyl sulfate, both *in vitro* and *in vivo* (Fernandez-Miragall and Martinez-Salas, 2007). Changes in local reorganization of the apical region were further supported by UV-psoralen crosslink (Fernandez-Miragall and Martinez-Salas, 2007).

Taking into consideration the inhibition showed by the two ASOs complementary to the GNRA hairpin in the bicistronic RNA and FMDV RNA, it could be deduced that the more critical region of the GNRA hairpin geared towards the 5´ side, as evidenced by the inhibitory effects of the ASO 183. However, the changes from the inhibitory *in vitro* to non-inhibitory *in vivo* of the ASO 192, complementary to the 3´side of the GNRA hairpin, and its high accessibility compared with the 5´ end, suggest that this region is involved in intramolecular interactions occurring in the apical region of the central domain.

The non-inhibitory effect of ASO 176, that anneals to the bulge of the GNRA hairpin, in *in vitro* and *in vivo* of both bicistronic and FMDV RNA (Fig. 26) denotes that this region is likely engaged in a tight RNA-RNA interaction that cannot be disturbed by the ASO. This premise is further supported by the absence of protein

interaction in this region as well as the lack of accessibility in the mobility shift assay (Fig. 26), as also observed in RNA accessibility in the microarray assay (Fernandez-Sanchez, 2010). This hypothesis, however, may require further studies to provide molecular explanations.

Meanwhile, the shift in the inhibitory pattern of ASO 247 complementary to the C-rich motif, *in vitro* and *in vivo* (Fig. 26) could be attributed to the protection offered by host proteins, consistent with the proposal that this conserved region binds to poly-C binding protein (PCBP) (Pacheco et al., 2008; Walter et al., 1999).

The RAAA motif is a conserved purine-rich motif that, along with the GNRA, is thought to be involved in the correct folding of the IRES (Fernandez et al., 2011; Martinez-Salas, 2008). It is well establish that to perform its function, the RNA must conform into a three-dimensional structure stabilized by tertiary contacts (Batey et al., 1999; Tinoco and Bustamante, 1999). Tertiary contacts between distant RNA sequences were observed in the FMDV IRES (Fernandez-Miragall et al., 2006). Different from the inhibitory pattern generated by the ASOs complementary to the GNRA, translation is greatly reduced when the RAAA region is blocked by ASO from either 5´ or 3´ side both in the bicistronic and FMDV RNA (Fig. 26, 27 and 28). The reduction in translation efficiency signified the participation of these sequences in IRES activity that is sensitive to the disturbance of the ASO. Conversely, the reduction of virus yield was only noted in ASO 207 complementary to the 5´ side of RAAA (Fig. 26). This is an indication that this conserved motif is involved in biologically relevant RNA interactions.

The RNA mobility shift assay has demonstrated that nts in the most apical region of the central domain were accessible to ASO (Fig. 21)**,** owing to the presence of bulges and hairpins. The virus yield inhibition by the 3´side of the GNRA and RAAA conserved motifs ASO 192 and 213 indicates a direct correlation between high accessibility and virus yield, while an inverse correlation is noted in ASO 183 and 207 (Fig. 26). The accessibility in the RNA mobility shift assay of the GNRA, RAAA and the C-rich motifs is consistent with RNA probing (Fernandez-Miragall and Martinez-Salas, 2003; Fernandez-Miragall and Martinez-Salas, 2007) while in the microarray assay, the accessibility was noted in the GNRA and C-rich motifs but not in the RAAA (Fernandez-Sanchez, 2010).

III.III The 5´ side of the GNRA and RAAA stem loop are candidate targets to inhibition of ASOs.

The reduced translation *in vitro* and low virus yield *in vivo* showed that the ASOs targeting the GNRA and RAAA motifs were able to inhibit protein synthesis both, in bicistronic RNA and FMDV RNA with different degree of potency. While the 3´and 5´ directions of both motifs proved to be inhibitory if blocked by the ASO *in vitro*, only the 5´ nts in these regions (183 and 207) were inhibitory *in vivo* (Fig. 26), conveying the presence of critical sequences in the 5´side of the two motifs.

The high inhibitory capacity (low virus yield), yet low and moderate accessibility of 5´ side of GNRA and RAAA motifs (Fig. 26), further support the idea that this region is playing a key role in getting hold of a correct IRES conformation inside the cell. The low accessibility implied that even a slight disturbance in this region might cause a severe effect on translation. In support of this theory, attacks by DMS in the nts located in the 5´ side of the RAAA motif were noted *in vivo*, indicating the accessibility of this region inside the cell (Fernandez-Miragall and Martinez-Salas, 2007).

IV. The apical region of the IRES central domain adopts a flexible structure

The different regions of the IRES exhibited distinct capacity to form retarded complex with their respective complementary ASO in the context of a complete IRES extended to the 2nd AUG, with the AUG1 shown as the most accessible region.

According to the RNA complex formation, the full length IRES and D3 wild type also showed changes in degree of accessibility. Most notably, the changes in the most distal parts of the D3 wildtype became more accessible (104 and 300) (Fig. 21**),** possibly as a result of the removal of the preceding and succeeding nts from the domain 1-2 and domain 4. Another remarkable change is the lesser accessibility noted in the 3´GNRA and the 3´RAAA regions with their complementary ASOs 192 and 213, shifting from more accessible in the full length RNA to a far less accessible in domain 3 wildtype (Fig. 22**)**. This change also occurred in the accessibility RAAA motif with ASO 207, although to a lesser degree. Subtle changes in accessibility of the GNRA and RAAA region could have been due to a change in the conformation

dependent on the presence of other domains. Loss of long-range RNA-RNA interactions may have affected the conformation of the GNRA hairpin and RAAA stem-loop.

Evidences of the RNA flexibility in the apical region were observed when the integrity of the apical region is challenged. Mutating the GNRA motif to GUAG did not bring any changes in the accessibility of the nts around the 3´ end of the GNRA hairpin (Fig. 22 and 23). However, the decrease in the efficiency of the ASO 183 binding, suggests changes in the RNA folding if mutated to GUAG, possibly by altering the pairing of GNRA motif to other receptor region. This decrease was comparable to the diminished RNA-RNA interactions between a GUAG oligonucleotide with the wildtype domain 3 done previously (Fernandez-Miragall and Martinez-Salas, 2003). In contrast to the GNRA motif, a slight elevation of accessibility was noted in the RAAA motif in GUAG mutant IRES (Fig. 22 and 23), indicating that the RAAA stem-loop may have loosened its structure as a result of the GUAG mutation. Relative to this finding, a mutation in the GUAG also caused a gross reorganization of the RAAA probed by RNase T1 digestion, loosening the base-pairing in RAAA stem (Fernandez-Miragall and Martinez-Salas, 2003).

Conversely, an increase in the accessibility of the target region of ASO 183, 192 and 213 was observed in the RAAA mutant (Fig. 22 and 23). The increase in accessibility of the GNRA motif in the CGCCC IRES mutant may insinuate a reorganization caused by the mutation due to the loss of RNA-RNA contact between sequences in the apical region with their receptors. It has been proposed that GNRA tetraloop interacts with a C:G pair as its receptor RNA (Jaeger et al., 1994; Michel and Westhof, 1990) and reorganization of the apical region due to mutations deviates it from the tetraloop structure (Fernandez-Miragall et al., 2006).

RNA structure of the IRES shows a double-stranded, G:C rich sequences in the 5´ side of the GNRA motif (Fernandez-Miragall et al., 2009). The inaccessibility of ASO 164 and 176 in the whole IRES, D3 alone or IRES mutants is highly indicative of the integrity of these regions (Fig. 21, 22 and 24). The consistent inaccessibility of the 176 ASO is in contrast to the reactivity results obtained in the SHAPE analysis (Fernandez et al., 2011), while the inaccessibility of the 164 region is consistent with the findings of a base-paired nts protected from the RNase T1 attack (Fernandez-

Miragall and Martinez-Salas, 2003). The translation efficiency *in vitro* and high virus yield *in vivo* also confirmed the inaccessibility of these regions to ASO. Future experiments exploring RNA organization of these region using newer technologies may provide explanation for the variation in accessibilities shown by different approaches.

V. Concluding remarks

Previous efforts to reveal IRES regions protected or susceptible from attacks have provided insights on RNA structure and its role in the translation process. RNA probing (Fernandez-Miragall et al., 2009) and SHAPE (Fernandez-Sanchez, 2010) data has provided detailed information on the presence of accessible nts in the IRES elements. Incorporating the results obtained in this study will provide stronger evidence on the complexity and critical function of the FMDV IRES in gene expression.

A secondary structure of the IRES with the accessible and protected nts revealed by RNA probing, SHAPE and ASO accessibility is provided in (Fig. 27 and 28). The inhibition exhibited by the ASO complementary to the 3´region of the IRES (domain 5), where the bulk of the eIFs and host factors congregate (Pacheco and Martinez-Salas, 2010) has highlighted the importance of this region in the translation process. A potent inhibition in the translation of poliovirus genome was achieved by blocking the 3´region of the PV IRES using morpholino oligomers (Stone et al., 2008), similar to the inhibition observed in the ASO complementary to the 3´region of the FMDV IRES obtained in this study.

Correlation of accessibility with inhibition of viral gene expression has been done by exploring the viral genome of HCV with a siRNA (Sagan et al., 2011). Taking into consideration that their work covers only one region of the HCV IRES, their results were similar to ours (with some exceptions) in that regions with less accessibility were less likely to be inhibited or disrupted in their functions. Thus, will have higher translation efficiency, while more accessible regions were likely to be inhibited.

The reduced translational efficiency *in vitro* and low virus yield *in vivo* have

further demonstrated the capacity of the ASO to abrogate the translational capability of the IRES either by preventing its correct conformation or physically blocking the binding of host proteins. This ASO-IRES hindrance can be put into perspective to control FMDV viral gene expression. Specific target sequences of the IRES element, aside from the two AUGs, as portrayed in this study, can be useful to down-regulate viral gene expression to a level that can be effectively used for viral infection control.

Variation in the accessibility of the central domain to ASO when mutations introduced in the GNRA and RAAA conserved motifs has proven that the IRES engages in a intra-molecular adjustments when its primary sequence in the domain 3 apical stem-loops are challenged.

The relevance of the IRES element for protein synthesis has been proven in many studies (Belsham and Brangwyn, 1990; Borman and Jackson, 1992; Brown et al., 1994; Fernandez-Miragall and Martinez-Salas, 2003; Glass et al., 1993; Kuhn et al., 1990; Pfingsten and Kieft, 2008). The discovery of the IRES existence in picornavirus genome has paved the way for an alternative view on translation initiation apart from the accepted belief of cap-dependent translation (Belsham, 2009; Fernandez-Miragall et al., 2009; Jang et al., 1988; Pelletier and Sonenberg, 1988). Furthermore, a number of studies controlling viral protein synthesis have proven to be effective against viral multiplication by targeting the highly structured IRES or other part of the viral genome in picornaviruses and other viruses by antisense RNA, DNA or its derivatives and modifications. This has also provided us alternative strategies against a vast range of pathogenic RNA and DNA viruses that pose serious threat to humans and animals (Haasnoot and Berkhout, 2009; Lim et al., 2006; Mescalchin and Restle, 2011; Spurgers et al., 2008)

The results obtained in this study has provided information on essential targets to interrupt IRES function. Therefore, these targets can be an effective tool in controlling the FMDV infection. This work further supports the concept of the relevance of IRES folding and its critical role in gene expression.

CONCLUSIONS

Down-regulation of FMDV IRES-dependent translation proves the existence of susceptible regions in the 5´UTR of the viral RNA critical for the expression of the FMDV genome.

FMDV AUG1 and AUG2 start codons behave differently *in-vitro* and *in-vivo*. AUG1 start codon is the most accessible region while AUG2 is the most susceptible to inhibition. FMDV genome is expressed *in-vivo* through AUG2 if the AUG1 ASO is present, while it is abrogated if AUG2 is blocked.

Each domain of the IRES element possesses critical sequences capable of influencing the global function of the IRES. These critical regions can be exploited to command the IRES role in FMDV virus infection.

The inhibition of IRES element translation exhibited by the ASO relative to its accessibility revealed an inverse relationship with few exceptions.

ASO-dependent Inhibitions are limited to specific regions of the IRES. The inhibition showed by ASO complementary to the GNRA and RAAA motifs, domain 5, J stem-loop of domain 4 and the proximal region of domain 2 demonstrated that the entire IRES structure is required for internal initiation.

Regions known to bind proteins are efficient targets of inhibitory ASOs. Domain 5 is the most accessible region and also the most susceptible to inhibition.

CONCLUSIONES

El descenso de la traducción dependiente del IRES de FMDV demuestra la existencia de una región susceptible en el 5'UTR de RNA viral crítico para la expresión del genoma del FMDV.

Las regiones AUG1 y AUG2 del FMDV se comportan de manera diferente *in-vitro* e *in-vivo*. La región que contiene codón de inicio AUG1 es la más accesible, mientras que la el AUG2 es la más susceptible a la inhibición. El genoma del FMDV se expresa *in-vivo* a través de AUG2 aún en presencia del ASO AUG1 mientras que la traducción se suprime si el AUG2 está bloqueado.

Cada dominio del elemento IRES posee secuencias críticas capaz de influir en la función global del IRES. Estas regiones pueden ser utilizadas para controlar el papel del IRES en la infección por el virus FMDV.

La inhibición de la traducción dependiendo de IRES exhibida por la ASO en relación a su accesibilidad reveló una relación inversa con algunas excepciones.

La inhibición dependientes de ASO es especifica de algunas regiones del IRES. La inhibición mostrada por ASO complementario a los motivos GNRA, RAAA, el dominio 5, la horquilla J del dominio 4 y la región proximal del dominio 2 demostró que toda la estructura del IRES se requiere para la iniciación interna.

Regiones que se unen con proteínas pueden servir como dianas de ASO inhibidores. El dominio 5 es la región más accesible y, también, la más susceptible a la inhibición.

REFERENCES

Anderson, E.C., Hunt, S.L. and Jackson, R.J. (2007) Internal initiation of translation from the human rhinovirus-2 internal ribosome entry site requires the binding of Unr to two distinct sites on the 5' untranslated region. J Gen Virol 88(Pt 11), 3043-52.

Andreev, D.E., Fernandez-Miragall, O., Ramajo, J., Dmitriev, S.E., Terenin, I.M., Martinez-Salas, E. and Shatsky, I.N. (2007) Differential factor requirement to assemble translation initiation complexes at the alternative start codons of foot-and-mouth disease virus RNA. RNA 13(8), 1366-74.

Baird, S.D., Turcotte, M., Korneluk, R.G. and Holcik, M. (2006) Searching for IRES. Rna 12(10), 1755-85.

Balvay, L., Soto Rifo, R., Ricci, E.P., Decimo, D. and Ohlmann, T. (2009) Structural and functional diversity of viral IRESes. Biochim Biophys Acta 1789(9-10), 542-57.

Batey, R.T., Rambo, R.P. and Doudna, J.A. (1999) Tertiary Motifs in RNA Structure and Folding. Angew Chem Int Ed Engl 38(16), 2326-2343.

Belsham, G.J. (1992) Dual initiation sites of protein synthesis on foot-and-mouth disease virus RNA are selected following internal entry and scanning of ribosomes in vivo. EMBO J 11(3), 1105-10.

Belsham, G.J. (2009) Divergent picornavirus IRES elements. Virus Res 139(2), 183-92.

Belsham, G.J. and Brangwyn, J.K. (1990) A region of the 5' noncoding region of foot-and-mouth disease virus RNA directs efficient internal initiation of protein synthesis within cells: involvement with the role of L protease in translational control. J Virol 64(11), 5389-95.

Belsham, G.J. and Martínez-Salas, E. (2004) Genome Organisation, Translation and Replication of Foot-and-mouth Disease Virus RNA. FMDV Current Perspective, 19-76.

Belsham, G.J. and Sonenberg, N. (1996) RNA-protein interactions in regulation of picornavirus RNA translation. Microbiol Rev 60(3), 499-511.

Bigeriego, P., Rosas, M.F., Zamora, E., Martinez-Salas, E. and Sobrino, F. (1999) Heterotypic inhibition of foot-and-mouth disease virus infection by combinations of RNA transcripts corresponding to the 5' and 3' regions. Antiviral Res 44(2), 133-41.

Blyn, L.B., Towner, J.S., Semler, B.L. and Ehrenfeld, E. (1997) Requirement of poly(rC) binding protein 2 for translation of poliovirus RNA. J Virol 71(8), 6243-6.

Borman, A. and Jackson, R.J. (1992) Initiation of translation of human rhinovirus RNA: mapping the internal ribosome entry site. Virology 188(2), 685-96.

Boussadia, O., Niepmann, M., Creancier, L., Prats, A.C., Dautry, F. and Jacquemin-Sablon, H. (2003) Unr is required in vivo for efficient initiation of translation from the internal ribosome entry sites of both rhinovirus and poliovirus. J Virol 77(6), 3353-9.

Brocard, M., Paulous, S., Komarova, A.V., Deveaux, V. and Kean, K.M. (2007) Evidence that PTB does not stimulate HCV IRES-driven translation. Virus Genes 35(1), 5-15.

Brown, E.A., Zajac, A.J. and Lemon, S.M. (1994) In vitro characterization of an internal ribosomal entry site (IRES) present within the 5' nontranslated region of hepatitis A virus RNA: comparison with the IRES of encephalomyocarditis virus. J Virol 68(2), 1066-74.

Buck, C.B., Shen, X., Egan, M.A., Pierson, T.C., Walker, C.M. and Siliciano, R.F. (2001) The human immunodeficiency virus type 1 gag gene encodes an internal ribosome entry site. J Virol 75(1), 181-91.

Butcher, S.E., Dieckmann, T. and Feigon, J. (1997) Solution structure of a GAAA tetraloop receptor RNA. EMBO J 16(24), 7490-9.

Cao, X., Bergmann, I.E., Fullkrug, R. and Beck, E. (1995) Functional analysis of the two alternative translation initiation sites of foot-and-mouth disease virus. J Virol 69(1), 560-3.

Carrillo, C., Tulman, E.R., Delhon, G., Lu, Z., Carreno, A., Vagnozzi, A., Kutish, G.F. and Rock, D.L. (2005) Comparative genomics of foot-and-mouth disease virus. J Virol 79(10), 6487-504.

Chan, J.H., Lim, S. and Wong, W.S. (2006) Antisense oligonucleotides: from design to therapeutic application. Clin Exp Pharmacol Physiol 33(5-6), 533-40.

Chen, W., Yan, W., Du, Q., Fei, L., Liu, M., Ni, Z., Sheng, Z. and Zheng, Z. (2004) RNA interference targeting VP1 inhibits foot-and-mouth disease virus replication in BHK-21 cells and suckling mice. J Virol 78(13), 6900-7.

Cong, W., Cui, S., Chen, J., Zuo, X., Lu, Y., Yan, W. and Zheng, Z. (2010) Construction of a multiple targeting RNAi plasmid that inhibits target gene expression and FMDV replication in BHK-21 cells and suckling mice. Vet Res Commun 34(4), 335-46.

Correll, C.C. and Swinger, K. (2003) Common and distinctive features of GNRA tetraloops based on a GUAA tetraloop structure at 1.4 A resolution. RNA 9(3), 355-63.

Costa-Mattioli, M., Svitkin, Y. and Sonenberg, N. (2004) La autoantigen is necessary for optimal function of the poliovirus and hepatitis C virus internal ribosome entry site in vivo and in vitro. Mol Cell Biol 24(15), 6861-70.

Cotten, M., Oberhauser, B., Brunar, H., Holzner, A., Issakides, G., Noe, C.R., Schaffner, G., Wagner, E. and Birnstiel, M.L. (1991) 2'-O-methyl, 2'-O-ethyl oligoribonucleotides and phosphorothioate oligodeoxyribonucleotides as inhibitors of the in vitro U7 snRNP-dependent mRNA processing event. Nucleic Acids Res 19(10), 2629-35.

Darfeuille, F., Hansen, J.B., Orum, H., Di Primo, C. and Toulme, J.J. (2004) LNA/DNA chimeric oligomers mimic RNA aptamers targeted to the TAR RNA element of HIV-1. Nucleic Acids Res 32(10), 3101-7.

Deas, T.S., Binduga-Gajewska, I., Tilgner, M., Ren, P., Stein, D.A., Moulton, H.M., Iversen, P.L., Kauffman, E.B., Kramer, L.D. and Shi, P.Y. (2005) Inhibition of flavivirus infections by antisense oligomers specifically suppressing viral translation and RNA replication. J Virol 79(8), 4599-609.

Devaney, M.A., Vakharia, V.N., Lloyd, R.E., Ehrenfeld, E. and Grubman, M.J. (1988) Leader protein of foot-and-mouth disease virus is required for cleavage of the p220 component of the cap-binding protein complex. J Virol 62(11), 4407-9.

Dias, N. and Stein, C.A. (2002) Antisense oligonucleotides: basic concepts and mechanisms. Mol Cancer Ther 1(5), 347-55.

Domingo, E., Baranowski, E., Escarmis, C. and Sobrino, F. (2002) Foot-and-mouth disease virus. Comp Immunol Microbiol Infect Dis 25(5-6), 297-308.

Du, Z., Ulyanov, N.B., Yu, J., Andino, R. and James, T.L. (2004) NMR structures of loop B RNAs from the stem-loop IV domain of the enterovirus internal ribosome entry site: a single C to U substitution drastically changes the shape and flexibility of RNA. Biochemistry 43(19), 5757-71.

el-Awady, M.K., el-Din, N.G., el-Garf, W.T., Youssef, S.S., Omran, M.H., el-Abd, J. and Goueli, S.A. (2006) Antisense oligonucleotide inhibition of hepatitis C virus genotype 4 replication in HepG2 cells. Cancer Cell Int 6, 18.

Enterlein, S., Warfield, K.L., Swenson, D.L., Stein, D.A., Smith, J.L., Gamble, C.S., Kroeker, A.D., Iversen, P.L., Bavari, S. and Muhlberger, E. (2006) VP35 knockdown inhibits Ebola virus amplification and protects against lethal infection in mice. Antimicrob Agents Chemother 50(3), 984-93.

Fernandez, N., Garcia-Sacristan, A., Ramajo, J., Briones, C. and Martinez-Salas, E. (2011) Structural analysis provides insights into the modular organization of picornavirus IRES. Virology 409(2), 251-61.

Fernandez-Miragall, O., Lopez de Quinto, S. and Martinez-Salas, E. (2009) Relevance of RNA structure for the activity of picornavirus IRES elements. Virus Res 139(2), 172-82.

Fernandez-Miragall, O. and Martinez-Salas, E. (2003) Structural organization of a viral IRES depends on the integrity of the GNRA motif. Rna 9(11), 1333-44.

Fernandez-Miragall, O. and Martinez-Salas, E. (2007) In vivo footprint of a picornavirus internal ribosome entry site reveals differences in accessibility to specific RNA structural elements. J Gen Virol 88(Pt 11), 3053-62.

Fernandez-Miragall, O., Ramos, R., Ramajo, J. and Martinez-Salas, E. (2006) Evidence of reciprocal tertiary interactions between conserved motifs involved in organizing RNA structure essential for internal initiation of translation. Rna 12(2), 223-34.

Fernandez-Sanchez, N. (2010) Análisis Estructural y funcional del IRES de Picornavirus. Doctoral Thesis, Universidad Autonoma de Madrid.

Filbin, M.E. and Kieft, J.S. (2009) Toward a structural understanding of IRES RNA function. Curr Opin Struct Biol 19(3), 267-76.

Forss, S., Strebel, K., Beck, E. and Schaller, H. (1984) Nucleotide sequence and genome organization of foot-and-mouth disease virus. Nucleic Acids Res 12(16), 6587-601.

Garcia-Arriaza, J., Manrubia, S.C., Toja, M., Domingo, E. and Escarmis, C. (2004) Evolutionary transition toward defective RNAs that are infectious by complementation. J Virol 78(21), 11678-85.

Ge, Q., Pastey, M., Kobasa, D., Puthavathana, P., Lupfer, C., Bestwick, R.K., Iversen, P.L., Chen, J. and Stein, D.A. (2006) Inhibition of multiple subtypes of influenza A virus in cell cultures with morpholino oligomers. Antimicrob Agents Chemother 50(11), 3724-33.

Gerber, K., Wimmer, E. and Paul, A.V. (2001) Biochemical and genetic studies of the initiation of human rhinovirus 2 RNA replication: identification of a cis-replicating element in the coding sequence of 2A(pro). J Virol 75(22), 10979-90.

Gitlin, L., Karelsky, S. and Andino, R. (2002) Short interfering RNA confers intracellular antiviral immunity in human cells. Nature 418(6896), 430-4.

Glass, M.J., Jia, X.Y. and Summers, D.F. (1993) Identification of the hepatitis A virus internal ribosome entry site: in vivo and in vitro analysis of bicistronic RNAs containing the HAV 5' noncoding region. Virology 193(2), 842-52.

Gonzalez-Carmona, M.A., Vogt, A., Heinicke, T., Quasdorff, M., Hoffmann, P., Yildiz, Y., Schneider, C., Serwe, M., Bartenschlager, R., Sauerbruch, T. and Caselmann, W.H. (2010) Inhibition of hepatitis C virus gene expression by adenoviral vectors encoding antisense RNA in vitro and in vivo. J Hepatol.

Goodfellow, I., Chaudhry, Y., Richardson, A., Meredith, J., Almond, J.W., Barclay, W. and Evans, D.J. (2000) Identification of a cis-acting replication element within the poliovirus coding region. J Virol 74(10), 4590-600.

Grubman, M.J. and Baxt, B. (2004) Foot-and-mouth disease. Clin Microbiol Rev 17(2), 465-93.

Gu, S., Ji, J., Kim, J.D., Yee, J.K. and Rossi, J.J. (2006) Inhibition of infectious human immunodeficiency virus type 1 virions via lentiviral vector encoded short antisense RNAs. Oligonucleotides 16(4), 287-95.

Gutierrez, A., Martinez-Salas, E., Pintado, B. and Sobrino, F. (1994) Specific inhibition of aphthovirus infection by RNAs transcribed from both the 5' and the 3' noncoding regions. J Virol 68(11), 7426-32.

Gutierrez, A., Rodriguez, A., Pintado, B. and Sobrino, F. (1993) Transient inhibition of foot-and-mouth disease virus infection of BHK-21 cells by antisense oligonucleotides directed against the second functional initiator AUG. Antiviral Res 22(1), 1-13.

Haasnoot, J. and Berkhout, B. (2009) Nucleic acids-based therapeutics in the battle against pathogenic viruses. Handb Exp Pharmacol(189), 243-63.

Haasnoot, J., Westerhout, E.M. and Berkhout, B. (2007) RNA interference against viruses: strike and counterstrike. Nat Biotechnol 25(12), 1435-43.

Hanecak, R., Brown-Driver, V., Fox, M.C., Azad, R.F., Furusako, S., Nozaki, C., Ford, C., Sasmor, H. and Anderson, K.P. (1996) Antisense oligonucleotide inhibition of hepatitis C virus gene expression in transformed hepatocytes. J Virol 70(8), 5203-12.

Hatta, T., Ishikawa, M., Takai, K., Nakada, S., Yokota, T., Hata, T., Miura, K. and Takaku, H. (1998) Inhibition of influenza virus RNA polymerase by 5'-capped short RNA fragments. Biochem Biophys Res Commun 249(1), 103-6.

Helene, C. and Toulme, J.J. (1990) Specific regulation of gene expression by antisense, sense and antigene nucleic acids. Biochim Biophys Acta 1049(2), 99-125.

Hellen, C.U. and Sarnow, P. (2001) Internal ribosome entry sites in eukaryotic mRNA molecules. Genes Dev 15(13), 1593-612.

Hinnebusch, A.G. (2006) eIF3: a versatile scaffold for translation initiation complexes. Trends Biochem Sci 31(10), 553-62.

Inagawa, T., Nakashima, H., Karwowski, B., Guga, P., Stec, W.J., Takeuchi, H. and Takaku, H. (2002) Inhibition of human immunodeficiency virus type 1 replication by P-stereodefined oligo(nucleoside phosphorothioate)s in a long-term infection model. FEBS Lett 528(1-3), 48-52.

Jackson, R.J., Hellen, C.U. and Pestova, T.V. (2010) The mechanism of eukaryotic translation initiation and principles of its regulation. Nat Rev Mol Cell Biol 11(2), 113-27.

Jaeger, L., Michel, F. and Westhof, E. (1994) Involvement of a GNRA tetraloop in long-range RNA tertiary interactions. J Mol Biol 236(5), 1271-6.

Jang, S.K., Krausslich, H.G., Nicklin, M.J., Duke, G.M., Palmenberg, A.C. and Wimmer, E. (1988) A segment of the 5' nontranslated region of encephalomyocarditis virus RNA directs internal entry of ribosomes during in vitro translation. J Virol 62(8), 2636-43.

Jia, H., Ge, X., Guo, X., Yang, H., Yu, K., Chen, Z., Chen, Y. and Cha, Z. (2008) Specific small interfering RNAs-mediated inhibition of replication of porcine encephalomyocarditis virus in BHK-21 cells. Antiviral Res 79(2), 95-104.

Jiang, M. and Milner, J. (2002) Selective silencing of viral gene expression in HPV-positive human cervical carcinoma cells treated with siRNA, a primer of RNA interference. Oncogene 21(39), 6041-8.

Jin, Y., Zhang, G., Hu, Y., Ding, M., Li, Y., Cao, S., Xue, J., Sun, L.Q. and Wang, M. (2011) Inhibition of highly pathogenic avian H5N1 influenza virus propagation by RNA oligonucleotides targeting the PB2 gene in combination with celecoxib. J Gene Med 13(4), 243-9.

Jopling, C.L., Yi, M., Lancaster, A.M., Lemon, S.M. and Sarnow, P. (2005) Modulation of hepatitis C virus RNA abundance by a liver-specific MicroRNA. Science 309(5740), 1577-81.

Kafasla, P., Morgner, N., Robinson, C.V. and Jackson, R.J. (2010) Polypyrimidine tract-binding protein stimulates the poliovirus IRES by modulating eIF4G binding. EMBO J 29(21), 3710-22.

Kahana, R., Kuznetzova, L., Rogel, A., Shemesh, M., Hai, D., Yadin, H. and Stram, Y. (2004) Inhibition of foot-and-mouth disease virus replication by small interfering RNA. J Gen Virol 85(Pt 11), 3213-7.

Kanda, T., Kusov, Y., Yokosuka, O. and Gauss-Muller, V. (2004) Interference of hepatitis A virus replication by small interfering RNAs. Biochem Biophys Res Commun 318(2), 341-5.

Kieft, J.S. (2009) Comparing the three-dimensional structures of Dicistroviridae IGR IRES RNAs with other viral RNA structures. Virus Res 139(2), 148-56.

Kim, S.M., Lee, K.N., Park, J.Y., Ko, Y.J., Joo, Y.S., Kim, H.S. and Park, J.H. (2008) Therapeutic application of RNA interference against foot-and-mouth disease virus in vitro and in vivo. Antiviral Res 80(2), 178-84.

Kinney, R.M., Huang, C.Y., Rose, B.C., Kroeker, A.D., Dreher, T.W., Iversen, P.L. and Stein, D.A. (2005) Inhibition of dengue virus serotypes 1 to 4 in vero cell cultures with morpholino oligomers. J Virol 79(8), 5116-28.

Knowles, N.J. and Samuel, A.R. (2003) Molecular epidemiology of foot-and-mouth disease virus. Virus Res 91(1), 65-80.

Kolupaeva, V.G., Lomakin, I.B., Pestova, T.V. and Hellen, C.U. (2003) Eukaryotic initiation factors 4G and 4A mediate conformational changes downstream of the initiation codon of the encephalomyocarditis virus internal ribosomal entry site. Mol Cell Biol 23(2), 687-98.

Kolupaeva, V.G., Pestova, T.V., Hellen, C.U. and Shatsky, I.N. (1998) Translation eukaryotic initiation factor 4G recognizes a specific structural element within the internal ribosome entry site of encephalomyocarditis virus RNA. J Biol Chem 273(29), 18599-604.

Kozak, M. (1987) At least six nucleotides preceding the AUG initiator codon enhance translation in mammalian cells. J Mol Biol 196(4), 947-50.

Kuhn, R., Luz, N. and Beck, E. (1990) Functional analysis of the internal translation initiation site of foot-and-mouth disease virus. J Virol 64(10), 4625-31.

Kusov, Y., Kanda, T., Palmenberg, A., Sgro, J.Y. and Gauss-Muller, V. (2006) Silencing of hepatitis A virus infection by small interfering RNAs. J Virol 80(11), 5599-610.

Laxton, C., Brady, K., Moschos, S., Turnpenny, P., Rawal, J., Pryde, D.C., Sidders, B., Corbau, R., Pickford, C. and Murray, E.J. (2011) Selection, optimisation and pharmacokinetic properties of a novel, potent antiviral locked nucleic acid (LNA-) based antisense oligomer (ASO) targeting hepatitis C virus (HCV) internal ribosome entry site (IRES). Antimicrob Agents Chemotherapy.

Li, M.J., Bauer, G., Michienzi, A., Yee, J.K., Lee, N.S., Kim, J., Li, S., Castanotto, D., Zaia, J. and Rossi, J.J. (2003) Inhibition of HIV-1 infection by lentiviral vectors expressing Pol III-promoted anti-HIV RNAs. Mol Ther 8(2), 196-206.

Lim, T.W., Yuan, J., Liu, Z., Qiu, D., Sall, A. and Yang, D. (2006) Nucleic-acid-based antiviral agents against positive single-stranded RNA viruses. Curr Opin Mol Ther 8(2), 104-7.

Liu, Y.P., Westerink, J.T., Ter Brake, O. and Berkhout, B. (2011) RNAi-Inducing Lentiviral Vectors for Anti-HIV-1 Gene Therapy. Methods Mol Biol 721, 293-311.

Lopez de Quinto, S., Lafuente, E. and Martinez-Salas, E. (2001) IRES interaction with translation initiation factors: functional characterization of novel RNA contacts with eIF3, eIF4B, and eIF4GII. Rna 7(9), 1213-26.

Lopez de Quinto, S. and Martinez-Salas, E. (1997) Conserved structural motifs located in distal loops of aphthovirus internal ribosome entry site domain 3 are required for internal initiation of translation. J Virol 71(5), 4171-5.

Lopez de Quinto, S. and Martinez-Salas, E. (1999) Involvement of the aphthovirus RNA region located between the two functional AUGs in start codon selection. Virology 255(2), 324-36.

Lopez de Quinto, S. and Martinez-Salas, E. (2000) Interaction of the eIF4G initiation factor with the aphthovirus IRES is essential for internal translation initiation in vivo. RNA 6(10), 1380-92.

Lopez de Quinto, S., Saiz, M., de la Morena, D., Sobrino, F. and Martinez-Salas, E. (2002) IRES-driven translation is stimulated separately by the FMDV 3'-NCR and poly(A) sequences. Nucleic Acids Res 30(20), 4398-405.

Luz, N. and Beck, E. (1991) Interaction of a cellular 57-kilodalton protein with the internal translation initiation site of foot-and-mouth disease virus. J Virol 65(12), 6486-94.

Lv, K., Guo, Y., Zhang, Y., Wang, K., Li, K., Zhu, Y. and Sun, S. (2009) Transient inhibition of foot-and-mouth disease virus replication by siRNAs silencing VP1 protein coding region. Res Vet Sci 86(3), 443-52.

Macpherson, J.L., Boyd, M.P., Arndt, A.J., Todd, A.V., Fanning, G.C., Ely, J.A., Elliott, F., Knop, A., Raponi, M., Murray, J., Gerlach, W., Sun, L.Q., Penny, R., Symonds, G.P., Carr, A. and Cooper, D.A. (2005) Long-term survival and concomitant gene expression of ribozyme-transduced CD4+ T-lymphocytes in HIV-infected patients. J Gene Med 7(5), 552-64.

Marintchev, A. and Wagner, G. (2004) Translation initiation: structures, mechanisms and evolution. Q Rev Biophys 37(3-4), 197-284.

Martin-Acebes, M.A., Gonzalez-Magaldi, M., Rosas, M.F., Borrego, B., Brocchi, E., Armas-Portela, R. and Sobrino, F. (2008) Subcellular distribution of swine vesicular disease virus proteins and alterations induced in infected cells: a comparative study with foot-and-mouth disease virus and vesicular stomatitis virus. Virology 374(2), 432-43.

Martinez-Salas, E. (2008) The impact of RNA structure on picornavirus IRES activity. Trends Microbiol 16(5), 230-7.

Martinez-Salas, E., Pacheco, A., Serrano, P. and Fernandez, N. (2008) New insights into internal ribosome entry site elements relevant for viral gene expression. J Gen Virol 89(Pt 3), 611-26.

Martinez-Salas, E., Regalado, M.P. and Domingo, E. (1996) Identification of an essential region for internal initiation of translation in the aphthovirus internal ribosome entry site and implications for viral evolution. J Virol 70(2), 992-8.

Martinez-Salas, E. and Ryan, M.D. (2010) Translation and Protein Processing. The Picornaviruses, 20.

Mason, P.W., Bezborodova, S.V. and Henry, T.M. (2002) Identification and characterization of a cis-acting replication element (cre) adjacent to the internal ribosome entry site of foot-and-mouth disease virus. J Virol 76(19), 9686-94.

McKnight, K.L. and Lemon, S.M. (1998) The rhinovirus type 14 genome contains an internally located RNA structure that is required for viral replication. RNA 4(12), 1569-84.

Mescalchin, A. and Restle, T. (2011) Oligomeric nucleic acids as antivirals. Molecules 16(2), 1271-96.

Michel, F. and Westhof, E. (1990) Modelling of the three-dimensional architecture of group I catalytic introns based on comparative sequence analysis. J Mol Biol 216(3), 585-610.

Monie, T.P., Perrin, A.J., Birtley, J.R., Sweeney, T.R., Karakasiliotis, I., Chaudhry, Y., Roberts, L.O., Matthews, S., Goodfellow, I.G. and Curry, S. (2007) Structural insights into the transcriptional and translational roles of Ebp1. EMBO J 26(17), 3936-44.

Nayak, A., Goodfellow, I.G. and Belsham, G.J. (2005) Factors required for the Uridylylation of the foot-and-mouth disease virus 3B1, 3B2, and 3B3 peptides by the RNA-dependent RNA polymerase (3Dpol) in vitro. J Virol 79(12), 7698-706.

Neuman, B.W., Stein, D.A., Kroeker, A.D., Churchill, M.J., Kim, A.M., Kuhn, P., Dawson, P., Moulton, H.M., Bestwick, R.K., Iversen, P.L. and Buchmeier, M.J. (2005) Inhibition, escape, and attenuated growth of severe acute respiratory syndrome coronavirus treated with antisense morpholino oligomers. J Virol 79(15), 9665-76.

Pacheco, A., Lopez de Quinto, S., Ramajo, J., Fernandez, N. and Martinez-Salas, E. (2009) A novel role for Gemin5 in mRNA translation. Nucleic Acids Res 37(2), 582-90.

Pacheco, A. and Martinez-Salas, E. (2010) Insights into the biology of IRES elements through riboproteomic approaches. J Biomed Biotechnol 2010, 458927.

Pacheco, A., Reigadas, S. and Martinez-Salas, E. (2008) Riboproteomic analysis of polypeptides interacting with the internal ribosome-entry site element of foot-and-mouth disease viral RNA. Proteomics 8(22), 4782-90.

Paessler, S., Rijnbrand, R., Stein, D.A., Ni, H., Yun, N.E., Dziuba, N., Borisevich, V., Seregin, A., Ma, Y., Blouch, R., Iversen, P.L. and Zacks, M.A. (2008) Inhibition of alphavirus

infection in cell culture and in mice with antisense morpholino oligomers. Virology 376(2), 357-70.

Park, W.S., Miyano-Kurosaki, N., Abe, T., Takai, K., Yamamoto, N. and Takaku, H. (2000) Inhibition of HIV-1 replication by a new type of circular dumbbell RNA/DNA chimeric oligonucleotides. Biochem Biophys Res Commun 270(3), 953-60.

Paul, A.V., Rieder, E., Kim, D.W., van Boom, J.H. and Wimmer, E. (2000) Identification of an RNA hairpin in poliovirus RNA that serves as the primary template in the in vitro uridylylation of VPg. J Virol 74(22), 10359-70.

Pelletier, J. and Sonenberg, N. (1988) Internal initiation of translation of eukaryotic mRNA directed by a sequence derived from poliovirus RNA. Nature 334(6180), 320-5.

Pengyan, W., Yan, R., Zhiru, G. and Chuangfu, C. (2008) Inhibition of foot-and-mouth disease virus replication in vitro and in vivo by small interfering RNA. Virol J 5, 86.

Pestova, T.V., Kolupaeva, V.G., Lomakin, I.B., Pilipenko, E.V., Shatsky, I.N., Agol, V.I. and Hellen, C.U. (2001) Molecular mechanisms of translation initiation in eukaryotes. Proc Natl Acad Sci U S A 98(13), 7029-36.

Pfingsten, J.S. and Kieft, J.S. (2008) RNA structure-based ribosome recruitment: lessons from the Dicistroviridae intergenic region IRESes. Rna 14(7), 1255-63.

Phelan, M., Banks, R.J., Conn, G. and Ramesh, V. (2004) NMR studies of the structure and Mg2+ binding properties of a conserved RNA motif of EMCV picornavirus IRES element. Nucleic Acids Res 32(16), 4715-24.

Pilipenko, E.V., Gmyl, A.P., Maslova, S.V., Svitkin, Y.V., Sinyakov, A.N. and Agol, V.I. (1992) Prokaryotic-like cis elements in the cap-independent internal initiation of translation on picornavirus RNA. Cell 68(1), 119-31.

Pilipenko, E.V., Pestova, T.V., Kolupaeva, V.G., Khitrina, E.V., Poperechnaya, A.N., Agol, V.I. and Hellen, C.U. (2000) A cell cycle-dependent protein serves as a template-specific translation initiation factor. Genes Dev 14(16), 2028-45.

Ramos, R. and Martinez-Salas, E. (1999) Long-range RNA interactions between structural domains of the aphthovirus internal ribosome entry site (IRES). Rna 5(10), 1374-83.

Rieder, E., Paul, A.V., Kim, D.W., van Boom, J.H. and Wimmer, E. (2000) Genetic and biochemical studies of poliovirus cis-acting replication element cre in relation to VPg uridylylation. J Virol 74(22), 10371-80.

Roberts, L.O. and Groppelli, E. (2009) An atypical IRES within the 5' UTR of a dicistrovirus genome. Virus Res 139(2), 157-65.

Robertson, M.E., Seamons, R.A. and Belsham, G.J. (1999) A selection system for functional internal ribosome entry site (IRES) elements: analysis of the requirement for a conserved GNRA tetraloop in the encephalomyocarditis virus IRES. Rna 5(9), 1167-79.

Rosas, M.F., Martinez-Salas, E. and Sobrino, F. (2003) Stable expression of antisense RNAs targeted to the 5' non-coding region confers heterotypic inhibition to foot-and-mouth disease virus infection. J Gen Virol 84(Pt 2), 393-402.

Sagan, S.M., Nasheri, N., Luebbert, C. and Pezacki, J.P. (2011) The efficacy of siRNAs against hepatitis C virus is strongly influenced by structure and target site accessibility. Chem Biol 17(5), 515-27.

Saiz, M., Gomez, S., Martinez-Salas, E. and Sobrino, F. (2001) Deletion or substitution of the aphthovirus 3' NCR abrogates infectivity and virus replication. J Gen Virol 82(Pt 1), 93-101.

Saleh, L., Rust, R.C., Fullkrug, R., Beck, E., Bassili, G., Ochs, K. and Niepmann, M. (2001) Functional interaction of translation initiation factor eIF4G with the foot-and-mouth disease virus internal ribosome entry site. J Gen Virol 82(Pt 4), 757-63.

Sangar, D.V., Newton, S.E., Rowlands, D.J. and Clarke, B.E. (1987) All foot and mouth disease virus serotypes initiate protein synthesis at two separate AUGs. Nucleic Acids Res 15(8), 3305-15.

Schubert, S., Grunert, H.P., Zeichhardt, H., Werk, D., Erdmann, V.A. and Kurreck, J. (2005) Maintaining inhibition: siRNA double expression vectors against coxsackieviral RNAs. J Mol Biol 346(2), 457-65.

Semler, B.L. and Waterman, M.L. (2008) IRES-mediated pathways to polysomes: nuclear versus cytoplasmic routes. Trends Microbiol 16(1), 1-5.

Serrano, P., Pulido, M.R., Saiz, M. and Martinez-Salas, E. (2006) The 3' end of the foot-and-mouth disease virus genome establishes two distinct long-range RNA-RNA interactions with the 5' end region. J Gen Virol 87(Pt 10), 3013-22.

Serrano, P., Ramajo, J. and Martinez-Salas, E. (2009) Rescue of internal initiation of translation by RNA complementation provides evidence for a distribution of functions between individual IRES domains. Virology 388(1), 221-9.

Sobrino, F., Davila, M., Ortin, J. and Domingo, E. (1983) Multiple genetic variants arise in the course of replication of foot-and-mouth disease virus in cell culture. Virology 128(2), 310-8.

Sonenberg, N. and Hinnebusch, A.G. (2009) Regulation of translation initiation in eukaryotes: mechanisms and biological targets. Cell 136(4), 731-45.

Sorin, E.J., Engelhardt, M.A., Herschlag, D. and Pande, V.S. (2002) RNA simulations: probing hairpin unfolding and the dynamics of a GNRA tetraloop. J Mol Biol 317(4), 493-506.

Spurgers, K.B., Sharkey, C.M., Warfield, K.L. and Bavari, S. (2008) Oligonucleotide antiviral therapeutics: antisense and RNA interference for highly pathogenic RNA viruses. Antiviral Res 78(1), 26-36.

Stone, J.K., Rijnbrand, R., Stein, D.A., Ma, Y., Yang, Y., Iversen, P.L. and Andino, R. (2008) A morpholino oligomer targeting highly conserved internal ribosome entry site sequence is able to inhibit multiple species of picornavirus. Antimicrob Agents Chemother 52(6), 1970-81.

Tinoco, I., Jr. and Bustamante, C. (1999) How RNA folds. J Mol Biol 293(2), 271-81.

Vagnozzi, A., Stein, D.A., Iversen, P.L. and Rieder, E. (2007) Inhibition of foot-and-mouth disease virus infections in cell cultures with antisense morpholino oligomers. J Virol 81(21), 11669-80.

van den Born, E., Stein, D.A., Iversen, P.L. and Snijder, E.J. (2005) Antiviral activity of morpholino oligomers designed to block various aspects of Equine arteritis virus amplification in cell culture. J Gen Virol 86(Pt 11), 3081-90.

Vitravene. (2002) A randomized controlled clinical trial of intravitreous fomivirsen for treatment of newly diagnosed peripheral cytomegalovirus retinitis in patients with AIDS. Am J Ophthalmol 133(4), 467-74.

Wakita, T., Moradpour, D., Tokushihge, K. and Wands, J.R. (1999) Antiviral effects of antisense RNA on hepatitis C virus RNA translation and expression. J Med Virol 57(3), 217-22.

Walter, B.L., Nguyen, J.H., Ehrenfeld, E. and Semler, B.L. (1999) Differential utilization of poly(rC) binding protein 2 in translation directed by picornavirus IRES elements. RNA 5(12), 1570-85.

Warfield, K.L., Swenson, D.L., Olinger, G.G., Nichols, D.K., Pratt, W.D., Blouch, R., Stein, D.A., Aman, M.J., Iversen, P.L. and Bavari, S. (2006) Gene-specific countermeasures against Ebola virus based on antisense phosphorodiamidate morpholino oligomers. PLoS Pathog 2(1), e1.

Watrin, M., Dausse, E., Lebars, I., Rayner, B., Bugaut, A. and Toulme, J.J. (2009a) Aptamers targeting RNA molecules. Methods Mol Biol 535, 79-105.

Watrin, M., Von Pelchrzim, F., Dausse, E., Schroeder, R. and Toulme, J.J. (2009b) In vitro selection of RNA aptamers derived from a genomic human library against the TAR RNA element of HIV-1. Biochemistry 48(26), 6278-84.

Westhof E, A.P. (2000) RNA tertiary structures. Encyclopedia of Analytic Chemistry.

Wilkinson, K.A., Merino, E.J. and Weeks, K.M. (2006) Selective 2'-hydroxyl acylation analyzed by primer extension (SHAPE): quantitative RNA structure analysis at single nucleotide resolution. Nat Protoc 1(3), 1610-6.

Yang, D., Wilson, J.E., Anderson, D.R., Bohunek, L., Cordeiro, C., Kandolf, R. and McManus, B.M. (1997) In vitro mutational and inhibitory analysis of the cis-acting translational elements within the 5' untranslated region of coxsackievirus B3: potential targets for antiviral action of antisense oligomers. Virology 228(1), 63-73.

Yoo, B.H., Bochkareva, E., Bochkarev, A., Mou, T.C. and Gray, D.M. (2004) 2'-O-methyl-modified phosphorothioate antisense oligonucleotides have reduced non-specific effects in vitro. Nucleic Acids Res 32(6), 2008-16.

Yu, Y., Abaeva, I.S., Marintchev, A., Pestova, T.V. and Hellen, C.U. (2011) Common conformational changes induced in type 2 picornavirus IRESs by cognate trans-acting factors. Nucleic Acids Res.

Yuan, J., Cheung, P.K., Zhang, H.M., Chau, D. and Yang, D. (2005) Inhibition of coxsackievirus B3 replication by small interfering RNAs requires perfect sequence match in the central region of the viral positive strand. J Virol 79(4), 2151-9.

Yuan, J., Stein, D.A., Lim, T., Qiu, D., Coughlin, S., Liu, Z., Wang, Y., Blouch, R., Moulton, H.M., Iversen, P.L. and Yang, D. (2006) Inhibition of coxsackievirus B3 in cell cultures and in mice by peptide-conjugated morpholino oligomers targeting the internal ribosome entry site. J Virol 80(23), 11510-9.

Zhang, H., Hanecak, R., Brown-Driver, V., Azad, R., Conklin, B., Fox, M.C. and Anderson, K.P. (1999) Antisense oligonucleotide inhibition of hepatitis C virus (HCV) gene expression in livers of mice infected with an HCV-vaccinia virus recombinant. Antimicrob Agents Chemother 43(2), 347-53.

With great achievements follow humility.

The fulfillment of this work was made possible through the help of Agencia Española de Cooperacion Internacional para el Desarrollo of the Ministerio de Asuntos Exteriores y Cooperacion. This work was accomplished through the stewardship of my thesis adviser and mentor, Dr. Encarnación Martinez-Salas, of the Centro de Biologia Molecular "Severo Ochoa", Universidad Autonoma de Madrid-CSIC.